جامعة البحرين
المكتبة
LIBRARY
University of Bahrain

Kingdom of Bahrain

University of Bahrain

Deanship of Scientific Research

Ways to Improve Water Quality in Tubli Bay

By

Layla A. Rahim Janahi
ID#: 19850863

A Thesis submitted in partial fulfillment of the requirements for the degree of

Master of Science

in

Environment and Sustainable Development

2006

DECLARATION

I declare that this work is the result of my own investigation and that it has not already been accepted in substance for any degree, nor is it being currently submitted for any degree.

Signed: Layla Janahi	**Date:** 26.06.06

The Thesis defense committee considers the Thesis titled :

Ways to Improve Water Quality in Tubli Bay - Bahrain

Submitted by Layla A Janahi to the Deanship of Scientific Research satisfactory and acceptable for the Master of Environment and Sustainable Development.

Thesis Defense Committee:

.....	
Dr. Abdul Rahim Abbas Member	Department of Chemical Engineering
.....	
Dr. Member	Department of
.....	
Dr. Member	Department of

ACKNOWLEDGEMENT

Where do I start! And having started, where do I stop!

The past few years have been rich experience; incurring the development of many new friends and acquaintances, who have to varying degrees and in numerous contexts, helped me along the twisting and occasionally disheartening road of research. This is my opportunity to thanks all these people for their excellent contribution, suggestions, friendly ears, timely distractions and full-fat chocolate products when I needed them most.

Firstly, thanks must go to my supervisor, Mohanned ALSheriadeh, for his support and feedback throughout my period of research. Also in the department, I would like to thank Dr. Abdul Rahim Abbas for his excellent advice and kindness and many of my fellow master students for their friendship.

Finally I would like to express my deep thank to my wonderful family for their worm love and support throughout my period of study and research.

Thanks to all – it's been a ball

ABSTRACT

The environmental conditions in Tubli Bay have been deteriorating continuously for many years due to the reclamations around it, which reduced its area by 40% and destroyed most of the mangroves northwest of the Bay; the discharges of wastewater from a number of sources, mainly the Tubli wastewater treatment plant; and the discharges of silt from sand washing in the southern part of the Bay. The problem is aggravated further by restricting the inflow and outflow of the Bay due to the installment of cairns ahead of Sitra Causeway Bridge, the construction of a culvert under Majlis Al Tawoon Highway, and the Ma'meer Channel. Nowadays, new plans are set to construct a new bridge in place of the old Sitra Bridge and two new ones are in the pipeline. All of these developments form a driving force behind this work. The main objective is to investigate the existing flushing characteristics of the Bay and potential options to improve the flushing capacity that could be able to eliminate contaminants. To this end MIKE 21 model was used, it was calibrated and validated to the bay situation and then set up for predicting the flow characteristics and improvement options. The calibration was based on the results of a work done by COWI ALMOAYED GULF Company and validation by actual water level measurement at a point situated north of the Bay. Simulations were conducted for various scenarios illustrating the possible situations that could improve water flow in the bay and flush contaminants. The results of the simulations indicated that flow in the Bay is divided into distinct areas; inner Bay and south of Ras Sanad. Flushing the inner Bay is mainly by tidal prism mechanism and it is effective, and south of Ras Sanad by the bouncing of water at both sides of the culvert under Majlis Al Tawoon Highway. However, it is been concluded that flushing by water circulation around Nabih Saleh Island is negligible. Furthermore, it has been found that dredging a channel south of Ras Sand to Ma'meer Channel will not have much effect in water flushing inside the Bay. On the basis of the results it is recommended that in order to improve the water quality in the Bay all waste effluents are ceased and settled sludge at the deep area north of Tubli Bay be capped artificially or naturally by suspended solids deposition in the long run.

TABLE OF CONTENTS

		Page
	CHAPTER ONE: INTRODUCTION	**1**
1.1	INTRODUCTION	2
1.2	TUBLI BAY NATURAL SETTING	3
1.2.1	Bay Geography	3
1.2.2	Climate and Wind	5
1.2.3	Habitats and Species	6
1.2.4	Physical Features of Gulf Region	7
1.2.5	Bathymetry and Bottom Sediments Nature	7
1.3	THE BAY SITUATION	8
1.3.1	Tubli Bay Importance	8
1.3.2	Pressures/ Stresses on the Bay	10
1.3.3	Bay Degradation	12
1.3.4	Policies and Legislation	12
1.3.4.1	Decision Making Legislation and Regulation	12
1.4	OBJECTIVE OF THE STUDY	14
	CHAPTER TWO: MIKE 21	**15**
2.1	GENERAL DESCRIPTION OF MIKE 21	16
2.2	MODEL APPLICATION	16
2.3	FLOW, SEDIMENT AND CONTAMINANT TRANSPORT PROCESSES	18
2.3.1	Flow/ Hydrodynamic Governing Equations	18
2.3.2	Flow/ Hydrodynamic parameters	19
2.3.2.1	Bed Resistance	19
2.3.2.2	Courant Number	21
2.3.2.3	Eddy Viscosity	21
2.3.3	Environmental Hydraulics	23

2.4	ADVECTION – DISPERSION MODULE	24
2.4.1	Dispersion Coefficients	24
2.4.2	Dispersion Processes	25
2.4.2.1	General	25
2.4.2.2	Turbulence	27
2.4.3	Shear Flow	29
2.4.4	Subgrid Scale Processes	31
2.5	ESTIMATION OF COEFFICIENTS	33
2.5.1	Basic Formulations	33
2.5.2	The Evidence of Experience	36
2.6	GENERAL INTERPRETATION	39
	CHAPTER THREE: MODEL APPLICATIONS AND RESULTS DISCUSSION	**42**
3.1	MODEL APPLICATION	43
3.2	INPUT DATA	44
3.3	REFERENCE LEVEL	44
3.4	BATHYMETRY	44
3.5	WIND	45
3.6	WATER LEVEL DATA	48
3.6.1	Tidal levels	48
3.6.2	Metrological Effects	48
3.6.3	Measurements	48
3.7	CURRENTS DATA	50
3.8	MODELING DOMAIN	52
3.9	FLOW BOUNDARY AND INITIAL CONDITIONS	53
3.10	FIRST ORDER SENSITIVITY ANALYSIS	56
3.11	MODEL CALIBRATION AND VALIDATION	59
3.12	EXISTING FLOW AND TRANSPORT IN TUBLI BAY	68

3.12.1	Existing Flow	68
3.12.2	Tidal Hydraulics and Flushing	71
3.12.2.1	High Tide Levels	71
3.12.2.2	Low Tide Levels	71
3.12.2.3	Current Speeds in the Bridge Openings	71
3.12.3	Improvement Scenarios	77
3.12.3.1	Residence Time	86
3.12.4	The behavior of contaminant in the Bay	87
	CHAPTER FOUR	**92**
4.1	CONCLUSIONS	93
4.2	RECOMMENDATIONS	95
	CHAPTER FIVE	**96**
	REFERENCES	97

LIST OF TABLES

Table		Page
1.1	List of legislations relating to protection of the environment issued as Ministerial order	13
2.1	List of the transport processes indicated at MIKE 21 Model	25
2.2	Comparison between Elder's Coefficient and calibrated coefficient	36
2.3	Effective coefficients of scale 4	37
3.1	Probability of occurrence of mean hourly wind speed from different directions. Wind statistics from the weather station at Bahrain Airport (E 50°39' and N 26°16') for the period 1982-1991.	47
3.2	The sensitivity of model flow predictions to bed resistance at two stations in Tubli Bay	57
3.3	The sensitivity of concentration predictions to dispersion coefficient at two stations in Tubli Bay	59
3.4	In and outflow across sections outlined in Figure 3.13	77
3.5	Proposed scenarios	78
3.6	Discharge through various sections in Tubli Bay for various scenarios	81
3.7	Residence Time Calculation for each scenario in Tubli Bay	86

LIST OF FIGURES

Figure		Page
1.1	Satellite Image of Arabian Gulf	2
1.2	Satellite Image of Bahrain Island indicating Tubli Bay at the eastern side	4
3.1	The model domain – Tubli Bay (2611'N, 5034'E)	43
3.2	Tubli Bay Bathymetry referenced to Ain Al Abd datum and adjusted to Mina Salman mean surface level	45
3.3	Water level records in Tubli Bay May 1996	49
3.4	Measured current speed at Tubli Bay	51
3.5	Time series of 14-day spring-neap tidal cycle at Mina Salman	54
3.6	Time series of 14-day spring-neap tidal cycle south of Ma'ameer Channel	55
3.7	Points of sensitivity analysis, calibration and simulation in Tubli Bay	58
3.8	Comparison of water surface elevations at Point NT as produced by this work and CAG EIA study	61
3.9	Comparison of water surface elevations at Point ST as produced by this work and CAG EIA study	63
3.10	Comparison of water surface elevations at Point NC as produced by this work and CAG EIA study	65
3.11	Comparison of water surface elevations measured and calculated at Point NT	67
3.12	Comparison of speed measured and calculated at Point NT	68
3.13	Water surface profile points and discharge cross-sections	70
3.14	Current speeds at spring tide in the North Bridge section in the existing situation and with the proposed solution.	72
3.15	Current speeds at spring tide in the South Bridge section in the existing situation and with the proposed solution	72
3.16	Water surface profile of flood and ebb along the points indicated in Figure 3.13	73

3.17	High tide level in Tubli Bay over the 14-day cycle for various south bridge openings	79
3.18	Low tide level in Tubli Bay over the 14-day cycle for various south bridge openings	79
3.19	High tide level in Tubli Bay over the 14-day cycle for deepening south of the bay to Ma'ameer Tide Channel	80
3.20	Low tide level in Tubli Bay over the 14-day cycle for deepening south of the Bay to Ma'ameer Channel	80
3.21	Location of cairns in the Tubli Bay	83
3.22	Discharge at various cross-sections in Tubli Bay for various scenarios	85
3.23	Contaminant initial concentration distribution in the Bay	88
3.24	Contaminant concentration distribution in the Bay at the maximum flow	89
3.25	Initial concentration at three spots in the Bay	90
3.26	Concentration of three spots contaminant at the maximum flow	91

DEFINITION OF TERMS IN THE THESIS

Advection: The rate of change of an atmospheric property caused by the horizontal movement of air.

Celerity Rate that is rapid. Rapidity of motion; quickness; swiftness.

Ecosystem: An area that contains organisms (e.g., plants, animals, bacteria) interacting with one another and their non-living environment. Ecosystems can be of any size (e.g., forest, meadow, and log).

Eutriphication: A process by which an excess of plant nutrients such as nitrogen and phosphorous reduces the oxygen dissolved within a body of water, producing an environment that dose not readily support aquatic life.

Hydrodynamics It is water motion that applied to study a fluid dynamics of liquids, such as water, alcohol, oil, and blood.

Hydraulics The term is applied commonly to the study of the mechanical properties of water, other liquids, and even gases when the effects of compressibility are small

Mangroves: Mangrove plants occupy shallow water and intertidal zones in tropical and subtropical coastal regions, usually where protected from direct wave action, and thus characterized by muddy or fine sediment substrata.

Nutrient: Nutriens Any substance that can be metabolized by an organism to give energy and build tissue

Photosynthesis The process a plant uses to combine sunlight, water, and carbon dioxide to produce oxygen and sugar (energy).

Sustainable Development: Development that meets the needs of the present without compromising the ability of future generations to meet their own needs.

Tidal Prism: The change in the volume of water covering an area, such as a wetland, between a low tide and the subsequent high tide.

Total volume of water flow into in and out during each tidal cycle.

CHAPTER ONE

INTRODUCTION

1.1 INTRODUCTION

The Kingdom of Bahrain is an archipelago of 33 islands, located between the Qatar peninsula and the coast of Saudi Arabia between latitude 25 degrees 32' and 26 degrees 20' North and longitude 50 degrees 20' and 50 degrees 51' East. Taking its name from the largest of these islands (the Arabic word for two seas), the kingdom lies in the warm, shallow waters of the Arabian Gulf (Figure 1.1). Bahrain shares no land borders, but despite its small land area it has 161 km of coastline. The islands' soil is composed of limestone and saline sand, which is particularly noticeable on the southern side of the main island, an area characterized by desert. As the Kingdom is located in an arid region, the climate of Bahrain is characterized by high summer temperature, scanty and irregular rainfall, and high rate of evaporation, high relative humidity and persistent winds from the northwest. There are significant seasonal variations in the average monthly temperature. The hottest months are July and August with average temperatures reaching 43°C while December, January and February are the coldest months with an average of about 17°C. The mean daily maximum humidity is about 85% throughout the year while the mean daily minimum drops to about 40% in May and June. In fact rainfall is concentrated during the period of November to May, being more pronounced in January. June and August have no recorded rainfall, while July and September have only a trace. The monthly rainfall values in Bahrain exhibit a large degree of variability with a mean annual value of about 72 mm.

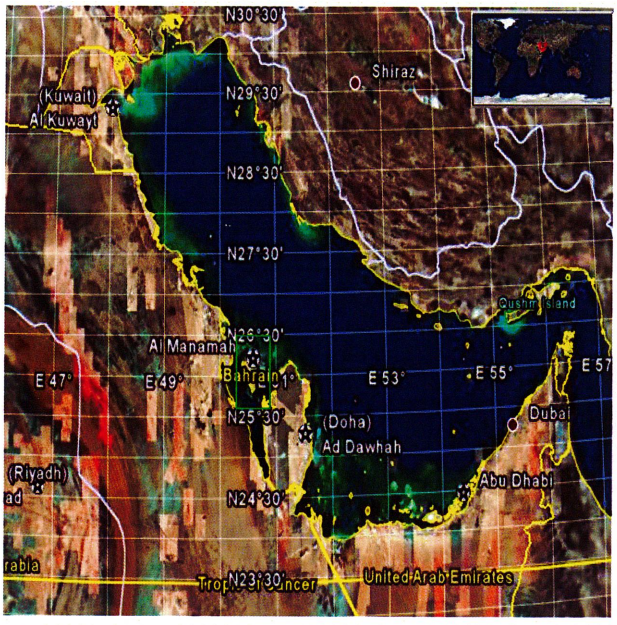


Figure 1.1: Satellite Image of Arabian Gulf (Google Earth)

To the north of the main island a wide fertile strip of land hosts the small and limited agricultural sector. This area is also where the majority of the population lives, in and around the capital city of Manama. The main island is linked to both Saudi Arabia and many of the smaller islands by causeways. Constructed in 1929, the oldest of these links Bahrain to Muharraq, the second-largest island and site of Bahrain's second most populous city, as well as the international airport. Another causeway to the island of Umm Al-Nasan carries on to the Saudi mainland town of al-Khubar.

The Kingdom is a small island with limited natural resources, high population growth rate (1.56% as of 2004 year – CIA World Factbook) and restricted space. The Country's fragile resources are under immense threat mainly due to high population growth, urban and tourism accelerated expansion and rapid industrialization. The waste generation from domestic, industrial and healthcare facilities and their uncontrolled and inappropriate disposa and pollution are causing major threat to the country's ecosystem creating adverse impacts on public health, land, water and air.

1.2 TUBLI BAY NATURAL SETTING

1.2.1 Bay Geography

Tubli bay is an inshore coastal bay located in 2611'N, 5034'E; at the northeast corner of the main island of Bahrain, almost surrounded by the capital city Manama (Figure 1.2). The bay covered an area of 12.56 km^2 (2,500 ha) as of 2002 (the Bay has been under threat from human activity). Infilling the coast for development has caused the size of the Bay to decrease from 23.5 square km in 1956 to 16.1 square km in 1996 (Environmental Affairs, 1996). It is a shallow, sheltered bay in an urban/industrial area, with salt marsh vegetation, extensive mudflats (mainly on the east side) and a large area of mangrove of *Avicennia* type (the last remaining area in the country) in the south-west corner of the bay at Ras Sanad. Tidal amplitude is up to 2.5 m and salinity exceeds 40 ppt.

The bay is characterized by large areas of intertidal mudflats and the last remaining stand of mangroves in Bahrain. It represents an important nursery area for fishes and prawns as well as

essential site for thousands of wintering and passage waders and waterfowl (Al-Sayed, 1995). In the past few years the bay was surrounded by plantation areas and fresh water springs and small streams. This feature gave it more ecological value as other category of birds present in the adjacent plantation area. Therefore, with respect to birds the bay still represents the most important site in the country migrating and wintering coastal water birds. Few bird species breed among mangrove trees like Black-winged Stilt, Moorhen. Since 1988, the mangrove area at Ras Sanad has been declared a Protected area and affiliated to the Environmental Affairs. Until present, land filling and reclamation are the critical problem. Vast area of inter tidal area has been lost in the last two decades. More conservation measures are needed to protect such important area.

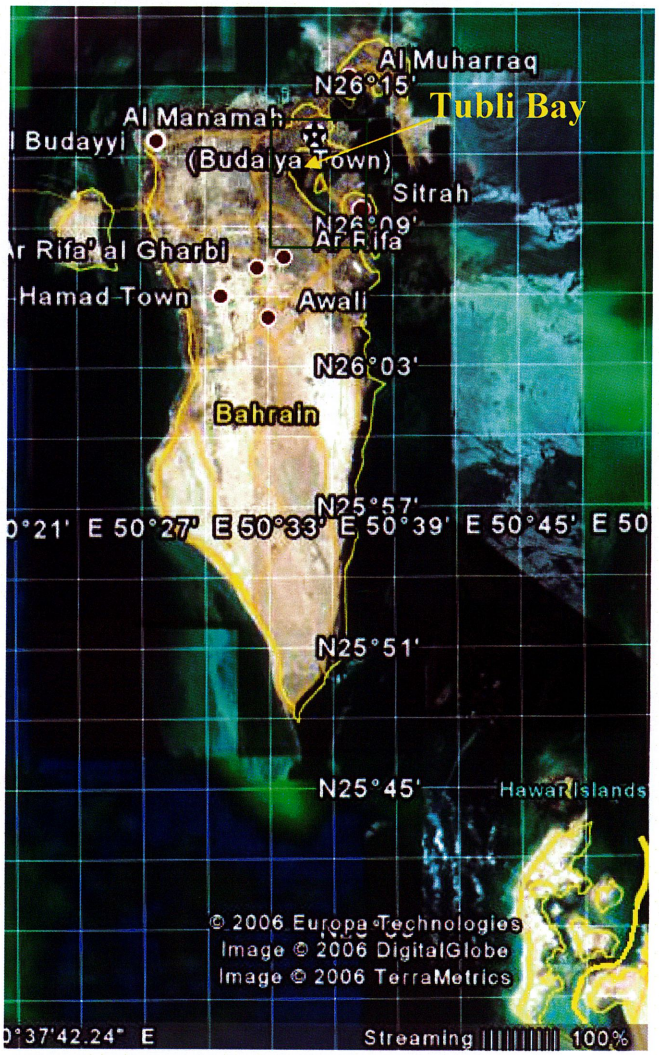


Figure 1.2: Satellite Image of Bahrain Island indicating Tubli Bay at the eastern side (Google Earth)

At the northern tip of the bay lies the major domestic wastewater treatment plant in Bahrain, Tubli Water Pollution Control Center (TWPCC). It discharges at present about 125,000 m^3d^{-1} of tertiary treated sewage effluent. Artesian fisheries were well-known practice in the bay and they were considered one of the most important recruitment areas for shrimps (*Penueaus simisulcatus*) (Al-Sayed, 1995).

However, population growth and developmental activities make the Bay vulnerable to environmental deterioration. The two main threats to it arise from land reclamation or sea infilling and wastewater discharges in general. Sources of wastewater are from sand-wash, industries and agricultural lands surrounding Tubli wastewater treatment plant. Brackish drainage water from the Adhari spring and adjacent agricultural farms collectively adds nutrients, such as nitrates and phosphates that are essential for the production of eutriphication. Long-term exposure of the bay to these effluents causes profound changes in the bay environment.

1.2.2 Climate and Wind

Bahrain has two seasons: an extremely hot summer and a relatively mild winter. During the summer months, from June to August, afternoon temperatures average 40° C and can reach 48° C during June and July. The combination of intense heat and high humidity makes this season uncomfortable. In addition, a hot, dry southeast wind, known locally as the **qaws**, periodically blows sand storms across the barren southern end of Bahrain toward Manama in the summer. The temperatures are moderate in the winter months, from November to March, when the range is between 10°C and 20°C. However, humidity often rises above 90 percent in the winter. From December to March, prevailing winds from the northwest, known as the **shammal**, bring damp air over the islands. Regardless of the season, daily temperatures are fairly uniform throughout the archipelago. Due to the small size of the country the climate is uniform everywhere. The wind direction is predominantly northwest winds known locally as **Al-Barah**.

1.2.3 Habitats and Species

Tubli Bay is characterized by its unique ecology. It is one of the only sheltered, low-energy areas in Bahrain and rich ecologically. It supports an important coastal habitat. The main plant species that Tubli Bay is mostly recognised for are "the mangrove trees". The Bay (and closely surrounding areas) is the only place in Bahrain where these ecologically important species still exist. Only one type of mangrove species exists, it is known as the Black Mangrove; *Avicennia marina.*

The Mangrove stand, protected by the Public Commission for the Protection of Marine Resources, Environment and wildlife of Bahrain, is situated at Ras Sanad in the southwestern part of the Bay. This particular mangrove stand, estimated to be 430,000 square meters in area, was designated as a nature reserve in 1988. Originally, mangroves were also to be found in many other areas of the Island.

The protected mangrove reserve at Ras Sanad has a tree density of 100%. The highest mangrove tree was approximately 3.5m tall. The average tree height recorded was approximately 2.3m tall.

Another important habitat dominating the Bay is the "seagrass ecosystem". The most common seagrass species in Tubli Bay is *Halodule uninervis.* This species of seagrass is a pioneer species and is tolerant of a wide range of environmental factors (temperature extremes for example). The mudflats are also very important components of Tubli Bay where they provide a habitat for many species that constitute a food source (e.g. snails and worms) for a large number of migrating birds in the area.

In the past the bay was a popular area for recreational purposes, due to its beauties and uniqueness. People of Bahrain spent the weekends along the bay shoreline for relaxation and enjoyment. The above information were obtained from (Halal, 1996).

1.2.4 Physical Features of Gulf Region

On the whole, there is little stratification of the water within the ROPME region (Regional Organization for the Protection of the Marine Environment), as the entire water column is well mixed due to strong winds. However, in the central part of the region during the summer months, temperature stratification may develop. There is a well-defined seasonal pattern in the sea surface temperatures. The widest temperature range occurs in the northwestern part of the area (15-35°C). The water circulation in the inner part of the region is driven by density gradients. Water of normal oceanic salinity enters through the Strait of Hormuz at the surface and through a compensatory out flowing current of high salinity water along the bottom. The general circulation pattern is counter clockwise. There is a water movement northwards along the Iranian coast and a corresponding one southward along the Arabian coast.

Due to the high rate of evaporation in the area, the salinity increase gradually from southern to northern parts of the region, with lower salinity along the Iranian side (e.g. in summer the surface salinity is 37°/$_{oo}$ (Electrical Conductivity of the extract off the Omani coast). Salinities as high as 70°/$_{oo}$ have been reported in the Gulf of Salwah. In the winter, the salinities are higher than the summer due to freshwater influx through the Shatt al'Arab and to evaporation. The strong tidal current of the area flushes out the waters, completely renewing its total volume every three years. Throughout most of the region dissolved oxygen is near saturation in surface waters. The above information were obtained from (UNEP, 1999).

1.2.5 Bathymetry and Bottom Sediments Nature

The composition of the sediment and the thickness of the oxidised surface layer are highly variable in Tubli Bay. The state of the sediment may be interpreted as an integrated measure of the water depth (bathymetry), accumulation of organic matter, oxygen concentration in bottom water and the water renewal by tidal currents.

Tubli Bay is a natural shallow and protected bay. The bathymetry of the Bay west of the Causeway is characterised by two deeper basins north and south of Nabih Saleh, intertidal

areas along the western and northern shores and large shallow mostly subtidal areas in the south of the Bay.

Extensive dredging in the northern basin has increased the water depth to more than 8 m in large areas. The water depth in the southern basin is mostly between 2 to 6 m. The water depth is below 2 m in the rest of the Bay.

The southern part of the Bay and the channel south of the culverts under Majlis Al Tawoon Highway is very shallow. The water depth and sediment in these areas is probably affected by discharges of silt from the surrounding sand washing plants.

Tubli Bay east of the Causeway is characterised by a fairly complex bathymetry, which includes sandy and rocky shallows intersected by natural tidal channels and narrow possibly partly dredged channels close to the present shorelines.

The sediment in Tubli Bay includes black mud, oxidised sand and hard bottom of shell gravel and caprock. The smell of the sediment and the colour and thickness of the surface sediment is indicative of the organic load and oxygen demand of the sediment and the rate of renewal of the bottom water.

Soft sediments of mud and fine sand predominate in the basins north and south of Nabih Salah and in the transition area between Tubli Bay and Khawr al Qulay'ah east of the Causeway. The mud sediments are mostly black, often with a strong smell of hydrogen sulphide (H_2S) and a thin brown oxidised surface layer.

1.3 THE BAY SITUATION

1.3.1 Tubli Bay importance

The whole of Tubli Bay is important. Its importance lies in its ecology and the interaction of its many elements. The seagrass ecosystem in the Bay and the mangroves at Ras Sanad are

closely linked by interactive processes. They have biological and physical functions which co-occur, these being intimately connected in successional sequences.

The seagrass bed acts as a hydrodynamic barrier that creates a low-energy zone favorable to mangroves. It also traps and stabilizes sediments, thus helping to prevent blocking of mangrove air roots. Mangroves, for their part, bind sediments that could smother seagrass. Mangroves and seagrass ecosystems produce nutrients which facilitate the optimum development of each system. This export of nutrients leads to a turnover of biomass and efficient carbon cycling, benefiting all elements of the Bay's ecosystem. Both ecosystems are connected through the movement of avifauna, which feed on seagrass beds and possibly carry nutrients back to the system by defecating in the mangroves. Both are sources of primary productivity and detritus production.

Seagrass provides substantial support grounds for marine organisms which use them, and the mangroves, during several stages in their lives, for resting, feeding or reproduction.

The mudflats provide a habitat for bivalves and worms, and therefore a feeding ground for shrimp, crab, over-wintering waders and shorebirds as well as a substrate for nitrogen-fixing blue C*yanobacteria* and a storage unit for important dissolved substances.

These interactive processes play a critical, positive role in improving and maintaining the quality of the marine environment.

From the above, it is clear that the Bay should be treated as an ecological whole, each part being equally important for the efficient functioning of that whole. It is also important economically, because it is a nursery and feeding ground for commercial fisheries. These fisheries are socially important to the people of Bahrain, especially those who rely on them for their livelihood. Tubli Bay, however, has a value in itself regardless of its usefulness to people, as it provides a habitat and feeding ground for birds, fish, shrimp, crabs, reptiles and many other smaller organisms.

Protecting Tubli Bay from any further destruction is a necessity, for the reason that this area is very unique ecologically to Bahrain. The best management option to adopt would be the

sustainable development of Tubli Bay. Sustainable development would integrate ecological, social and economic sustainability. It aims to the best environmental, economic and social options. In this option, as the destructive activities on the Bay would be stopped and measures taken to reduce the effect of others, most of the adverse impacts on the Bay would be eliminated. Habitats would no longer be destroyed by infilling and accumulation of driftwood and rubbish in the mangrove pocket area would no longer be a problem.

Long-term ecological benefits could be gained by the adoption of this option. The interference to Tubli Bay would be minimal, photosynthesis and the dispersion of pollutants by the mangroves would be more efficient, and gradual recovery would take place. As a result, inshore and coastal fisheries can thrive. The above information were obtained from (Halal, 1996).

1.3.2 Pressures/ Stresses on the Bay

The marine environment of Tubli Bay is extremely stressed due to sewage discharges, land reclamation, silt discharge from sand washing, low tidal flow velocities and reduced flushing of the bay caused by the Sitra Causeway, as well as the reduction of tidal exchange to the south through the Ma'ameer Channel .

The Tubli Water Pollution Control Center (WPCC) is the main sewage treatment plant for the country and receives sewage from Muharraq, Central and Greater Manama, Isa Town and Hamad Town and Budaiya-Bani Jamrah. Future expansion is planned to include Dumistan and the western villages by connecting them to the Hamad Town sewer system. Tubli plant was commissioned in 1982 to treat 54,400m^3/day. The extension of this plant had led to an increase in the capacity to reach 124,000m^3/day of sewage per day. In 1999, the plant had further expanded and increased its design capacity to 200,000m^3/day. The plant is now receiving 170,000m^3 every day. It is planed to stop pumping the effluent in the bay by end of year 2005. Unfortunately, it is still pumping 60,000m^3/day of the effluent in the bay and but it will be stopped by end of 2006 and all of the effluent will be used for irrigation. (Al Aradi, 2006) (Personal Communication).

In addition to Tubli Sewage Treatment, Nuwidrat Sewage also flushes directly to the intertidal zone of Tubli Bay. Bad odor especially at low tide and pathogenic bacteria, microbes and parasites always exist in the bay with their reversible effects. High organic content will increase bacteria and therefore the dissolved oxygen will be depleted and this will limit the number of living organisms.

Tubli Bay received large quantities of fine silt from Abdulla Nass factory. This fine silt suspended at the water column and effected photosynthesis and eventually reduced water productivity. As Tubli Bay is characterized by its low wave energy, suspended fine silt formed thick layer of mud on the shore and therefore changed the nature of the intertidal flat and this may affect species diversity (Kareema, 2003).

Tubli Bay is characterized by its salt tolerant shrubs known as mangroves (A*vicennia marina*). Mangroves are evergreen halophytic plants growing in the intertidal zone in marine or estuarine tropical areas. The black mangrove (*Avicennia marina*) is the only species adapted to the extreme environmental conditions in the Gulf. Mangroves are found along the coasts of Tubli bay and Arad. The term mangrove refers to both the forest and the tree types, they can tolerate having their roots submerged in salt water. Their prop roots provide a surface of attachment for marine organisms in a muddy environment where hard surfaces are in short supply. Mangroves also trap and bind sediments and filter land based nutrients, promoting water clarity. Mangroves, like seagrasses, serve as nursery grounds for the juveniles of many commercially important fisheries species, while also providing habitat for a variety of small fishes, crabs and birds. It is breeding, spawning, nursery and feeding habitats for a diverse fauna of invertebrates and for a number of important fish, shrimp, crabs and other marine organisms. It provides shelter, nesting and feeding opportunities for birds. They also protect coasts against erosion by breaking storm waves and dampening tidal currents. They protect coasts against erosion by breaking storm waves and dampening tidal currents (Abdulqader, 1994).

Tubli Bay and shallow areas south of Fasht Al-Adhom are known for their importance to Bahrain penaeid shrimps. The role of these shallow waters in the Bahrain penaeid shrimps life cycle was studied by Abdulqader (1994) in Tubli Bay. Tubli Bay is an important nursery

ground for both *P. semisulcatus* and *M. stebbingi*. However, this bay does not support the entire stock of *P. semisulcatus*. Post-spawning return migration to shallow waters is noted for *P. Semisulcatus*. Tubli Bay is of minor importance as a nursery ground for both *P. Latisulcatus* and *M. Kutchensis*. Other penaeid species found in Bahrain water are not dependent on Tubli Bay during their life Cycles. High abundance of all stages of the different penaeid species found in the Tubli Bay were found to coincide with seasonal rise of sea water temperature (Abdulqader, 1994).

Reclamation will increase the turbidity of the water column of the intertidal area, which therefore destruct and damage the whole system which has been mentioned earlier in this section. Reclamation materials include sand, steel, wood, stones, domestic waste and others. Those materials create pollution to the marine organisms. For example, accumulation of fine silt creates a thick layer of mud. Dissolved oxygen is low in the muddy shore which will lead to limit species diversity.

1.3.3 Bay Degradation

Population growth and developmental activities make the Bay vulnerable to environmental deterioration. The two main threats to this bay arise from reclamation and wastewater dumping, such as sand-wash wastewater, industrial wastewater, agricultural wastewater and municipal wastewater. Wastewater outfall from Tubli municipal sewage treatment plant discharges tertiary treated fresh water at a rate of 125,000 m^2/day at the northern end of the Bay. Brackish water drainage from the Adhari spring and adjacent agricultural farm collectively add more nutrients such as nitrates and phosphates that are essential for algal eutriphication.

1.3.4 Policies and Legislation

1.3.4.1 Decision Making Legislation and Regulation

Based on the laws, rules and agenda 21 discussed on the international level, the present study concentrates on improving the current situation of the bay. Taking the privilege of the

construction job that will be carried on the Sitra Bridge. Below all the degrees and convention to protect the marine environment was discussed in the section.

Ministerial Order No. 1 1998 lays down regulations for environmental assessments of projects including specifically public utilities, construction operations accompanied by dredging of bedrock or soil, or reclamation of seashores, bays and lowlands. According to this order all new projects to be under taken and existing projects to be developed must fill in an Environmental Impacts Assessment Information Form. The Directorate of Environment shall, in the light of the information and in accordance with the rules and regulations herein, determine the extent and the need for submitting a full environmental impact assessment report. The Director General of Environmental Affairs is the authority to sign the licenses (to approve the project) provided for in Decree Law No. 21 1996.

Ministerial Order No. 10 of 1999 with respect to environmental standards lays down quality criteria for air and water discharge from industry. This regulation will apply for temporary installations on the construction site.

Table 1.1: List of legislations relating to protection of the environment issued as Ministerial orders

Year	Subject
1981	To control fishing
1984	To protect date palm trees
1986	To protect dugong
1986	To control gill nets and shrimp nets
1986	To limit trawling to areas greater than 20m depth
1986	To prohibit use of drift nets
1989	To control the use of pesticides
1995	Protection of Tubli Bay (Mangrove protected area)

1.4 OBJECTIVE OF THE STUDY

New plans are currently underway to construct a new wider bridge in place of the old Sitra Bridge. The new bridge should be designed and constructed while allowing for adequate water circulation in the bay. The main objective of this work is to consider the effect of several north and south bridge opening scenarios on the water circulation in the bay and hence on its environmental conditions. The effects of Ma'meer channel on the bay conditions were also investigated. The well known hydrodynamic software simulation package, namely Mike 21, was used for this study.

CHAPTER TWO

MIKE 21 MODEL

2.1 GENERAL DESCRIPTION OF MIKE 21

MIKE 21 is a professional software package containing a comprehensive modeling system for 2D free-surface flows as will be mentioned below.

MIKE 21 Flow Model can be used to simulate a wide range of hydraulic and related items, including:

- Tidal exchange and currents
- Storm surges
- Heat and recirculation
- Water quality

The material used below in this chapter is a summary obtained from MIKE 21 manuals (MIKE 21, 2003).

2.2 MODEL APPLICATION

Danish Hydraulic Institute's (DHI) numerical model MIKE 21, Version 2003 is used. It consists of a basic Hydraulic module 'MIKE 21 HD' that simulates the hydrodynamics of phenomenon in lakes, estuaries, bays, coastal areas and seas where stratification can be neglected. Four other modules are coupled with MIKE 21 HD to simulate phenomenon like Advection-Dispersion (MIKE 21 AD), Water quality (MIKE 21 WQ), Eutriphication (MIKE 21 EU) and Heavy metals (MIKE 21 ME). The following gives a brief description of each of the above mentioned modules.

- ***MIKE 21 HD: HYDRODYNAMIC MODULE***

The hydrodynamic module in MIKE 21 Flow model (MIKE 21 HD) is a general numerical modeling system for the simulation for the water level and flow in estuaries, bays and coastal area. It simulates unsteady two-dimensional flows in one layer (vertical homogonous) and has been applied in a large number of studies.

- ***MIKE 21 AD: ADVECTION DISPERSION MODULE***

The advection dispersion module of MIKE 21 simulates the spreading of a dissolved or suspended substance in an aquatic environment under the influence of the fluid transport and associated natural dispersion process. The substance may be a pollutant, which may be treated as conservative or subject to linear decay: salt, heat and dissolved/suspended contaminants.

Similarly to the HD module, the concentration of the substance is calculated in each point of a rectangular grid covering the area of interest.

The HD module provides information on the transport, (i.e. currents and water depths) in each grid point. Other data required include substance concentrations and discharge quantities at outfalls, together with concentrations at the boundaries.

The system solves the equation of conservation of mass for a dissolved or suspended substance using a two dimensional form of the QUICKEST finite difference scheme.

- ***MIKE 21 WQ: WATER QUALITY MODULE***

The water quality module of MIKE 21 is used to assess the environmental problems related to domestic and industrial pollution sources, riverine inputs and agricultural run off in coastal areas.

The model simulates the resulting concentrations of bacteria threatening bathing water quality, oxygen depletion due to the release of BOD, excess concentrations of nutrients (ammonia and phosphate) and chemical substances. The included processes influencing these concentrations are functions of the environmental conditions (e.g. light intensity, water temperature and salinity).

The WQ Module is integrated with the AD Module, which describes the physical transport processes in each grid point of the model. The process equations are solved using a rational extrapolation method in an integrated two step procedure with the AD Module.

2.3 FLOW, SEDIMENT AND CONTAMINANT TRANSPORT PROCESSES

2.3.1 Flow/ Hydrodynamic Governing Equations

The hydrodynamic module in the MIKE 21 Flow Model (MIKE 21 HD) is a general numerical modelling system for the simulation of water levels and flows in estuaries, bays and coastal areas. It simulates unsteady two dimensional flows in one layer (vertically homogeneous) fluids and has been applied in a large number of studies.

The following equations, the conservation of mass and momentum integrated over the vertical, describe the flow and water level variations:

$$\frac{\partial \zeta}{\partial t}+\frac{\partial p}{\partial x}+\frac{\partial q}{\partial y}=\frac{\partial d}{\partial t} \tag{2.1}$$

$$\frac{\partial p}{\partial t}+\frac{\partial}{\partial x}\left(\frac{p^2}{h}\right)+\frac{\partial}{\partial y}\left(\frac{pq}{h}\right)+gh\frac{\partial \zeta}{\partial x}+\frac{gp\sqrt{p^2+q^2}}{C^2.h^2}-\frac{1}{\rho_w}\left[\frac{\partial}{\partial x}(h\tau_{xx})+\frac{\partial}{\partial y}(h\tau_{xy})\right]-\Omega q$$

$$-fVV_x+\frac{h}{\rho_w}\frac{\partial}{\partial x}(p_a)=0 \tag{2.2}$$

$$\frac{\partial q}{\partial t}+\frac{\partial}{\partial y}\left(\frac{q^2}{h}\right)+\frac{\partial}{\partial x}\left(\frac{pq}{h}\right)+gh\frac{\partial \zeta}{\partial y}+\frac{gq\sqrt{p^2+q^2}}{C^2.h^2}-\frac{1}{\rho_w}\left[\frac{\partial}{\partial y}(h\tau_{yy})+\frac{\partial}{\partial x}(h\tau_{xy})\right]+\Omega p$$

$$-fVV_y+\frac{h}{\rho_w}\frac{\partial}{\partial y}(p_a)=0 \tag{2.3}$$

Where,

h(x,y,t)	- water depth (= ζ-d, m)
d(x,y,t)	- time varying water depth (m)
ζ(X,Y,t)	- surface elevation (m)
p,q (x,y,t)	- flux densities in x and y directions (m^3/ s/ m) = (uh,vh); (u,v) = depth averaged velocities in x and y directions
C(X,Y)	- Chezy resistance ($m^{1/2}$/s)

G	- acceleration due to gravity (m/s^2)
f(V)	- wind friction factor
V,Vx,Vy (X,Y,t)	- wind speed and components in x and y direction (m/s)
Ω (x,y)	- Coriolis parameter, latitude dependent (s^{-1})
P_a (x,y,t)	- atmospheric pressure ($kg/m/s^2$)
ρ_w	- density of water (kg/m^3)
x,y	- space coordinates (m)
t	- time (s)
$\tau_{xx},\tau_{xy},\tau_{yy}$	- components of effective shear stress

2.3.2 Flow/ Hydrodynamic parameters

2.3.2.1 Bed Resistance

You can chose between two ways of describing the bed resistance in the MIKE 21 Flow Model:
either as a Chezy number or as a Manning number. In both cases the bed resistance used is

$$\frac{g \cdot u \cdot |u|}{C^2} \qquad (2.4)$$

where g is gravity, u is velocity and C is the Chezy number. Manning numbers are converted to Chezy numbers as follows

$$C = M.\ h^{1/6} \qquad (2.5)$$

where M is the Manning number and h is the water depth. The units of Chezy numbers and Manning numbers are respectively $m^{1/2}/s$ and $m^{1/3}/s$.

Specifying the Bed Resistance

A bed resistance number is assigned to each grid point in the model area. You can specify this in MIKE 21 in two ways:

- as one value which is given to all grid points
- as a map similar to that for bathymetry with a resistance value for each grid point

Recommended values

If the relative variation of the water depth is considerable you should specify Manning numbers. Values in the range 20 - 40 $m^{1/3}/s$ are normally used with a suggested value of 32 $m^{1/3}/s$ if no other information is available. In an estuary with tidal channels you can use a value of 25 $m^{1/3}/s$.

If you apply Chezy numbers, a model calibration can normally be achieved with values in the range 30 - 50 $m^{1/2}/s$.

Because of the definition of the resistance numbers the following apply:

- Using a smaller resistance number increases the bed resistance,
- Using a greater resistance number decreases the bed resistance.

Remarks and Hints

If the boundary conditions at one of your boundaries are inaccurate and you therefore have stability problems (blow ups) at this boundary, you can specify a small band (2 to 4 grid lines) with a very high resistance. Manning numbers in the range 5 - 10 $m^{1/3}/s$ have been applied successfully. However, this method should only be used if it is impossible to improve the boundary conditions. Furthermore, the simulation results in the area around the small resistance numbers should be used with caution.

When carrying out a tidal calibration you can use the bed resistance to increase or decrease the tidal amplitude. The tidal phase is adjusted by changing the water depth. When the depths have been read from a sea chart, increasing the depth is all the more justifiable as these charts often give the minimum depths, which are more important to shipping than the maximum depths.

Because $h^{1/6}$ is calculated for each grid point and at each time step when the Manning formulation is selected rather than the Chezy formulation, the computational time is increased.

2.3.2.2 Courant Number

The Courant number is defined as follows:

$$C_R = c\frac{\Delta t}{\Delta x} \tag{2.6}$$

where c is the celerity, Δt the time step and Δx the grid spacing. For a tidal wave the celerity is

$$c = \sqrt{gh} \tag{2.7}$$

where g is gravity and h is the water depth.

As the information (about water levels and fluxes) in the computational grid travels at a speed corresponding to the celerity, the Courant number actually expresses how many grid points the information moves in one Lime step.

Recommended value

Normally you can have a maximum Courant number in your model of up to 5. The maximum value which you can use without having stability problems does, however, depend on your bathymetry:

- If you are modeling an estuary with tidal channels you should adhere to the rules given under Bathymetry. Alternatively you can use a maximum Courant number of 1, in which case you should have no problems in resolving the flow in the channels.
- The MIKE 21 Flow Model is designed for Courant numbers up to about 20. You should, however, only allow these very high numbers in areas where the bathymetry is very smooth.

2.3.2.3 Eddy Viscosity

The effective shear stresses in the momentum equations contain momentum fluxes due to turbulence, vertical integration and subgrid scale fluctuations. The terms are included using an eddy viscosity formulation to provide damping of short wave length oscillations and to represent subgrid scale effects.

The formulation of the eddy viscosity in the equations has been implemented in two ways:

- Flux based formulation

$$\frac{\partial}{\partial x}\left\{E\frac{\partial P}{\partial x}\right\}+\frac{\partial}{\partial y}\left\{E\frac{\partial P}{\partial y}\right\} \text{ (x – momentum)} \qquad (2.8)$$

where P is the flux in the x-direction and E is the eddy viscosity coefficient.

- Velocity based formulation

$$\frac{\partial}{\partial x}\left\{h\cdot E\frac{\partial u}{\partial x}\right\}+\frac{\partial}{\partial y}\left\{h\cdot E\frac{\partial u}{\partial y}\right\} \qquad (2.9)$$

where u is the velocity in the x-direction and h the water depth.

Strictly speaking the first formulation is only correct at a constant depth and should be applied with great care in order to avoid falsification of the flow pattern.

The velocity based formulation, which is more correct, is unfortunately also more difficult to implement in the numerical algorithm. This is because the system uses the fluxes as the unknown parameters and not the velocities. Therefore the velocity based formulation is implemented by using the velocities from the previous time step. This can, however, lead to stability problems when the eddy viscosity coefficient E becomes large. The coefficient must fulfil the criterion:

$$\frac{E\cdot\Delta t}{\Delta x^2}\leq\frac{1}{2} \qquad (2.10)$$

Specifying the Eddy Viscosity

The eddy viscosity coefficient E can be specified in three different ways:

- As a constant value for the entire computational domain
- From a type 2 data file giving the value at each grid point
- A time-varying function of the local gradients in the velocity field. This formulation is based on the so-called Smagorinsky concept, which yields:

$$E = C_s{}^2\Delta^2\left[\left(\frac{\partial U}{\partial x}\right)^2\right]+\frac{1}{2}\left(\frac{\partial U}{\partial y}+\frac{\partial V}{\partial x}\right)^2+\left(\frac{\partial V}{\partial y}\right)^2 \qquad (2.11)$$

where U,V are depth averaged velocity components in the x and y direction, A is the grid spacing and C_s is a constant to be chosen in the interval of 0.25 to 1.0.

The Smagorinsky facility is combined with the following formulation of the shear stresses:

$$\frac{\partial}{\partial x}\left(hE\frac{\partial U}{\partial x}\right)+\frac{\partial}{\partial y}\left[\frac{1}{2}hE\left(\frac{\partial U}{\partial y}+\frac{\partial V}{\partial x}\right)\right] \qquad (2.12)$$

If you choose the Smagorinsky formulation you must specify the Smagorinsky factor C_s.

Remarks and Hints

In the same way as for the bed resistance you can use the eddy coefficients to damp out numerical instability (see Bed Resistance). You should only use this as a last resort to your stability problem: the schematisation of the bathymetry and the boundary conditions are the primary causes for a blow up,

When you use the Smagorinsky formulation of the turbulence the CPU time for a simulation is increased.

2.3.3 Environmental Hydraulics

The MIKE 21 AD equation is shown below. The numerical algorithm and solution technique applied in the model is described in a paper. This is followed by a discussion of dispersion coefficients.

MIKE 21 AD solves the so called advection dispersion equation for dissolved or suspended substances in two dimensions. This is in fact the mass conservation equation. Discharge quantities and compound concentrations at source and sink points are included together with a decay rate.

$$\frac{\partial}{\partial t}(hc)+\frac{\partial}{\partial x}(uhc)+\frac{\partial}{\partial x}(vhc)=\frac{\partial}{\partial x}\left[h\cdot D_x\cdot\frac{\partial c}{\partial x}\right]+\frac{\partial}{\partial y}\left[h\cdot D_y\frac{\partial c}{\partial y}\right]-F\cdot h\cdot c+S \qquad (2.13)$$

Where:

c : compound concentration (arbitrary units)

u,v : horizontal velocity components in the x,y directions (m/s)

h : water depth (m)

D_x,D_Y : dispersion coefficients in the x,y directions (m^2/s)

F : linear decay coefficient (sec^{-1})

S :Q_s,(c_s-c)

Q_s : source/sink discharge ($m^3/s/m^2$)

C_s : concentration of compound in the source/sink discharge.

Information on u, v and h at each time step is provided by the hydrodynamic module.

2.4 ADVECTION - DISPERSION MODULE

2.4.1 Dispersion Coefficients

Dispersion is commonly used as a general term to refer to the scattering of fluid particles that depend both on random type processes (diffusion) and on the effect of velocity gradients (shear), as schematised in Table 1. The diffusive processes are never resolved, which led to early attempts two parameters the mass fluxes of solutes due to molecular and turbulent motions, respectively. They assumed that the mass fluxes could be set to be proportional to the concentration gradients, the constants of proportionality being called the molecular and turbulent diffusion coefficients, respectively. This approximation was extended to shear flows, the combined effect of differential advection and diffusion being thus represented by the so called dispersion coefficients. Taylor's analysis was applied to shallow water flows in order to describe the shear effects of the vertical velocity gradients.

The concept of dispersion of mass of any substance in solution or suspension in a flow can be extended to other properties of the flow. Resorting to Backmeteffs principle of momentum transfer, it follows that the velocity fluctuations act as a mechanism of transfer of momentum between adjacent scales of circulation, for example they provide for the dispersion of momentum. The corresponding coefficients are the so called viscosity coefficients.

Table 2.1 List of the transport processes indicated at MIKE 21 Model

MAIN TRANSPORT PROCESSES	
1- ADVECTION Movement of fluid particles due to the resolved flow processes	
2- DISPERSION Scattering of fluid particles due to non- Resolved flow processes	a) SHEAR Spatial velocity gradients b) DIFFUSION - Molecular motion - Turbulent

2.4.2 Dispersion Processes

2.4.2.1 General

The commonly recognised filtering procedures used in the development of the momentum and transport dispersion equations are:

Scale 1

Filter out the random molecular motion	→molecular diffusion →viscosity

Scale 2

Filter out the Turbulent motion	→turbulent diffusion

Below a given scale →eddy-viscosity

Scale 3

Depth averaging to →dispersion

Filter out the →bed & surface shear stresses

vertical velocity

Scale 4

Profile for →horizontal shear stresses

2-D models -shear viscosity

Scale 1, which corresponds to filtering out the random molecular motions, is the basis of Newton's law of viscosity

$$\tau_{zx} = \mu \frac{\partial u}{\partial z} \qquad (2.14)$$

where viscosity μ may be regarded as a measure of the resistance of the flow to deformation imposed by tangential stresses τ, which are generated by the transfer of momentum due to velocity fluctuations normal to the corresponding surface. With respect to the fluctuations due to molecular motions, their effect on the transfer of momentum is independent of the flow conditions, thus the dynamic viscosity μ is a characteristic of the fluid. The corresponding dynamic equilibrium equations are the well known Navier-Stokes equations, where the influence of the non-resolved scales of random molecular motions are accounted for by the following empirical terms (in the x_i direction)

$$\nu\left[\frac{\partial^2 u_i}{\partial x^2}+\frac{\partial^2 u_i}{\partial y^2}+\frac{\partial^2 u_i}{\partial z^2}\right], \quad i= 1,2,3 \qquad (2.15)$$

$\nu = \mu/\rho$ being the Kinematic viscosity (L^2T^{-1}).

The random molecular motions also induce the transfer of mass of any substance dissolved or in suspension in the fluid, which according to Fick's law is given by

$$T_i = D^m \frac{\partial c}{\partial x_i} \tag{2.16}$$

where c represents the concentration of the constituent and D^m the molecular diffusion coefficient. Applying a conservation principle to an arbitrary volume of control, an empirical term similar to 2.15 will appear

$$D^m \left[\frac{\partial^2 c}{\partial x^2} + \frac{\partial^2 c}{\partial y^2} + \frac{\partial^2 c}{\partial z^2} \right] \tag{2.17}$$

2.4.2.2 Turbulence

Although molecular agitation is always present even for fluids at rest, under flow conditions fluid particles experience additional random motions of much higher magnitude, so that their paths are very irregular and sinuous. It is apparent when observing recorded time series of instantaneous velocities u^I, that the flow is characterised by an unsteady fluctuating velocity u' superimposed on a temporal steady mean velocity u, such that

$$u^I(x,t) = u(x,t) + u'(x,t) \tag{2.18}$$

$$\overline{u^I(x,t)} = \frac{1}{\Delta T} \int_{t-\Delta T}^{t} u^I(x,t)dt = u(x,t) \tag{2.19}$$

$$\overline{u^I(x,t)} = \frac{1}{\Delta T} \int_{t-\Delta T}^{t} u'(x,t)dt = 0 \tag{2.20}$$

In these conditions it is possible to filter out the fluctuations under a selected time scale ΔT, by integrating the Navier-Stokes equations over ΔT. As a result the following new terms will be obtained

$$\frac{\partial}{\partial x_j} \left[\partial \overline{u_i' u_j'} \right] \tag{2.21}$$

Similarly for the conservation of property c, the result is,

$$\frac{\partial}{\partial x_j}\left[\overline{\partial u_i' c'}\right] \tag{2.22}$$

In the classical theory of turbulence the terms $-\rho u_i' u_j'$, called Reynold's stresses, are empirically correlated to the resolved scales through a new coefficient v^T , the "eddy viscosity", such that

$$-\rho\overline{u_i' u_j'} = \rho v^T \frac{\partial u_h}{\partial x_j} \tag{2.23}$$

Which makes it possible to write the new terms in the following form

$$\frac{\partial}{\partial x}\left[v^T \frac{\partial u_i}{\partial x}\right] + \frac{\partial}{\partial y}\left[v^T \frac{\partial u_i}{\partial y}\right] + \frac{\partial}{\partial z}\left[v^T \frac{\partial u_i}{\partial z}\right] \tag{2.24}$$

It is apparent that v^T is now dependent on the flow conditions. For the evaluation of v^T several models have been developed, each corresponding to a particular kind of turbulence (e.g. isotropy). One of the formulations adopted by DHI is based on the so called Smagorinsky model of isotropic turbulence, given by

$$v^T = \rho \ell^2 (X_i) (S_{ij} S_{ji})^{1/2} \tag{2.25}$$

where ℓ (x_i) is a characteristic mixing length and S_{ij} the second order strain tensor. It is obvious that considering v^T constant, expression (2.24) reduces to the form of expression (2.15) established for molecular motion (Boussinesq approximation).

In general it is difficult to determine v^T but as a reference, for uniform channel flow it is often assumed to take a value given approximately by

$$v^T \approx \frac{1}{10} h u^* \tag{2.26}$$

where h is the water depth and u* the friction velocity.

Introducing the Reynold's analogy for turbulent flows, that expresses the principle that the transfer processes of dissolved or suspended matter are equivalent to the transfer processes of momentum, and consequently the turbulent diffusion coefficient D^T will be such that $D^T = \nu$, the new dispersive terms of the conversation equation becoming

$$\frac{\partial}{\partial x}\left[D^T \frac{\partial c}{\partial x}\right]+\frac{\partial}{\partial y}\left[D^T \frac{\partial c}{\partial y}\right]+\frac{\partial}{\partial z}\left[D^T \frac{\partial c}{\partial z}\right] \qquad (2.27)$$

2.4.3 Shear Flow

As in many coastal engineering applications the depth is much smaller than the horizontal dimensions of the domain under study, two-dimensional models are usually adequate to describe the main flow processes. Nevertheless the depth integration will imply the filtering of the vertical velocity profiles, which are responsible for additional spreading in the direction of the flow. Flows with velocity gradients are often referred to as "shear flows", and the associated spreading mechanism discussed is currently known as the "shear effect". Hence to account for "shear flows" in a depth integrated model, additional empirical terms have to be included.

The filtering procedure can now be based on the following relationships:

$$u = (U + U') \qquad (2.28)$$

$$\overline{U'} = \frac{1}{h}\int_h^\zeta U' dz = 0 \qquad (2.29)$$

$$\overline{u} = \frac{1}{h}\int_\zeta^h (U + U')dz = U \qquad (2.30)$$

Where U represents the depth-integrated velocity and U' the deviation of the velocity profile from the average U, at general depth z.

Introducing these relationships in the Reynolds equations (Navier-Stokes equations after filtering out turbulence under a time scale AT), it is possible to demonstrate that the convective terms will be given by:

$$\frac{\partial}{\partial x}\int_{-h}^{\zeta} uudz + \frac{\partial}{\partial y}\int_{-h}^{\zeta} vudz = \frac{\partial}{\partial x}(hUU) + \frac{\partial}{\partial y}(hVU) \frac{\partial}{\partial x}\int_{-h}^{\zeta} (u')^2 dz + \frac{\partial}{\partial y}\int_{-h}^{\zeta} (u'v')^2 dz \qquad (2.31)$$

The last two terms represent the overall transfer of momentum over the depth due to the shear effect, and in an assumption similar to that applied to the turbulent transfer of momentum, it is common to accept the following correlations with the resolved dependent variables (depth-integrated):

$$\frac{1}{h}\int_{-h}^{\zeta} (U')^2 dz = -v_x^s \frac{\partial U}{\partial x} \qquad (2.32)$$

and

$$\frac{1}{h}\int_{-h}^{\zeta} (U'V) dz = -v_y^s \frac{\partial U}{\partial y} \qquad (2.33)$$

The above assumptions and the Reynolds analogy make it possible to finally write the new terms for the conservation of momentum and constituents in the following form

$$\frac{\partial}{\partial x}\left[v_i^s h \frac{\partial U_i}{\partial x}\right] + \frac{\partial}{\partial y}\left[v_i^s h \frac{\partial U_i}{\partial y}\right] + \frac{\partial}{\partial z}\left[v_i^s h \frac{\partial U_i}{\partial z}\right] \qquad (2.34)$$

and

$$\frac{\partial}{\partial x}\left[D_i^s h \frac{\partial U_i}{\partial x}\right] + \frac{\partial}{\partial y}\left[D_i^s h \frac{\partial U_i}{\partial y}\right] + \frac{\partial}{\partial z}\left[D_i^s h \frac{\partial U_i}{\partial z}\right] \qquad (2.35)$$

where $v_i^s = D_i^s$, with v_i^s and D_i^s representing the horizontal shear stresses and dispersion in depth- integrated shear flows (in the x_i direction). The coefficient v_i^s will be called hereafter the "shear viscosity".

In the case of uniform channel flow, the shear viscosity can be estimated by:

$$v_i^s = D_i^s = \frac{\alpha - (\alpha')^2}{2} C_z U h \tag{2.36}$$

with

$$\alpha = \frac{\int_{-h}^{\zeta} u^3 dz}{U^3 h} \tag{2.37}$$

and

$$\alpha' = \frac{\int_{-h}^{\zeta} u^2 dz}{U^2 h} \tag{2.38}$$

where C_z is the non-dimensional Chezy number, U the depth-averaged velocity (m/s) and h the water depth (m).

For example, considering a 10 meter deep channel with a depth-averaged velocity of 1 m/s and a non-dimensional Chezy number of 18, the shear viscosity coefficient that corresponds to an exponential velocity distribution along the vertical given by $KZ^{0.2}$ is $v^s = 4$ m^2/s.

As expected, these results suggest that the intensity of transfer of momentum and constituents is related to the magnitude of the scale considered, the molecular and turbulent effects being in practice negligible in comparison to the shear effect (10^{-6} to 10^{-1} m^2 /s against 4 m^2/s).

2.4.4 Subgrid Scale Processes

At this point it is convenient to emphasise that the concepts of viscosity and diffusion have been brought about by the need to take into account non resolved motions of the fluid particles, i.e. diffusion and dispersion are the result of advective processes associated with non resolved scales. This concept is the one that really matters when the filtering procedures are further extended to higher scales, as a consequence of the need for horizontal spatial discretization of the depth integrated equations. It implies that additional dispersion and viscosity will be required to account for higher order non resolved scales of motion, which magnitude will be dependent on the grid spacing Δx used in the numerical computations.

Once again it is only natural to expect that by increasing Δx, the dispersive coefficients will also increase, with practice confirming that they can be several orders of magnitude higher than the coefficients arising from the depth-integration. In the lower limit, $\Delta x \cong h$, the larger non resolved scales of circulation will be related to the shear flow and the extensive studies available on this subject provide very accurate first estimates for the empirical coefficients, so long as the velocity profile is well defined.

One of the main difficulties found when estimating dispersion coefficients, so as to take into account the horizontal spatial discretizations, is the characterisation of the new non resolved scales of motion, which can be greatly dependent on factors like local bathymetric configurations, density gradients and wind friction and set up. Although some general formulae can be used for guidance, the accuracy of the final values will always be greatly dependent on calibration and on the experience of the modeller.

In conclusion, the fact that the numerical resolution of the primitive equations has to resort to additional discretizations in space and time (generally, no analytical solutions are available), makes it necessary to extend filtering to larger scales of motion which are dependent on the model resolution, Δx. Thus, following the previous schernatisation a fourth scale must be considered, such that

Scale 4

Averaging over the model	→	additional dispersion
resolution Δx, Δt	→	additional viscosity

In what follows the additional dispersion and viscosity will be referred to as Subgrid Dispersion D^G and Subgrid Viscosity v^G.

2.5 ESTIMATION OF COEFFICIENTS

2.5.1 Basic Formulations

As a basis for the interpretation of dispersive coefficients, Elder's formulation will be used. Consider the mass conservation equation for a dissolved constituent in an open channel of infinite lateral extent, where the lateral and vertical velocity components are zero and the horizontal diffusion can be neglected, i.e.

$$\frac{\partial c}{\partial t}+\frac{\partial}{\partial x}(uc)=\frac{\partial}{\partial z}\left[D_z^{\,T}\frac{\partial c}{\partial z}\right] \tag{2.39}$$

Considering the vertical profile defined by equations (2.28) and taking into account the flux continuity for incompressible fluids, equation (2.30) can be written

$$\frac{\partial}{\partial t}(C+C')+(U+U')\frac{\partial}{\partial x}(C+C')=\frac{\partial}{\partial z}\left[D_z^{\,T}\frac{\partial C'}{\partial z}\right] \tag{2.40}$$

Introducing now a non inertial frame of reference moving at velocity U, C and C'will be functions of x'= x Ut and t'= t, which brings the previous equation to the following form

$$\frac{\partial}{\partial t}(C+C')+(U+U')\frac{\partial}{\partial x'}(C+C')=\frac{\partial}{\partial z}\left[D_z^{\,T}\frac{\partial C'}{\partial z}\right] \tag{2.41}$$

After a sufficiently long time, C and C' will become functions only of x' and t, respectively, which make it possible to finally write

$$U'\frac{\partial C}{\partial x'}=\frac{\partial}{\partial z}\left[D_z^{\,T}\frac{\partial C'}{\partial z}\right],t\to\infty \tag{2.42}$$

Proceeding by integrating the previous equation, one gets

$$C=\left[\int_0^z\frac{1}{D_z^{\,T}}\left(\int_0^z U'dz\right)dz\right]\frac{\partial C}{\partial x'} \tag{2.43}$$

Multiplying by U` and integrating again over the vertical, it yields

$$\frac{1}{h}\int_0^h (U'C')dz = \frac{\partial C}{\partial x'}\frac{1}{h}\left\{\int_0^h U'\left[\int_0^z \frac{1}{D_z^T}\left(\int_0^z U'dz\right)dz\right]dz\right\} \tag{2.44}$$

And it is now clear that the dispersion coefficient can be given by

$$D_x^s = \frac{1}{h}\left\{\int_0^h U'\left[\int_0^z \frac{1}{D_z^T}\left(\int_0^z U'dz\right)dz\right]dz\right\} \tag{2.45}$$

Elder evaluated D_x^s using Von Karman's logarithmic profile for the velocity

$$U'(z) = \frac{u^*}{\kappa}\left[1 + \ln\frac{z}{h}\right] \tag{2.46}$$

where u* is the shear velocity $(\tau_o/\rho)^{1/2}$ and κ(~0.41) the Von-Karman constant. The shear stress distribution is considered to be linear

$$\tau = \tau_o\left(1 - \frac{z}{h}\right) \tag{2.47}$$

the assumption is made that the turbulent transport of mass and momentum are identical (Reynold's analogy). Noting also that the vertical turbulent momentum transfer is given by

$$\tau = \rho \nu_z^T \frac{\partial U'}{\partial z} \tag{2.48}$$

It transpires that

$$D_z^T = \nu_z^T = u^* \kappa z\left(1 - \frac{z}{h}\right) \tag{2.49}$$

Considering now the independent variable in equation (2.47) given by ζ = z/h and taking into account (2.48) and (2.51), Elder obtained

$$D_z^{\ s} = \frac{u^* h}{\kappa^3} \left\{ \int_0 (1 + in\zeta) \left[\int_\zeta^{\zeta} \frac{\int_0 (1 + \ln\zeta) d\zeta}{\zeta(1-\zeta)} d\zeta \right] d\zeta \right\} \qquad (2.50)$$

Performing the integration, one gets

$$D_x^{\ s} = 0.404 \frac{u^* h}{\kappa^3} = K_E u^* h \qquad (2.51)$$

With $K_E = 5.9$ and $\kappa = 0.41$

Expressions similar to Elder's have been proposed with a wide variety of coefficients, as for example

For open channel flow:	$9.1\ u^*\ h$
For smooth channels:	$13\ u^*\ h$
For natural streams:	$7.25\ (u/u^*)^{1/4}\ u^*\ h$

Some evidence that the Reynolds analogy holds was provided as $v^T/D^T \cong 1$. It also confirmed the parabolic distribution of v^T and was found that the mean depth value was about:

$$D_z^{\ T} = 0.07\ u^* h \qquad (2.52)$$

which justifies its being neglected in comparison to horizontal dispersion due to shear flows.

In applications for natural streams, longitudinal dispersion coefficients as predicted by Elder's formula were found too small, values as much as 150 times higher having been reported. that The effective coefficients of horizontal dispersion are inversely proportional to the coefficient of vertical turbulent diffusion, which is also apparent in Elder's development (equation, 2.47). The mixing produced under a shearing current will thus be enhanced if some stability factors are present in the vertical, their effects becoming important for local Richardson numbers of about 0.5 to 1. According to Bowden the coefficient of vertical turbulent diffusion may then be reduced by a factor of 10 or 20, with a corresponding increase in the horizontal dispersion coefficients, to an order of 10^5 to 10^6 cm^2/sec.

The conclusions of these authors clearly show that other mechanisms of spreading may be dominant in comparison with shear effects. Fischer proposed that the main factor contributing to longitudinal dispersion was transversal diffusion and not vertical diffusion, i.e. the dominant mechanism of spreading should be associated with transversal circulations (this analysis having been done for natural streams). Bowden recognized that shear effects are likely to be most effective in estuaries and near the coastline, and that the existence of large horizontal eddies may dominate among the dispersion processes.

2.5.2 The Evidence of Experience

It is well demonstrated that dispersive effects due to physical processes at scales 1 and 2 are negligible in relation to those at scale 3. With respect to environmental flows, field measurements and modeling results also show that in most situations Elder's coefficient with several orders of magnitude are too small as mentioned previously. This is illustrated in Table 2.2, in which calibrated coefficients are compared with Elder's formula for 4 different applications with a two-dimensional circulation model (MIKE 21).

Table 2.2 Comparison between Elder's coefficient and calibrated coefficient

Case	h m	u m/s	u^* m/s	Δx m	Δt s	E.calib. m^2s	$6hu^*$ M^2/s
A	8	0.7	0.05	50	30	2-5	2.4
B	20	1.0	0.1	500	300	40-50	12
C	30	0.5	0.03	6000	600	~500	5.4
D	1000	0.1	0.003	30000	900	>6000	18

The magnitude of the calibrated coefficients can only be explained by considering processes at Scale 4, that for values of $\Delta x >> h$ usually dominate over processes in Scale 3.

Many modellers attempt to account for the filtered processes at Scale 4 by increasing the coefficient K_E in Elder's formulation, which will only be acceptable as long as those processes remain related to flow variations in the vertical. However, to represent subgrid processes it is

only natural to relate the effective coefficients of viscosity and dispersion to the length scale Δx and to the time scale Δt. Hence the effective coefficients for subgrid processes may be considered in the following possible forms:

$$K_1 \frac{\Delta x^2}{\Delta t} \quad (2.53)$$

$$K_2 \Delta x\, u \quad (2.54)$$

$$K_3 \Delta t\, u^2 \quad (2.55)$$

In Table 2.3 the three different forms of the effective coefficient for Scale 4 have been compared to calibrated results in five different situations.

Table 2.3 Effective coefficients of scale 4

Case	**h (m)**	**u (m/s)**	**Δx (m)**	**Δt (s)**	**$E_{cal.}$ (m^2/s)**	**K_1**	**K_2**	**K_3**
A	8	0.7	50	30	1 - 5	0.06 - 0.01	0.14 - 0.03	.34-.07
B	20	1.0	500	300	40-50	0.06	0.10	0.17
C	30	0.5	6000	600	~500	0.008	0.17	3.3
D	40	1.0	20	10	1 - 3	0.075 - 0.025	0.15 - 0.05	0.30-0.10
E	1000	0.1	30000	900	~6000	0.006	2.0	667

The form $K_2 \Delta x\, u$ appears to be promising since K_2 is almost constant in the five different cases.

It is important to emphasise that as formulae (2.55 & 2.57) are not based on a defined pattern of circulation, like Euler's formulation, the estimates can only be expected to be a rough approximation to the true values. Furthermore, as will be analysed in the next section, the values of the dispersive coefficients are dependent on the biggest non-resolved circulations, and not directly on Δx or Δt. This is very important, and makes it possible to justify that in situations where $\Delta x >> h$, the use of Elder's formulation may still be valid although the

associated dispersive processes will be irrelevant in comparison with other effects. Nevertheless, the above formulae, when complemented with field observations and experience obtained in similar situations; do provide valuable guidance for the calibration of two dimensional environmental models.

When Δx and h are of the same order of magnitude, the shear effects (processes at Scale 3) will be the ones responsible for the transfer of momentum and constituents. In practice, assuming that the friction velocity for coastal waters is about 6% of the mean depth velocity, Elder's formula will give

$$v_x^s \cong D_x^s \cong 5.9 * 0.06\ U\ h \cong 0.4\ U\ h \qquad (2.56)$$

Thus, for application in MIKE 21 when Ax a h the dispersive coefficients (shear viscosity and dispersion) are taken as a first approximation as, to be

$$v_x^s \cong D_x^s \cong 1.0\ U\ h \qquad (2.57)$$

with the factor 1.0 possibly varying by one order of magnitude according to calibration.

It should be stressed that in the above discussion direction x was assumed to be aligned with the flow direction, the coefficients thus obtained being representative of the longitudinal dispersive processes. In the case of shear effects the transverse or lateral processes are found to be approximately one order of magnitude smaller than the longitudinal ones, as indicated by tests reported by (Talbot & Talbot, 1974). For an arbitrary direction of the flow in a Cartesian coordinate system, cross terms would then be present, complicating the definition of the coefficients. Calling D_L^S, D_T^S longitudinal and lateral coefficients, a reasonable approach would be to project them on the x and y directions and disregard cross derivative terms. This can be accomplished by taking the ellipse of semi-axes D_L^S, D_T^S in which D_y^S is aligned with the current vector (u,v), and calculate D_x^S and D_y^S accordingly, eventually obtaining

$$\frac{1}{D_x^s} = \left[\left(\frac{\cos\alpha}{D_t^s} \right)^2 + \left(\frac{\sin\alpha}{D_T^s} \right)^2 \right]^{\frac{1}{2}} \qquad (2.58)$$

$$\frac{1}{D_y^s} = \left[\left(\frac{\cos\alpha}{D_t^s} \right)^2 + \left(\frac{\sin\alpha}{D_T^s} \right)^2 \right]^{\frac{1}{2}} \qquad (2.59)$$

Where α = arctan (v/u)

However, for dispersive processes associated with the largest scales, as is the case in subgrid flow circulations, the influence of flow direction is no longer relevant, which means that isotropy can be usually assumed.

2.6 GENERAL INTERPRETATION

It is possible to simulate realistically secondary large scale circulations by using two dimensional models. Continuing on the same subject referred to the existence of two fundamental mechanisms for the generation of circulations, where the resistance forces (bottom friction) are balanced by:

- the momentum transfer resolved at the scale of the spatial discretization adopted (convective accelerations)

- the momentum transfer non resolved at the scale of the spatial discretization adopted, represented by horizontal shear stresses (subgrid viscosity)

The first mechanism is dominant in many situations where the scales of flow circulation and space discretization Δx are much bigger than the depth of the flow, and the second one is fundamental to describe secondary circulations when $\Delta x < h$. Nevertheless, for some situations where $\Delta x >> h$ it is found in practice that the second mechanism is still necessary to describe the resolved scales of circulation. A possible explanation may be found in the following heuristic hypothesis:

- The transfer of momentum or constituents amongst resolved scales depends upon the relative magnitude of the minimum resolved scale and the maximum non resolved scale. The transfer is only effective when these scales have the same order of magnitude.

To analyse the consistency of this statement the following interpretations are made:

a) When the structure of the flow is well defined by a logarithmic profile of velocities and Δx is of the same order of magnitude of the depth h, the biggest non resolved scale is the velocity profile itself, Elder's formula being thus valid for the estimation of the effective viscosity and dispersion coefficients. The second mechanism is fundamental to describe flow circulation.

b) When $\Delta x >> h$ several situations may be found:

   a) The bottom is very regular and three dimensional effects are negligible. In this case the biggest non resolved scale will still be related to the depth, thus being much smaller than the minimum resolved scale. Consequently the transfer of momentum due to the non resolved scales (subgrid viscosity) is negligible. Euler's formula is still valid but the model will not be sensitive to the values of the viscosity coefficient. The circulation is only determined by the first mechanism, i.e., by the dissipative terms, as the non-resolved scales only contribute as energy absorbers.

   b) The bottom configurations and the existence of three-dimensional effects originate circulations, the scales of which are of the same order of magnitude of Δx, i.e., important in relation to the minimum resolved scales. In this case the transfer of momentum due to the non resolved scales becomes significant. This can be easily illustrated by the experience of many authors, who for calibration of regional models using large grid spacings ($\geq$ 5000 m) employed dispersion coefficients proportional to Δx or/and h. As an example one of the formulae commonly used is given by $E = K \Delta x^2/\Delta t$ with $0.01 < K < 0.06$. For a regular mesh with a 30,000 m grid spacing, a 15 min. time step and an average depth of 1000 m, we get $10{,}000 < E < 60{,}000$ m2/s, i.e. 10 h $< E <$ 60 h.

      For his global oceanic tidal model used a dispersion coefficient linearly proportional to the depth and -x, that gives values consistent with the previous formula.

c) It is logical to expect that by using the Prandtl model for the determination of the dispersive coefficients, the mixing length will be related to the magnitude of the maximum non resolved scales. Using the Smagorinsky formulation and considering the mixing length given by

$$\ell = C_s \Delta x \qquad (2.60)$$

It is recommended to use values of Cs in the range (0.4 to 0.8). These values are consistent with the hypothesis formulated before, i.e. the transfer processes of momentum and constituents are only important when the non resolved circulations are of the same order of magnitude as Δx.

CHAPTER THREE

MODEL APPLICATIONS AND RESULTS DISCUSSION

3.1 MODEL APPLICATION

The model is used to study the flow and transport processes in Tubli Bay of Bahrain (Figure 3.1) for the purpose of examining the flushing and assimilative capacity of the bay contaminants. The application, as will be explained later, is a based on scenarios or cases which describe the conditions that enable us to understand the flow and contaminant transport processes in the bay, so the proposed scenarios sometimes are unrealistic from practical point view, but intrinsic in them there is an idea that can help explaining certain processes. Some cases were imported from COWI ALMOAYED GULF (CAG) Sitra Causeway environmental impact assessment study to double check on the conclusions reached in this study.

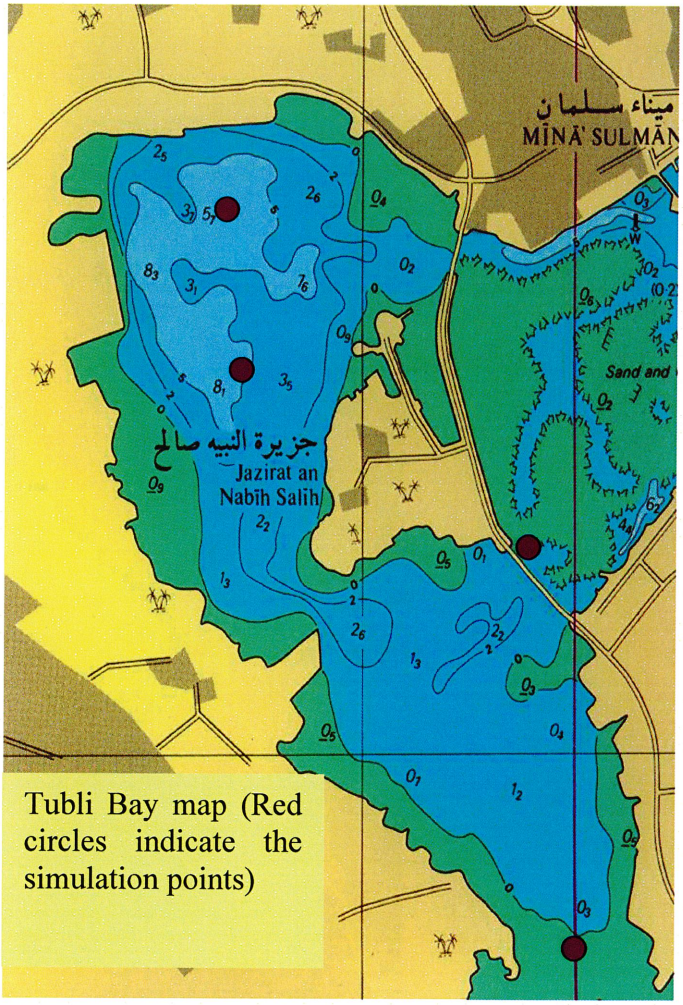


Figure 3.1: The model domain - Tubli Bay (2611′N, 5034′E)

3.2 INPUT DATA

The physical oceanographic data of Tubli Bay was obtained from DHI through COWI ALMOAYED GULF Company based in Bahrain (pers comm). The original data was obtained by this company from various sources to conduct an environmental impact assessment for the replacement of the old Sitra Bridge. The obtained data consists of the bay bathymetry, tidal elevation and speed at some points like Mina Salman, Yacht Club, and a point north of Tubli Bay (Figure 3.1), in addition to meteorological data describing the whole Bahrain like wind speed and direction. For verification, similar data was obtained from other resources like Survey Directorate of the Survey & Land Registration Bureau at Mina Salman and GEOMATIC of the Bahrain Center for Studies and Research. The verification revealed that COWI ALMOAYED GULF Company data is more complete and serves the purpose better, and so we used it (COWI, 2004). A brief introduction of COWI obtained data is described in the coming sections.

3.3 REFERENCE LEVEL

According to CAG any positional information, whether horizontal or vertical, used in their study is referenced to the datum at Ain Al Abd. The used map projection is the Universal Transverse Mercator (UTM). Unless stated otherwise, the Bahrain National Height Datum (BND) is used as vertical datum. In Bahrain depths illustrated by the navigational charts are given relative to the Chart Datum (CD), which is approximately the Lowest Astronomical Tide (LAT), at the given location. The CD relation to the BND is given as BND = CD + 1.46 m.

3.4 BATHYMETRY

The COWI Tubli Bay Bathymetric data was obtained from the Survey Directorate of the Survey & Land Registration Bureau, and adjusted to the mean surface water level at Mina Salman for the model application. Figure 3.2 describes the bay bathymetry adopted in Sitra Causeway study and for this thesis work sensitivity analysis.

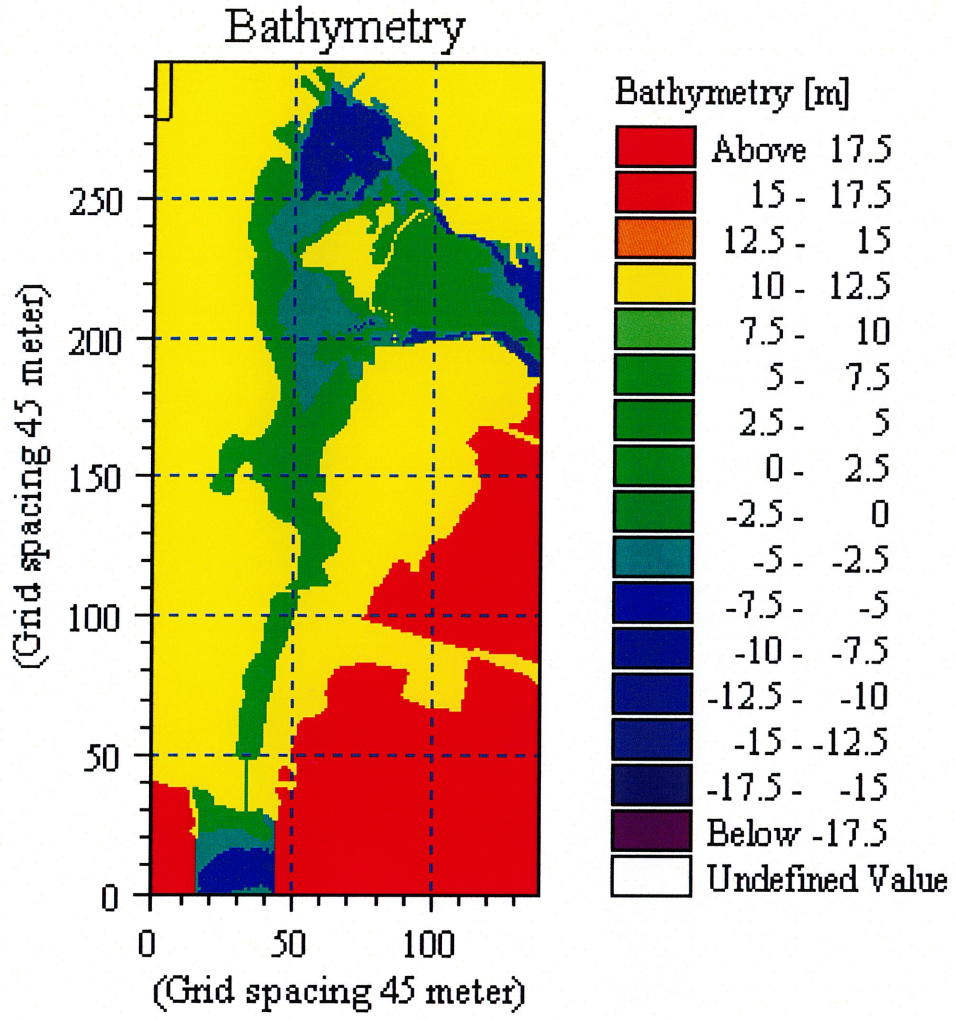


Figure 3.2: Tubli Bay bathymetry referenced to Ain Al Abd datum and adjusted to Mina Salman mean surface water level.

3.5 WIND

As stated by CAG wind data of the area was collected from Civil Aviation Affairs/Directorate of Meteorology, and analysed by CAG, the results output is presented in Table 3.1.

On the basis of the results in Table 3.1 approximately 62% of the time the wind blows from directions WNW clockwise through N with 23% of occurrences from NNW. Winds with an

average speed above 10 m/s are most frequent from these four directions, mostly from direction NNW. The frequency of occurrence of these winds (above 10 m/s) is about 1.48%. Furthermore, approximately 70% of the time the wind in the area has speeds below 6 m/s, indicating passage of only minor important weather systems under normal conditions.

Table 3.1: Probability of occurrence of mean hourly wind speed from different directions. Wind statistics from the weather station at Bahrain Airport (E 50°39' and N 26°16') for the period 1982-1991.

Wind	Percentage of occurrence for different wind directions (degree north)																
m/s	N	NNE	NE	ENE	E	ESE	SE	SSE	S	SSW	SW	WSW	W	WNW	NW	NNW	Total
<2	2.30	1.71	0.68	0.68	1.37	1.36	1.41	1.84	1.28	0.91	0.78	1.21	1.29	2.19	2.40	3.31	24.72
2-4	2.80	1.36	0.83	0.73	1.75	1.40	1.20	1.38	0.88	1.01	0.62	0.45	1.08	3.86	2.64	3.81	25.80
4-6	3.43	0.98	0.52	0.35	0.85	0.88	0.76	0.85	0.42	0.46	0.10	0.15	0.32	1.98	2.58	4.59	19.22
6-8	4.29	0.37	0.07	0.04	0.45	0.57	0.45	0.64	0.02	0.02	-	-	0.02	1.43	2.78	5.20	16.35
8-10	2.50	0.29	-	-	0.29	0.19	0.29	0.19	-	-	-	-	-	1.12	2.46	5.09	12.42
10-12	0.22	-	-	-	-	-	-	-	-	-	-	-	-	0.15	0.26	0.76	1.39
12-14	-	-	-	-	-	-	-	-	-	-	-	-	-	-	-	0.09	0.09
>14	-	-	-	-	-	-	-	-	-	-	-	-	-	-	-	-	-
Total	15.50	4.71	2.10	1.80	4.71	4.40	4.11	4.90	2.60	2.40	1.50	1.81	2.71	10.70	13.10	22.90	100

3.6 WATER LEVEL DATA

As a background water level is an important factor in the hydraulics of free surface flow. It is determined in any water system by tidal levels and other meteorological effects like wind and meteorological pressure.

3.6.1 Tidal levels

In Bahrain tidal levels vary as a result of barriers tides in their way down to Gulf of Salwa, a good example is Fasht al Azm coral reef laying east of Bahrain that acts as a barrier to the tide going down to the Gulf of Salwa and reduces its amplitude. The spring tide amplitude on the north side of the reef is in the order of 1.7 m, while on the south side of it is about 0.4 m at Umm Jalid Island. Likely, the amplitude at Mina Salman is 1.8 m and in Maamir Channel it is only 0.5 m.

3.6.2 Meteorological Effects

In addition to change in water level due to tide and wind barometric pressure causes change in water level. Wind produces wind set up/down on the water surface; the higher the wind speed and the longer fetch are the larger and longer the wave they produce. In a closed water body it creates a slight tilting on the water surface. Similarly, the low barometric pressure that associated with storms is the higher the water level rise it produces, a low pressure tends to raise the sea level by about 10 mm for each 1 mbar below the average air pressure.
As a result of the low speed of the dominant northwestern direction wind and because Tubli Bay is a small closed water body these combined make the rise of water level due to wind blow up not significant and can be easily neglected in the model simulations.

3.6.3 Measurements

Actual observations of water level are available from Mina Salman for various periods from 1988 to 1998. The water level recording station records the water level in 10 minutes interval. Figure 3.3 shows part of a time series of the water level recording from Mina Salman. Similar

data of the same period is available for the Yacht Club in Sitra. One further data is presented for a point located north of the bay (Figure 3.1).

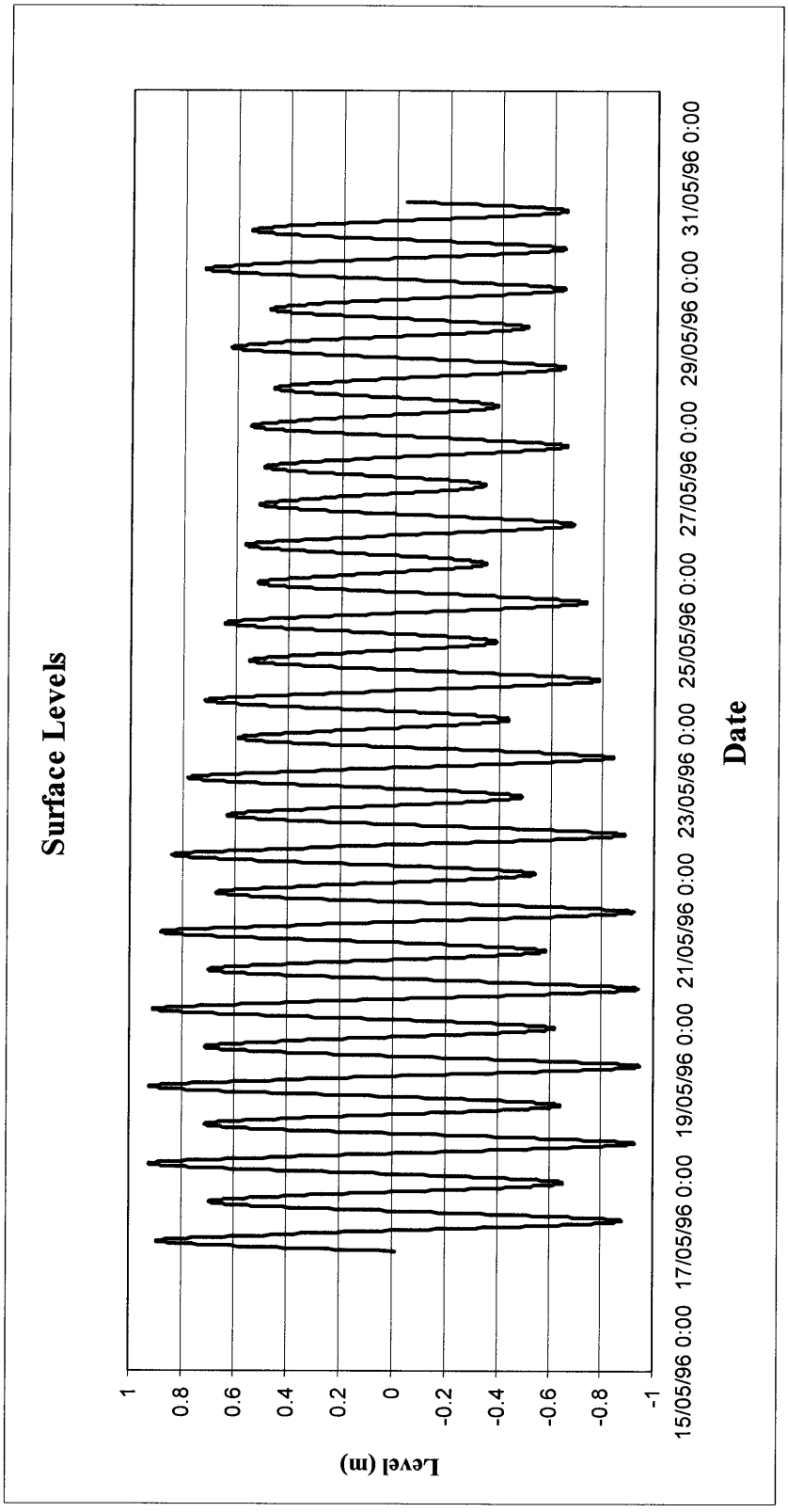


Figure 3.3: Water level records in Tubli Bay May 1996.

3.7 CURRENTS DATA

The current data in Tubli Bay and the surrounding areas as obtained from the Survey Directorate of the Survey & Land Registration Bureau is displayed is shown in the figure 3.4. The data belongs to a point located north of Tubli Bay. The speed is the average of 6 tidal cycles measured near the surface and the direction of the wind was NW.

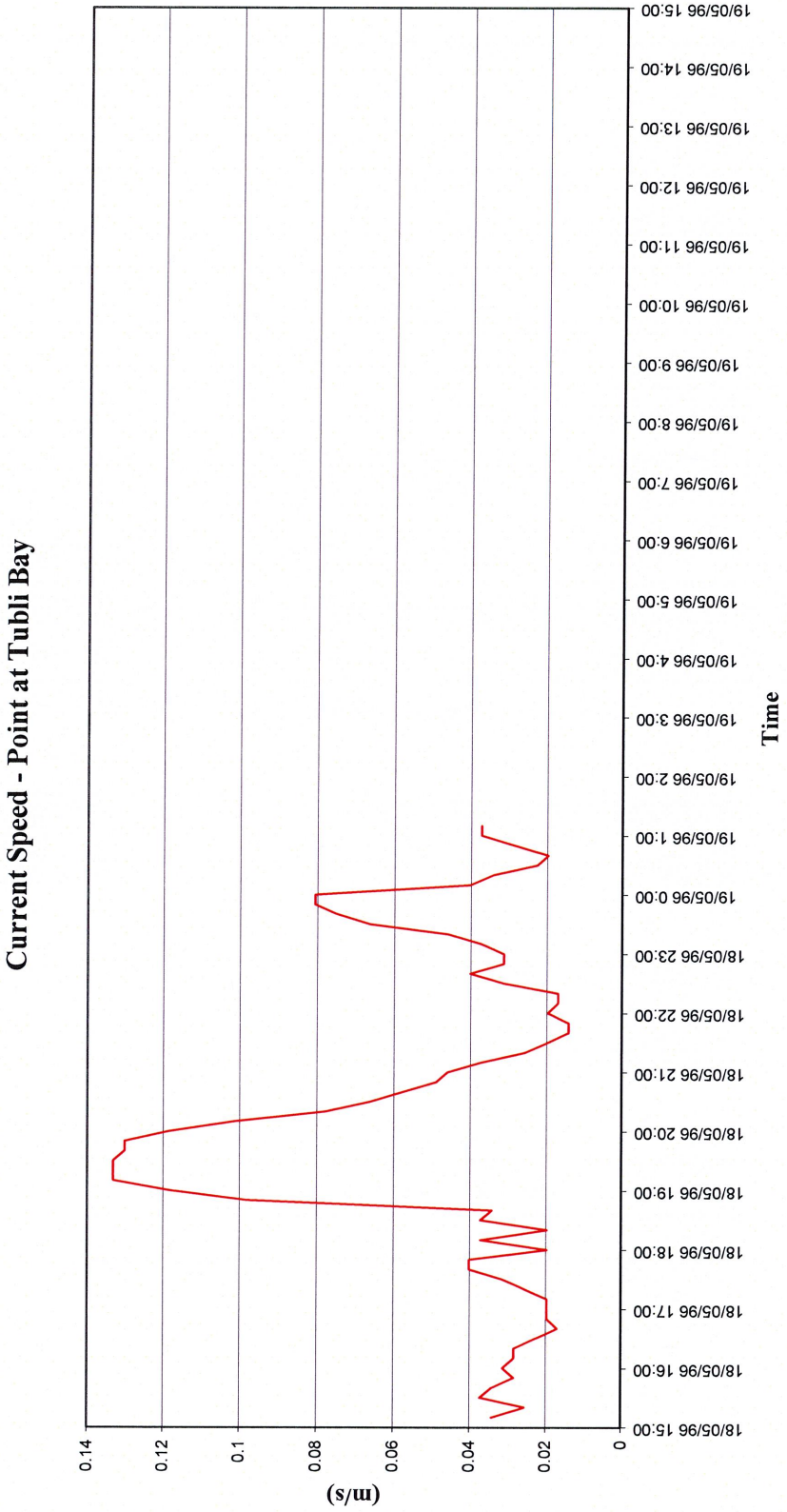


Figure 3.4: Measured current speed at Tubli Bay.

3.8 MODELING DOMAIN

Before starting, simulations data needs some preprocessing. The bathymetric data has to be read in such a way by which MIKE 21 in order to discern the delineation line between land and water during the simulations. If the data was not so, the user should manually trace the delineation line. It is important to note that all bathymetric data were adjusted to the mean sea level datum at Mina Salman. In case of Tubli Bay, the delineation line was manually traced and the modeled area cells designating land that stay dry during the maximum elevation flood tide were assigned an elevation value of 10 m, which is higher than the sum of any other elevation in Tubli Bay bathymetric map and the maximum flood tide elevation at Mina Salman. This value guarantees land to stay dry during the simulations.
Once the delineation line has been discerned the user lays a rectangular mesh of length, width and orientation of his choice. The number of mesh cells, however, is governed like in any other numerical model (see Box 1 for more details) by the computer CPU time and storage, the resolution and accuracy needed, and the available data. Because MIKE 21 is a finite difference model the orientation should be selected so as the mesh boundaries hit the actual boundary conditions, and hopefully the direction of flow entering and the leaving the domain is perpendicular to the mesh boundaries.

Once the land and water has been delineated on the bathymetric map and the mesh has been selected the mesh will be imposed on the bathymetric to extract elevations on the bathymetric map at the mesh points. At this point the mesh contains the bathymetric information of elevation and dry land and water flags.

Moreover, two boundaries was specified for the project after applying a set of flow models starting with overall and coarser models covering larger areas and than gradually focus on smaller areas close to the study area to account for the tidal currents entering from deep water in the Arabian Gulf into the shallower areas surrounding Bahrain and Tubli. These two boundaries were Mina Salman in the north of the Sitra causeway and Yacht Club in the south.

Box 1: Selection of domains in numerical models

The selection of the domain size, shape and orientation are usually governed by a number of constraints, among them are the following:

- Model numerical method- because the present version of MIKE 21 uses finite difference technique the model domain needs to be rectangular in shape and because of problems of stability and numerical dispersion the cells need to be square in shape.
- Location of boundary conditions
- Orientation of the flow entering and leaving the modeling area
- Stability and convergence problems of the model governing equations- non-linear governing equations and equations of hyperbolic type are difficult to convergence in comparison to linear and elliptic type equations.

Applying the above to Tubli Bay case produced a mesh of 139x300 cells, each of 45x45m dimensions (6,255mx13,500m), tilted 325° from true north, and mesh boundaries hit the actual boundary conditions at Mina Salman and south of Ma'ameer Channel (Figure 3.2 - Bathymetry Map). As observed in Figure 3.2, the mesh boundary that hits Mina Salman is not perpendicular to the actual flow there because making it so requires a mesh of much bigger number of cells, a simple remedy to this is by taking the actual flow direction at the boundary and make it the simulations default.

3.9 FLOW BOUNDARY AND INITIAL CONDITIONS

The flow boundary conditions at the eastern boundary of the flow domain are the tidal level at Mina Salman from 15th to 30th of May 1996, 14-day spring-neap tidal cycle. Similarly, the southern boundary conditions were of tidal level at the Yacht Club of the same period of the eastern boundary. Because of the existing constrictions of culvert and Ma'ameer channel, boundary conditions at the southern domain boundary are expected to have little effect on the

flow of the present situation in Tubli Bay compared with the eastern boundary. Therefore, the southern boundary was neglected.

Initial conditions were all assigned the value of tidal level at Mina Salman at the time of simulation start up (15th of May 1996 1:30PM) (refer to figures 3.5 and 3.6).

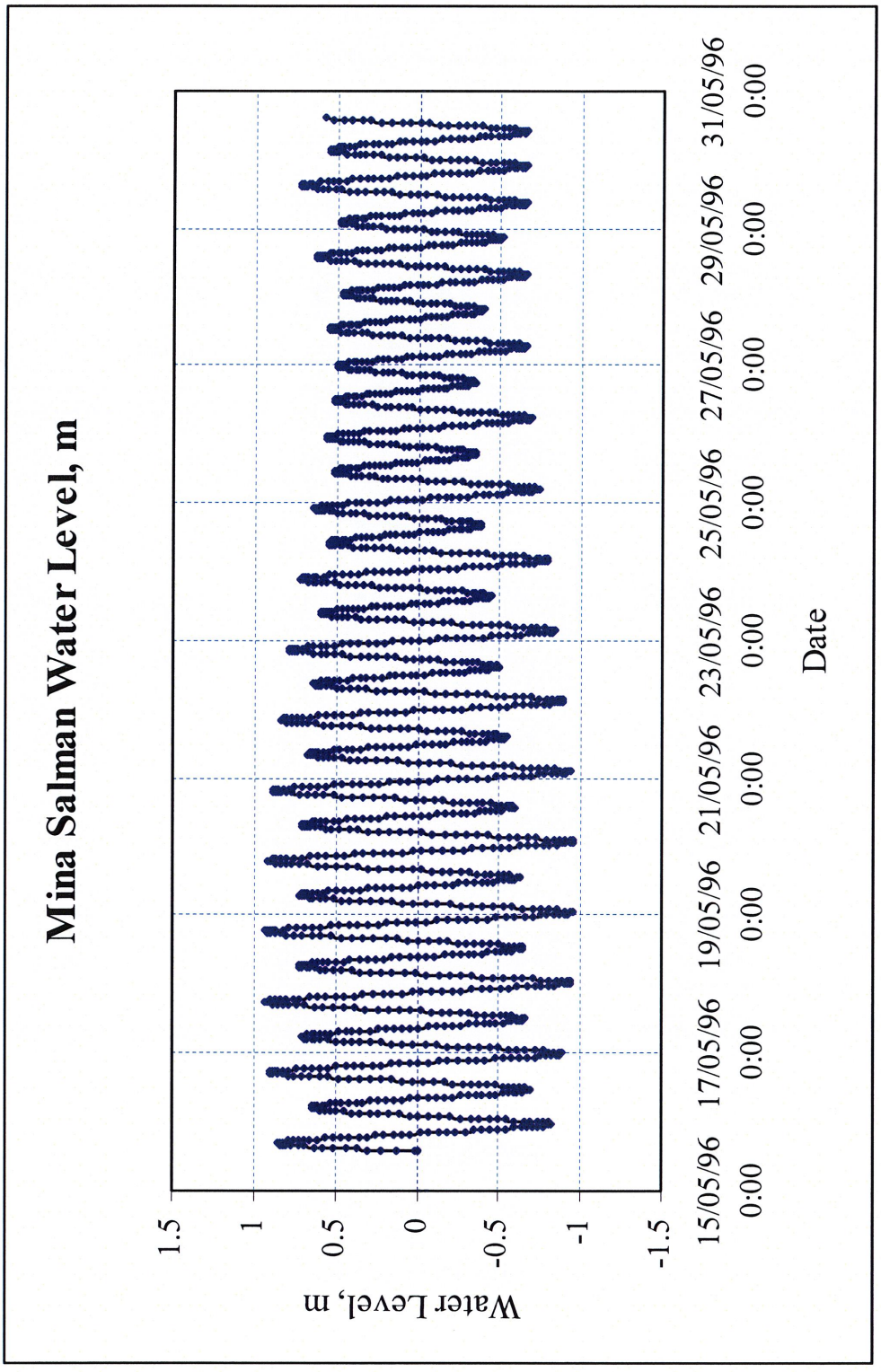


Figure 3.5: Time series of 14-day spring-neap tidal cycle at Mina Salman

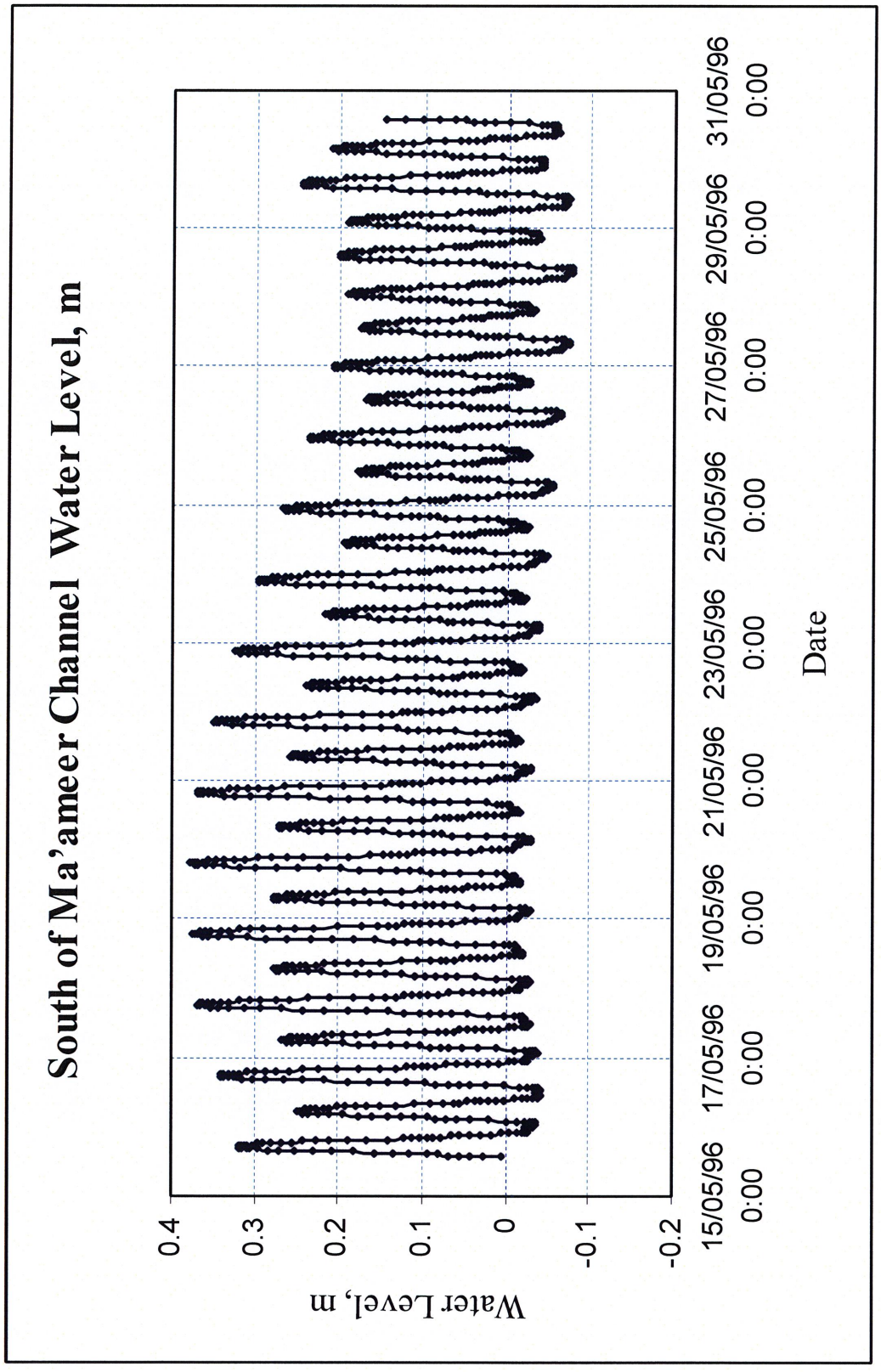


Figure 3.6: Time series of 14-day spring-neap tidal cycle south of Ma'ameer Channel

3.10 FIRST-ORDER SENSITIVITY ANALYSIS

Governing equations in general consist of variables, forcing functions and parameters. The variables are the spatial and temporal dimensions (x,y,z,t), the forcing functions are the driving external factors like the driving wind force, and the parameters are system properties that specify the governing equations to the undertaking.

To display the effect of the parameter value or bed resistance on the results a sensitivity analysis was conducted. As the name implies it measures the results sensitivity to a change in parameter/s. Mathematically, this could be dealt with as below.

Using first order Taylor series, the forward and backward expansion of it could be written as:

$$C(k+\Delta k) = C(k) + \frac{\partial(k)}{\partial k}\Delta k \qquad (3.1)$$

Where, C(k) is the targeted result, k is the parameter, in this work it is the bed resistance or Manning number.

$$C(k+\Delta k) = C(k) - \frac{\partial(k)}{\partial k}\Delta k \qquad (3.2)$$

Subtraction the above two equations yields,

$$\Delta C = \frac{\partial(k)}{\partial k}\Delta k \qquad (3.3)$$

Divide the above equation by C and rearrange gives,

$$\frac{\Delta C}{C} = \frac{\partial(k)}{\partial k}\frac{\Delta k}{C} \qquad (3.4)$$

Or

$$\frac{\Delta C}{C} = CN_k \frac{\Delta k}{k} \qquad (3.5)$$

Where, CN_k is the condition number for the parameter k ($CN_k = \frac{\partial C(k)}{\partial k}\frac{k}{C}$). In a way it provides a transfer function to propagate the parameter relative error (i.e., $\frac{\Delta k}{k}$) into the relative error of the prediction C (i.e., $\frac{\Delta C}{C}$).

For hydrodynamic simulations the condition number was calculated only for bed resistance parameter because it is believed that the other parameter 'eddy viscosity' is of little effect due to the low wind velocity in Tubli Bay. The bed resistance or Manning number 'k' of 23 $m^{1/3}/s$ value was perturbed in the model between 18 and 28 $m^{1/3}/s$, and the predictions 'Cs' calculated by MIKE 21 HD at points of interest were used to calculate the condition number 'CN_k' in accordance with the above equations. In Tubli Bay case, C was chosen to designate the height or time of the of the highest or lowest tidal level during the 14-day flood-neap cycle in two stations, namely North Tubli (NT) and North culvert (NC) shown in Figure 3.7. These stations were selected because they represent the most extreme flow situations in Tubli Bay, the former is the deepest and no constriction point and the later is the point where constriction exists. The calculation results are displayed in Table 3.2.

Table 3.2: The sensitivity of model flow predictions to bed resistance at two stations in Tubli Bay.

Bed Resistance	**Highest tide height** (m)		**Lowest tide height** (m)		**Highest tide time** (hr)		**Lowest tide time** (hr)	
	North Tubli	North Culvert	North Tubli	North Culvert	North Tubli	North Culvert	North Tubli	North Culvert
18	0.886	0.834	-0.595	-0.354	78	78	85.5	86.5
23	0.911	0.863	-0.659	-0.359	77.5	78	85.5	86.5
28	0.939	0.902	-0.710	-0.414	77.5	77.5	85	86.0
CN_{23}	+0.134	+0.181	+0.401	+0.384	-0.015	-0.015	-0.013	+0.013

It is evident from Table 3.2 that the relative error of the lowest tide height is about 3 (0.401/0.134) times greater than that of the highest tide height, and similarly it is about 30 (0.401/0.013) times greater than the lowest or highest tide time of occurrence. These results imply that the model calibration should be based on the low tide elevation of the actual observation points.

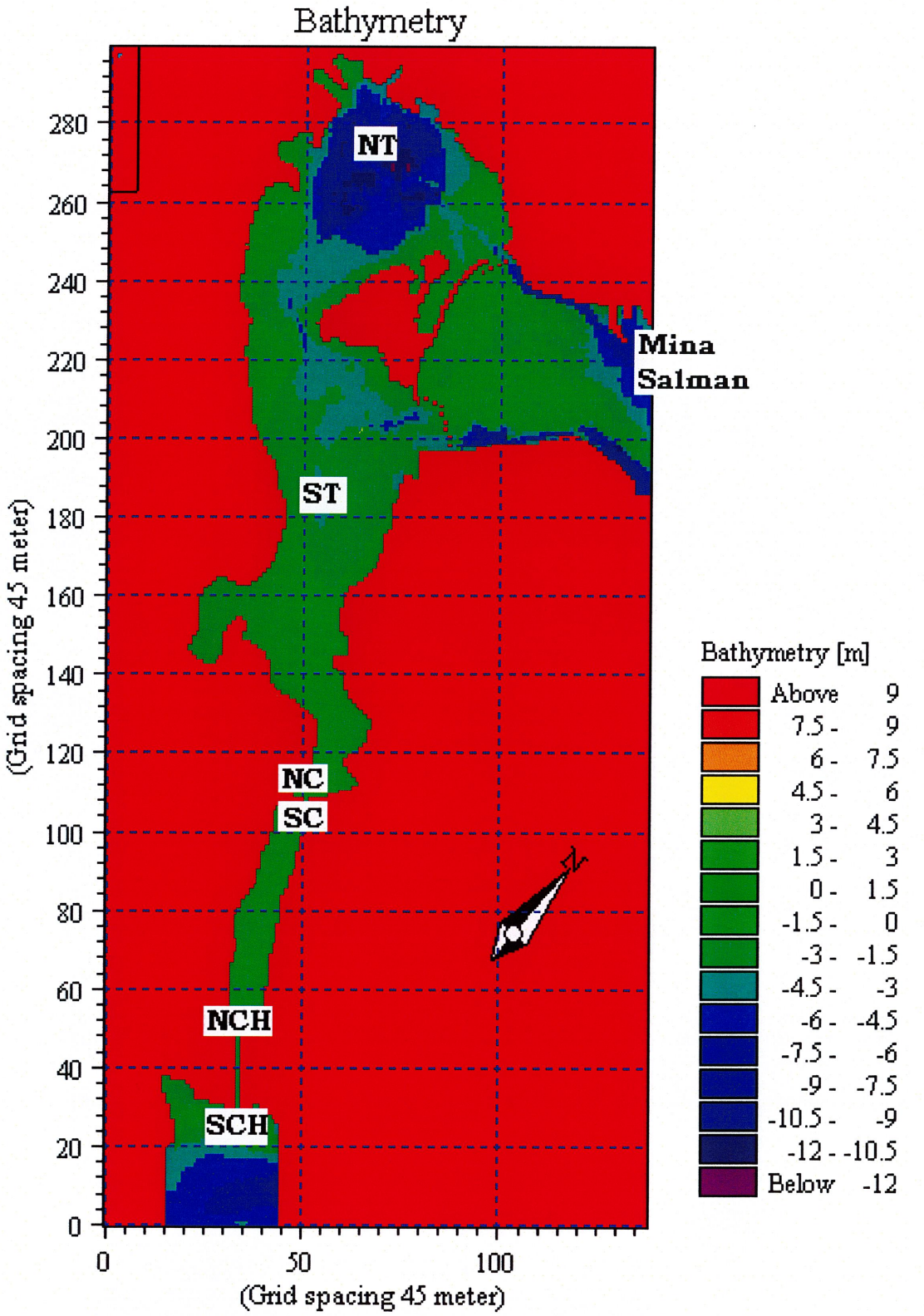


Figure 3.7: Points of sensitivity analysis, calibration and simulation in Tubli Bay

Similarly, sensitivity analysis was also performed on the dispersion coefficient of the same points mentioned above. The results of the analysis are presented in Table 3.3.

Table 3.3: The sensitivity of concentration predictions to dispersion coefficient at two stations in Tubli Bay

Dispersion Coefficient Cm^2/s	Mean Concentration	
	North Tubli	North Culvert
0.5	7.59	6.8
2.5	6.12	5.96
4.5	5.24	5.17
$CN_{2.5}$	-0.48	-0.34

Table 3.3 illustrates that concentration relative errors at these two points are comparable, and at the same time it seems that concentration contours are very much affected by the selected value of dispersion coefficient in Tubli Bay. The negative sign in Table 3.3 implies that plume point concentrations decrease and areal extend increases with increasing dispersion coefficient. Therefore, it is advisable to estimate dispersion coefficient in any study of Tubli Bay flushing characteristics.

3.11 MODEL CALIBRATION AND VALIDATION

For MIKE 21 hydrodynamic simulations two parameters need estimation to make the governing equations specific to Tubli Bay case; these are eddy viscosity and bed resistance. Because wind speed and water flow currents in Tubli Bay are both small in magnitude, the model predictions are not going to be sensitive to eddy viscosity. On the contrary, bed resistance as explained in the sensitivity analysis has the major effect on flow in Tubli Bay due to two reasons: the shallow water depth and the presence of constrictions along the flow path from Mina Salman to Ma'ameer Channel.

On the basis of the above the model was calibrated by selecting a number of bed resistance values or Manning numbers between 20 and 60 $m^{1/3}/s$ based on a trial and error, and predicting the water surface elevation and speed at points shown in Figure 3.7. Eyeball comparisons were used to compare the predictions at these points with the simulated ones of

CAG EIA study (Points NT, ST and NC). The comparisons were based on the amplitude and time shift of the model produced time series and that of CAG study. The result of these comparisons indicated that a Manning number of 23 $m^{1/3}/s$ value gave the best fit (Figure 3.8 a and b, Figure 3.9 a and b and Figure 3.10 a and b). According to these figures the predicted values coincide very well with the CAG simulated ones at Point NT and ST. At Point NC the predictions deviate a little bit from CAG ones for low tide and the reason could be attributed to the slight difference in boundary conditions south of the Ma'ameer Channel between this work and GAC study. Therefore, from the comparison, the water level variations were accepted.

North Tubli (NT):

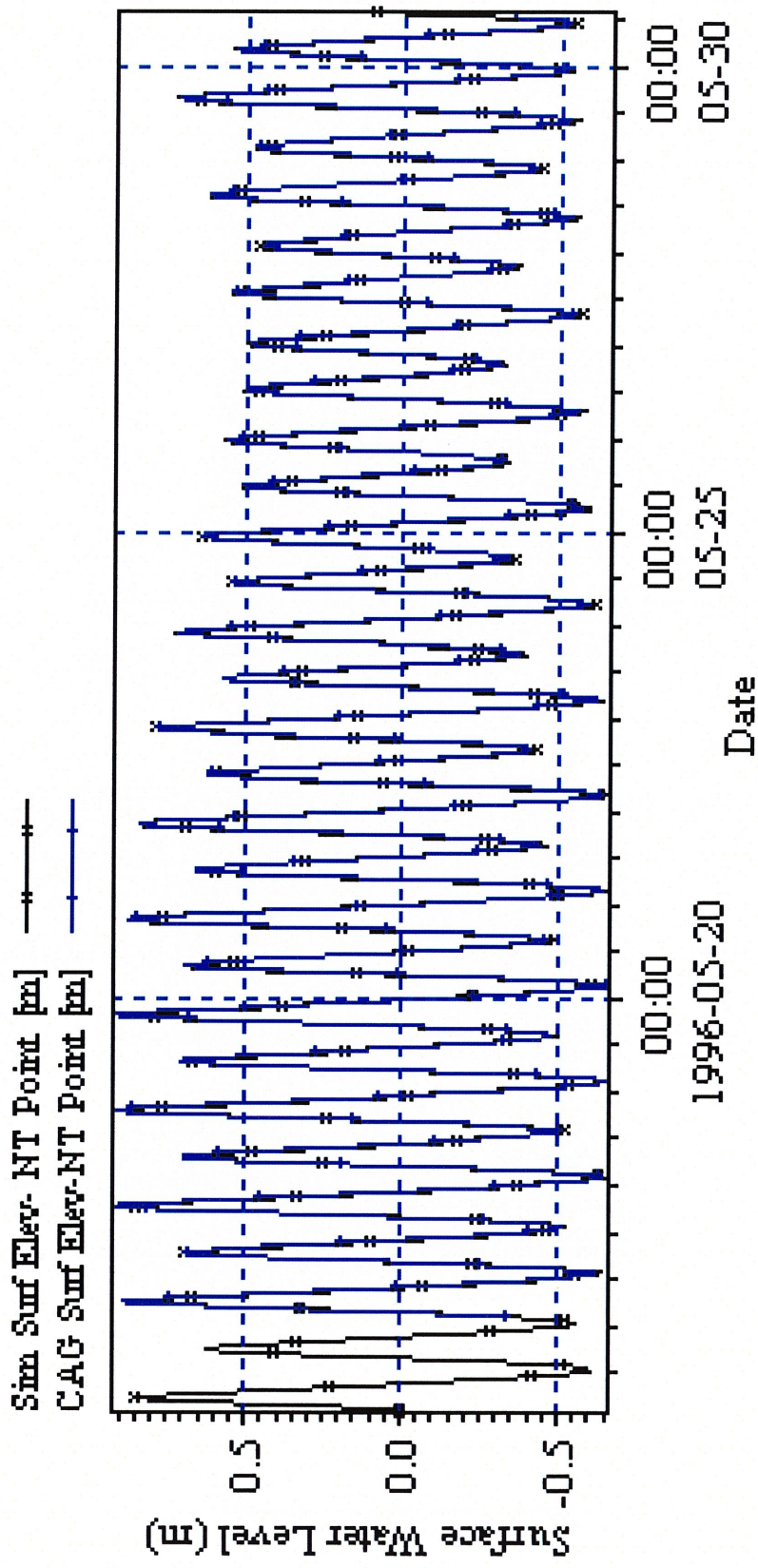


Figure 3.8, a: Comparison of water surface elevations at Point NT as produced by this work and CAG EIA study

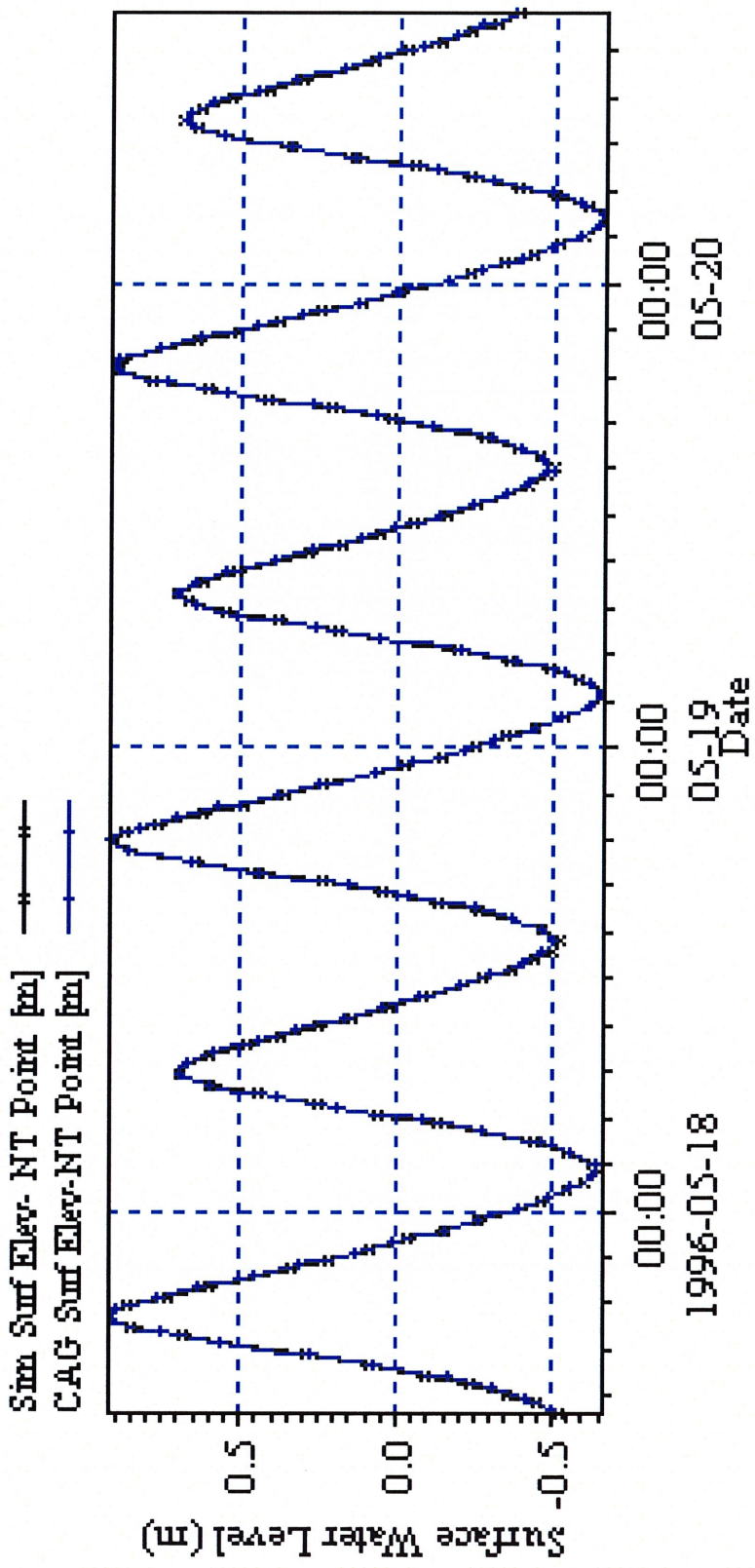


Figure 3.8, b: Comparison of water surface elevations at Point NT as produced by this work and CAG EIA study

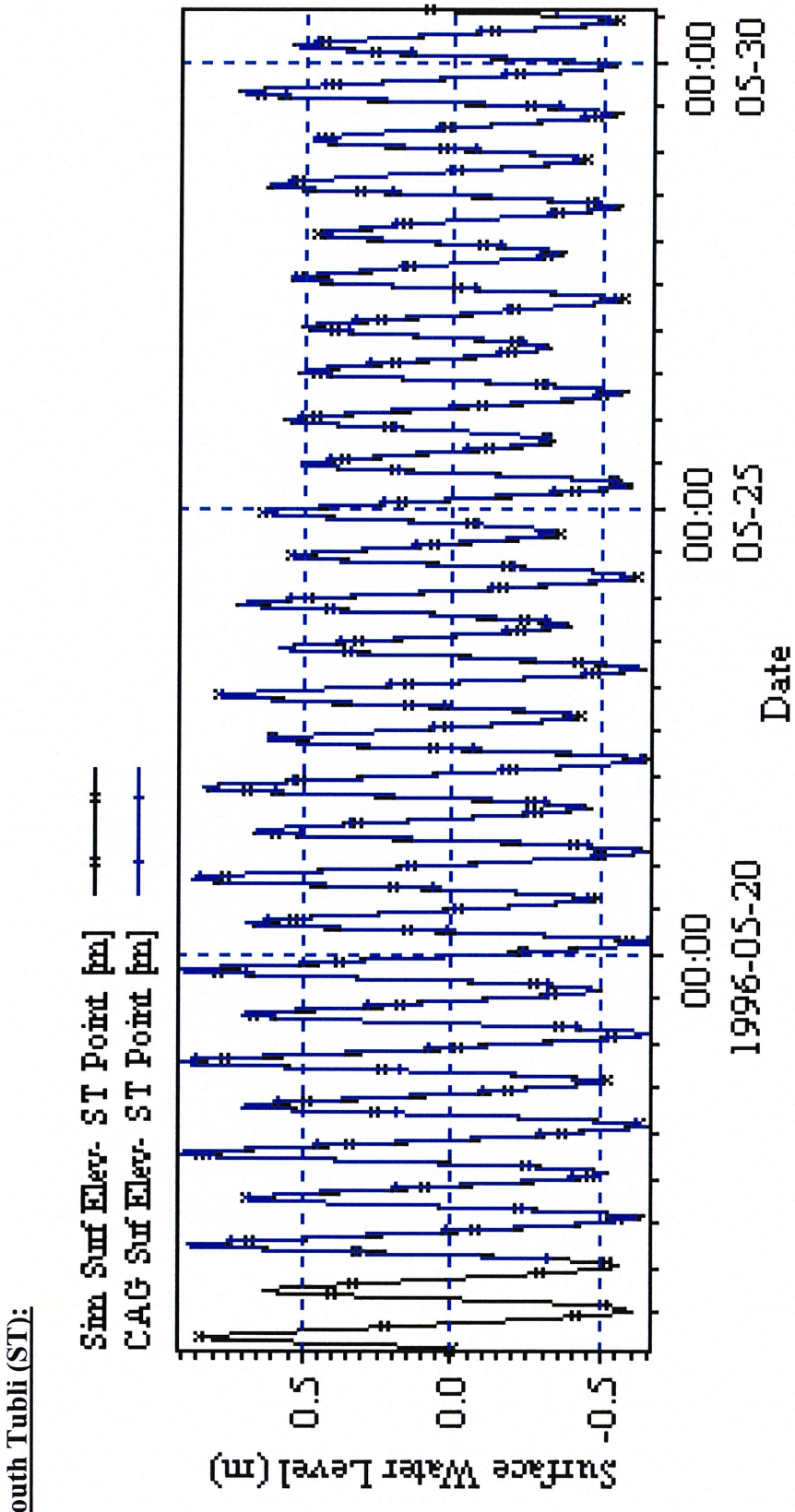


Figure 3.9, a: Comparison of water surface elevations at Point ST as produced by this work and CAG EIA study

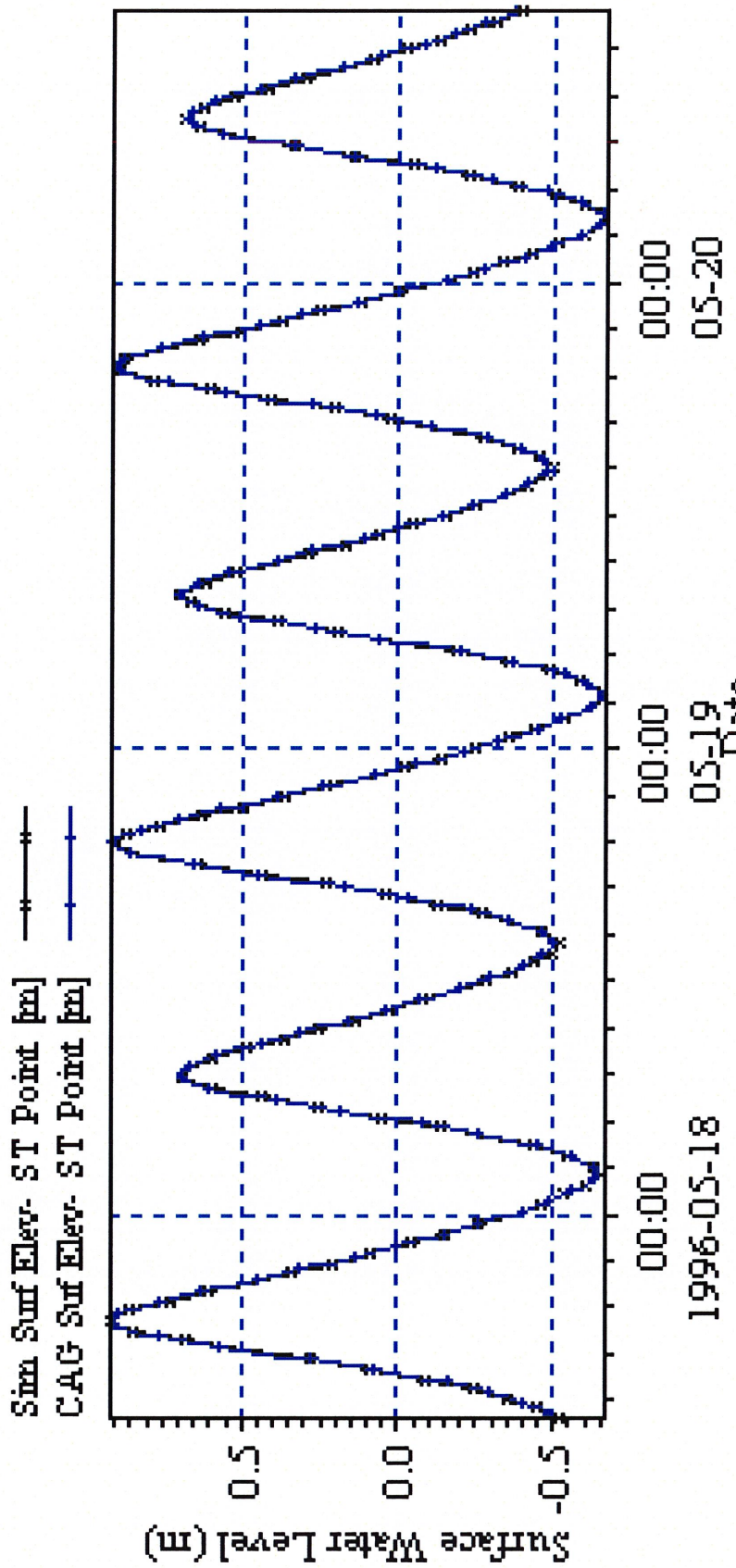


Figure 3.9, b: Comparison of water surface elevations at Point ST as produced by this work and CAG EIA study

North Culvert (NC):

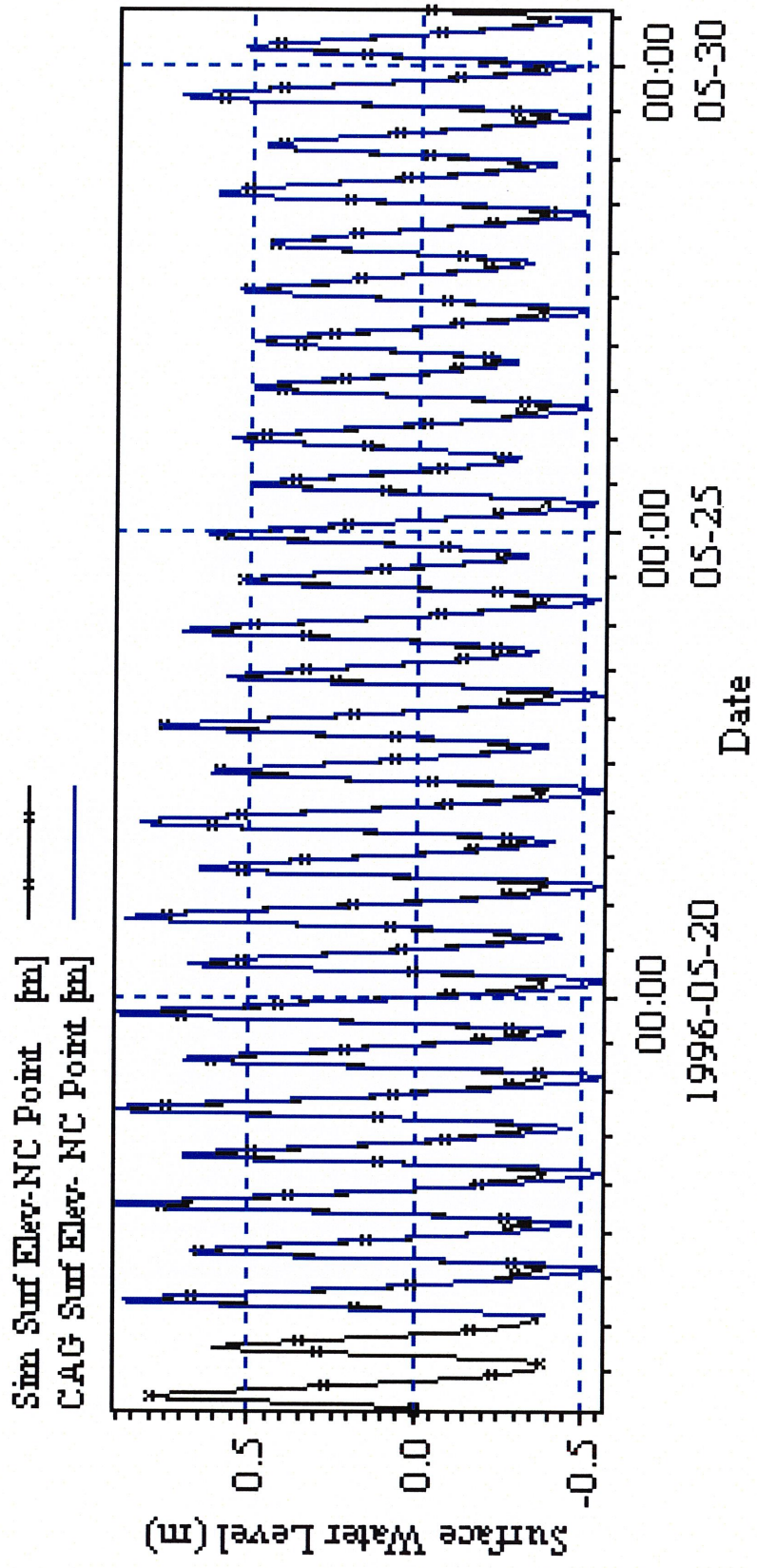


Figure 3.10, a: Comparison of water surface elevations at Point NC as produced by this work and CAG EIA study

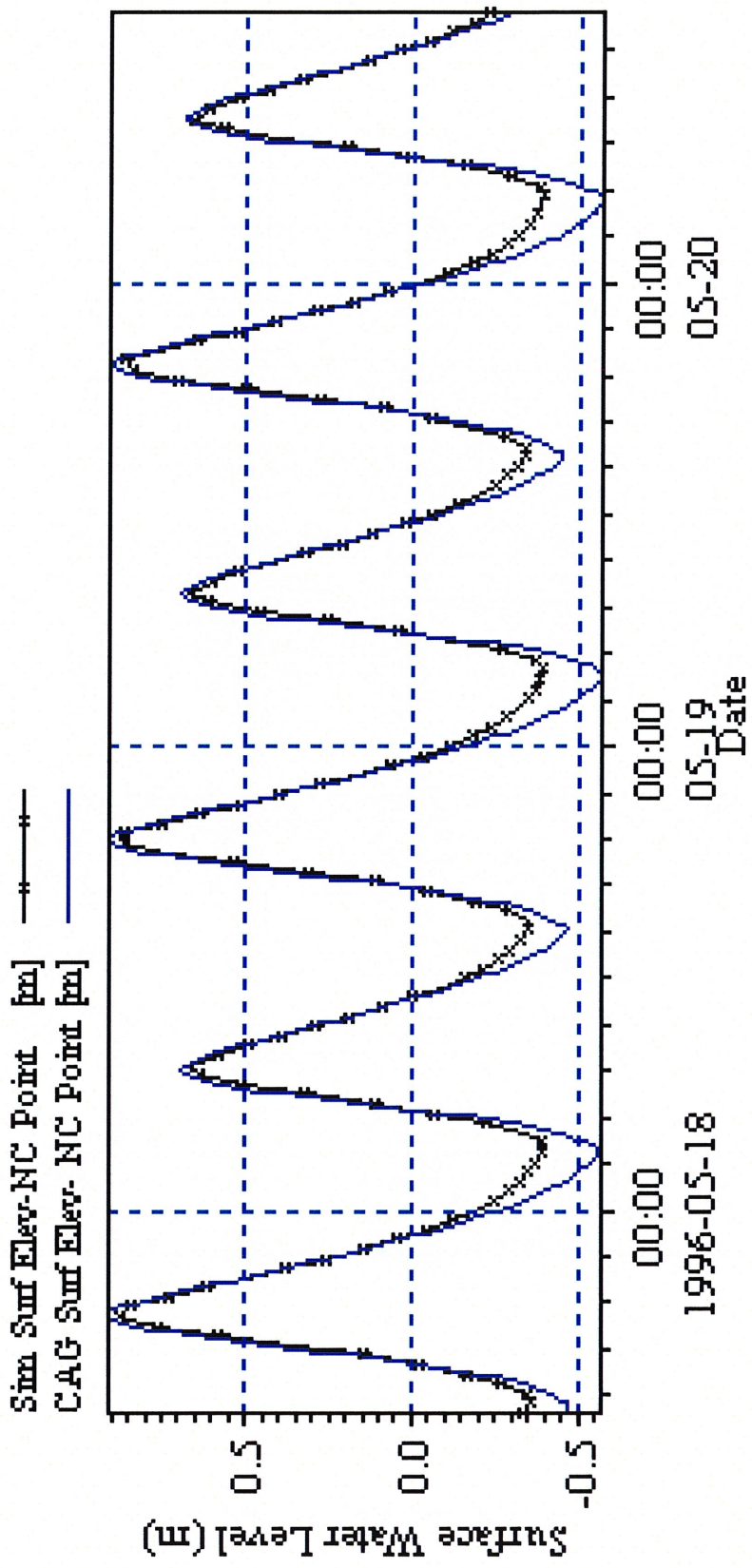


Figure 3.10, b: Comparison of water surface elevations at Point NC as produced by this work and CAG EIA study

Before applying the calibrated model on actual scenarios it is essential to validate it for the same calibrated parameters (in this case for Manning number equals 23 $m^{1/3}/s$), but with another set of measured water levels and/or currents at points not used in the calibration. Luckily, measured water level and current speeds are available at Point NT in Tubli Bay (see Figures 3.3 and 3.4), and so the model predictions were compared at this point with the actual ones. The result of the comparison is shown in Figures 3.11 and Figure 3.12, which clearly shows the good agreement between the predictions and the actual observations with respect to water level. But a relatively large difference is found in current speed, this is because the modeled current speed are depth average and only influenced by tidal motion, whereas the actual speed measured at the surface and thus influenced by wind.

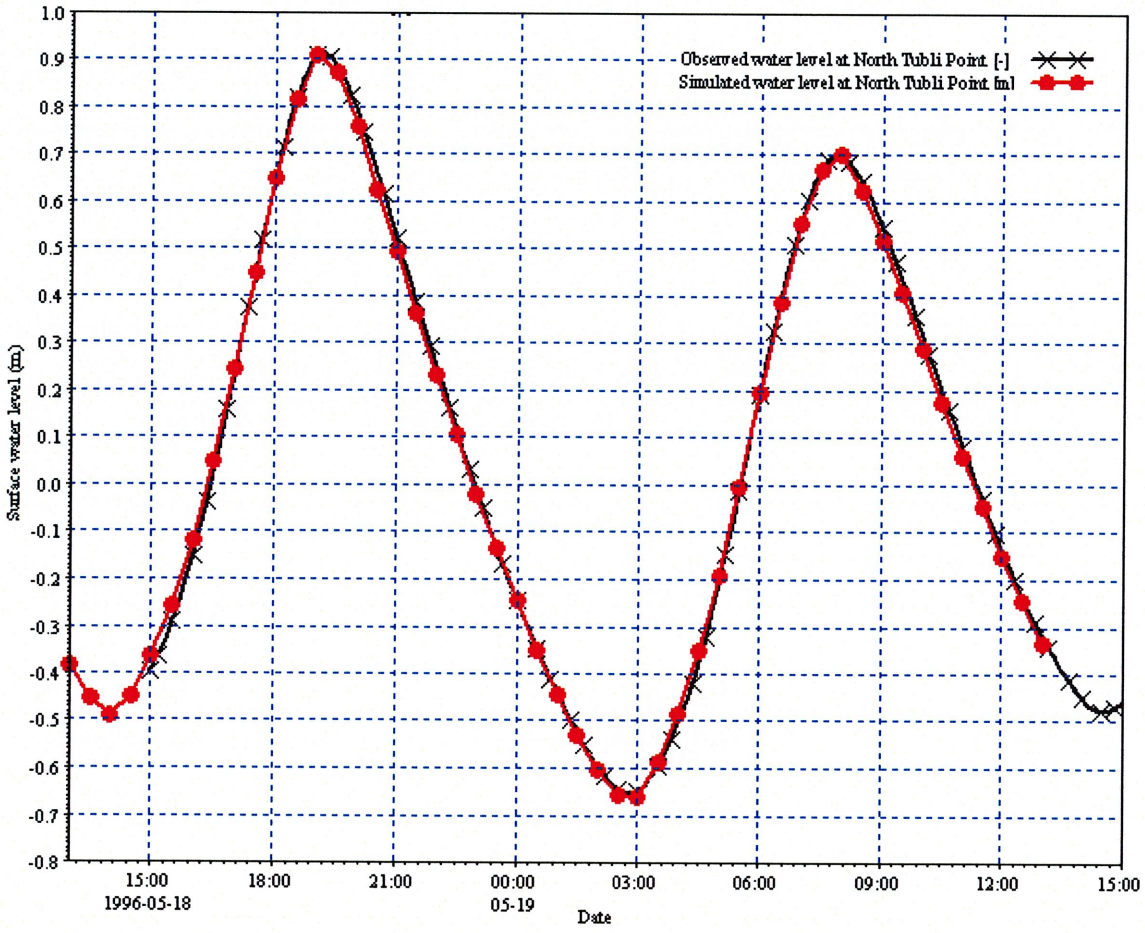


Figure 3.11: Comparison of water surface elevations measured and calculated at Point NT

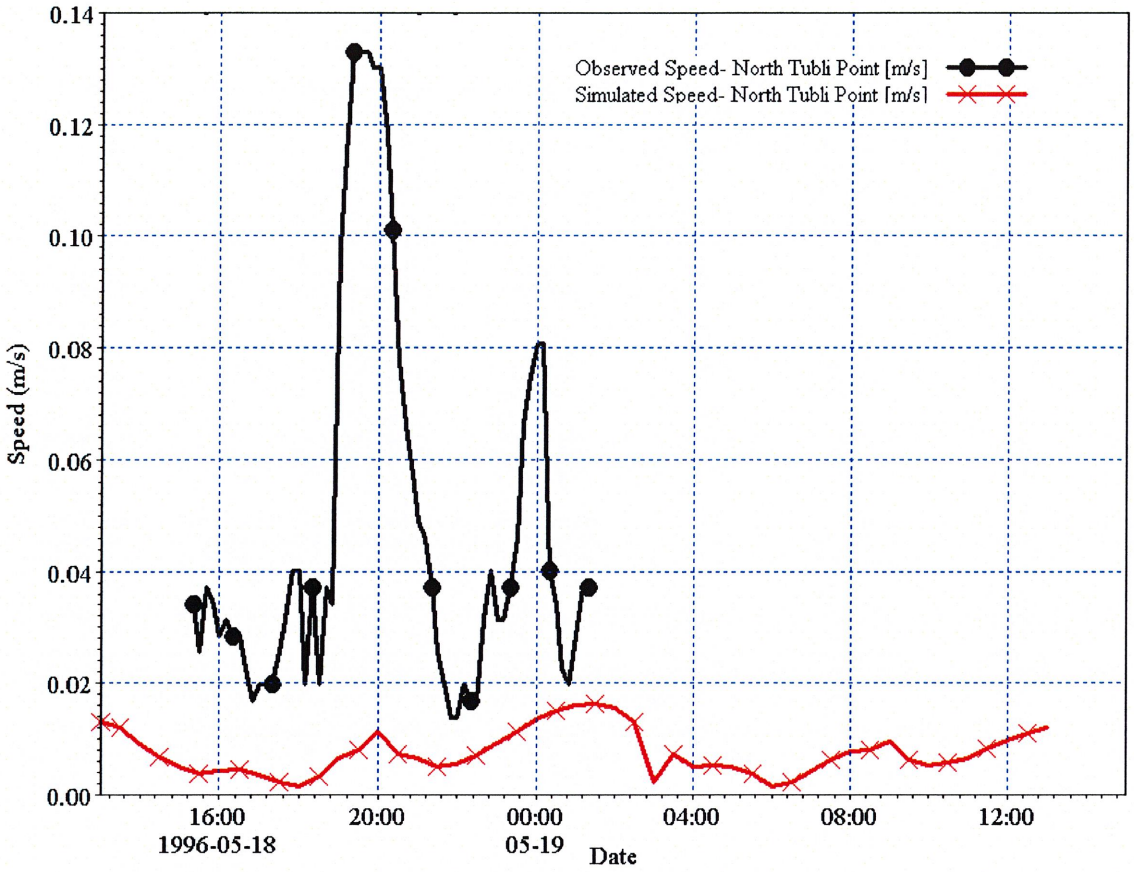


Figure 3.12: Comparison of speed measured and calculated at Point NT

3.12 EXISTING FLOW AND TRANSPORT IN TUBLI BAY

3.12.1 Existing Flow

After the model had been calibrated it is advisable to understand the existing flow characteristics in Tubli Bay. This helps us to understand the problems of flow circulation and flushing of the bay and at the same time corrective actions could be devised to enhance its flushing characteristics.

As indicated by CAG EIA study flushing of Tubli Bay could be attributed to two mechanisms: the tidal prism and circulation around Nabih Saleh Island and down into Ma'ameer Channel. These two mechanisms and their relative contribution to flushing in the

bay could be studied by first making a simulation of the existing situation, where cairns exist, and draw the water surface profile with time along a line from the eastern boundary at Mina Salman down to a point south of Ma'ameer Channel and passing through the points located north and south of Tubli Bay (for the profile path see Figure 3.13). The water surface profile at four times is drawn in Figure 3.14, these times are the situations of maximum flood flow, ebb starts up at Mina Salman, lowest water surface elevation in the Bay and the water levels at Mina Salman and in the Bay are the same.

Water surface elevations (level) at these times are keys to understand the flow in the Bay under the existing situation where cairns are present. At the time of maximum flood water surface elevation drops sharply through the cairns, stays at almost the same elevation in the northern parts of the Bay up to point south of the southern bridge, decreases gradually further down till it levels up through the culvert (almost stagnant as a result of flow coming from both sides of the culvert) and rises with steep slope through the channel. At this time water enters the Bay from the eastern boundary at Mina Salman and from south of the Ma'ameer Channel, but the former is much larger in quantity. At the time of ebb starts up at Mina Salman water surface elevation is highest in the Bay and almost of the same elevations all through the Bay up till the culvert, through the culvert as well as the channel it drops sharply or freely, but with a lesser slope in the later. The sharp drop through the culvert and the channel indicates that these two are real constrictions to flow and they may behave like control sections where flow changes it status from sub- to supercritical as it flows through them. At the time of lowest water surface elevation in the Bay and lowest tidal level at Mina Salman the culvert stays as a control section of flow coming into the Bay from south of the channel. Lastly, at the time levels at Mina Salman and the Bay are the same the culvert behaves too as a control section for flow going up from the south of the channel into the Bay. In brief, it can easily be said that water surface elevation in the Bay oscillates between two controls, the cairns and the culvert or the channel if the culvert is not present; therefore, the flow is largely governed by a control at cairns and another one at the culvert or the channel, but the later of much lesser effect.

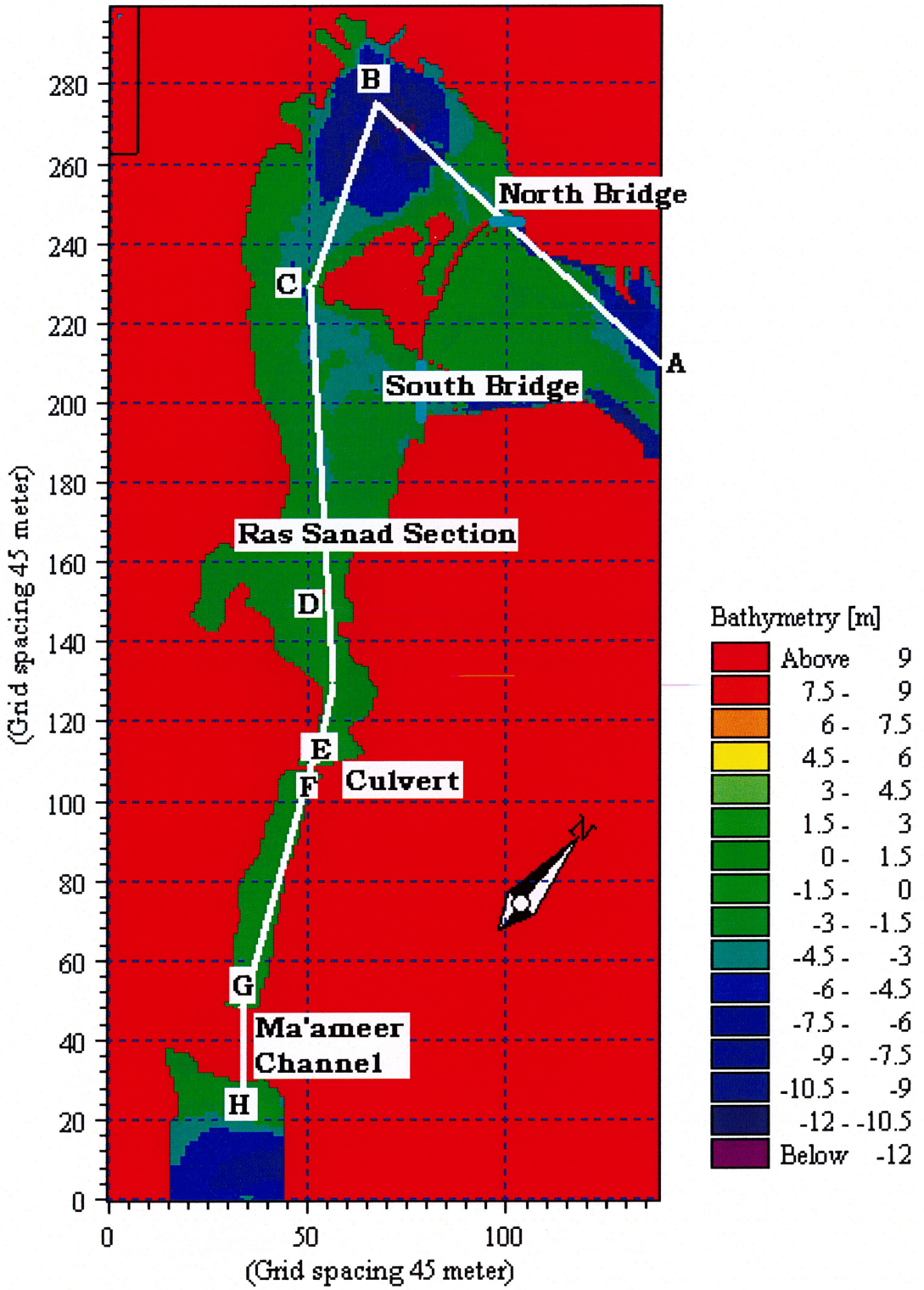


Figure 3.13: Water surface profile points and discharge cross-sections

3.12.2 Tidal Hydraulics and Flushing

The permanent impacts of the new Sitra Causeway on the tidal hydraulics and flushing are related to the high and low tide levels, currents in the bridge openings and flushing of Tubli Bay.

3.12.2.1 High Tide Levels

Compared to the existing situation, high tide levels will increase by about 2 cm with the proposed solution for the bridges. Such a small increase will not pose a threat to the safety of any coastal structures or to flooding of coastal areas. Its impact is negligible.

3.12.2.2 Low Tide Levels

Low tide levels will be about 5 cm lower than at present. This will result in a small increase in the area of inter-tidal flats exposed at low tide. The change is unlikely to be noticeable compared with the natural changes which occur between spring and neap tides where the low tide levels vary by 60 cm.

3.12.2.3 Current Speeds in the Bridge Openings

Representative current speeds in the bridge openings in the existing situation and with the proposed solution are shown in Figure 3.14 and Figure 3.15. With the new bridges the current speeds will exceed 1 m/s at spring tide. However, this is less than the maximum current speeds between the rock cairns at present. Therefore the currents are not expected to present any additional difficulties for the small craft using the area. The bridge spans will be increased from 12 m to 40-50 m and this will considerably reduce any danger to the small craft manoeuvring under the bridges. All the above information related to 3.12.2 was extracted from (CWOI, 2004).

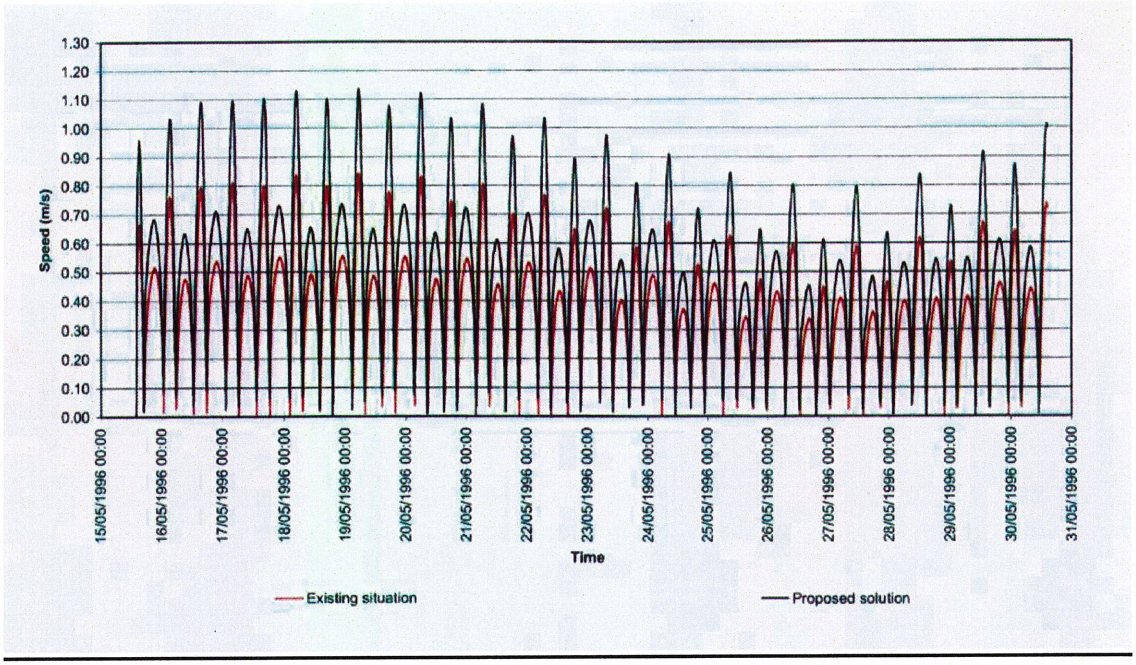


Figure 3.14: Current speeds at spring tide in the North Bridge section in the existing situation and with the proposed solution.

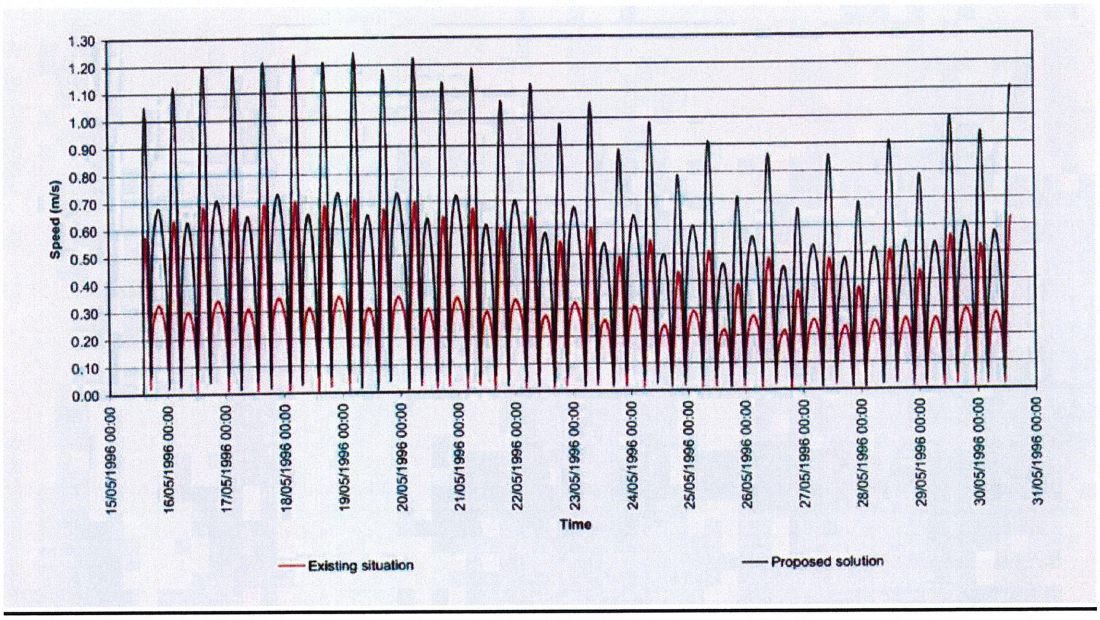


Figure 3.15: Current speeds at spring tide in the South Bridge section in the existing situation and with the proposed solution.

1- FLOOD:

a) Maximum flood into Tubli Bay:

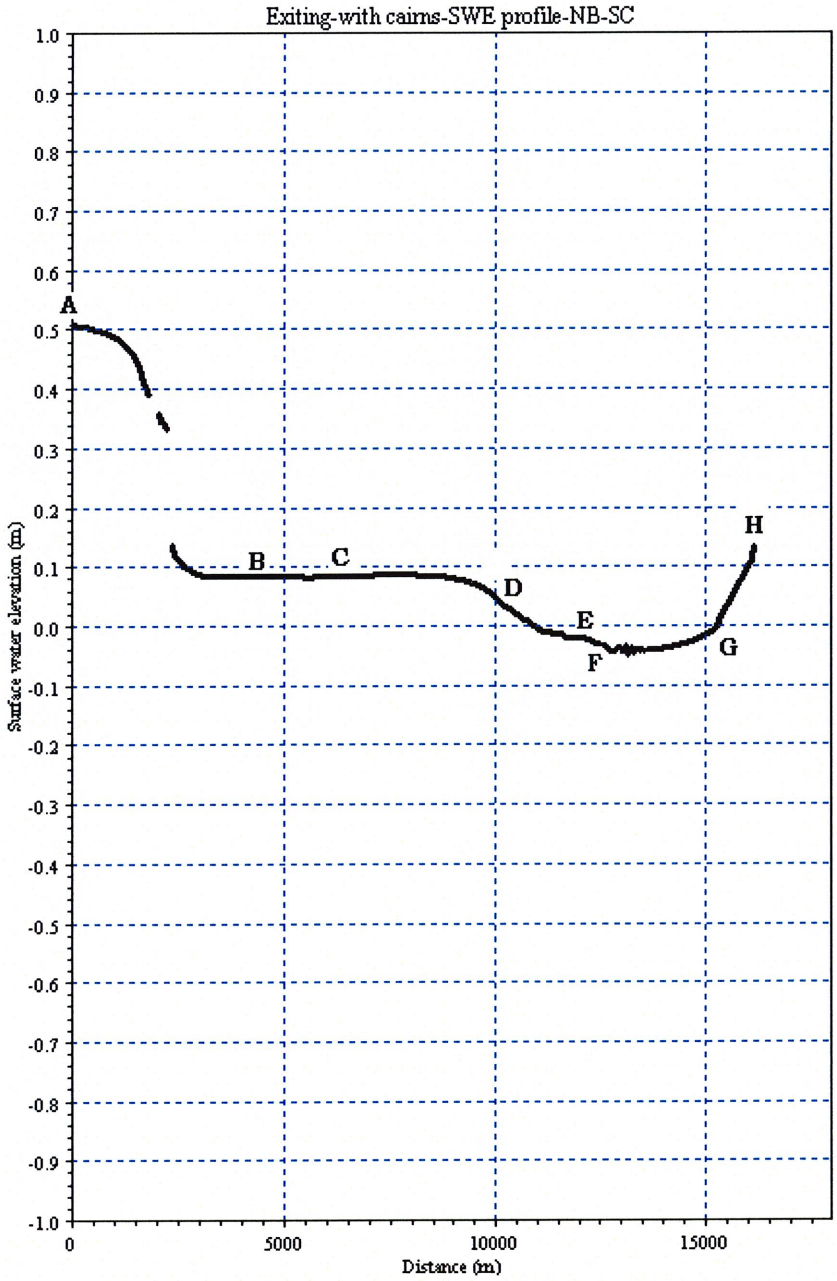
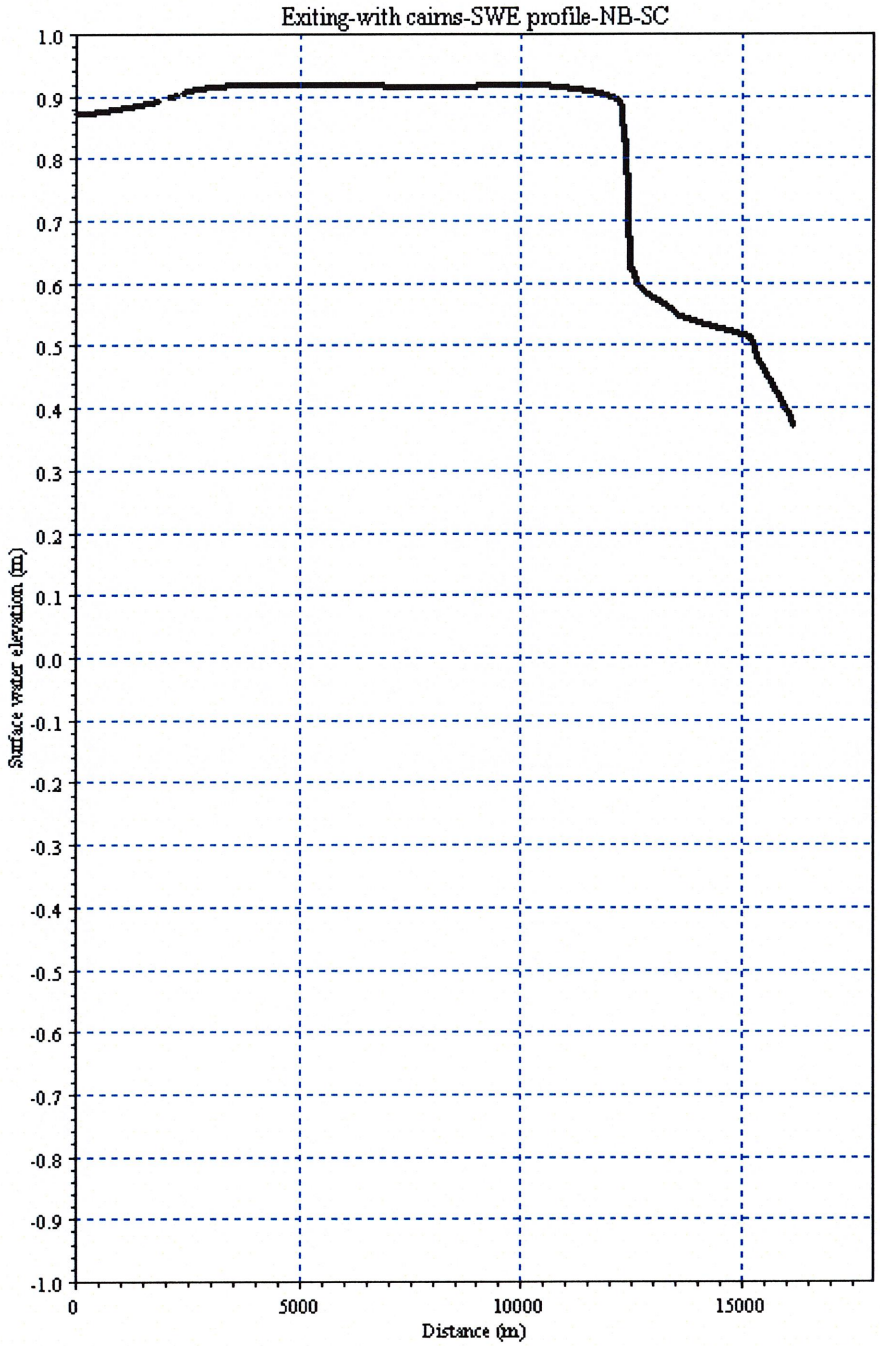


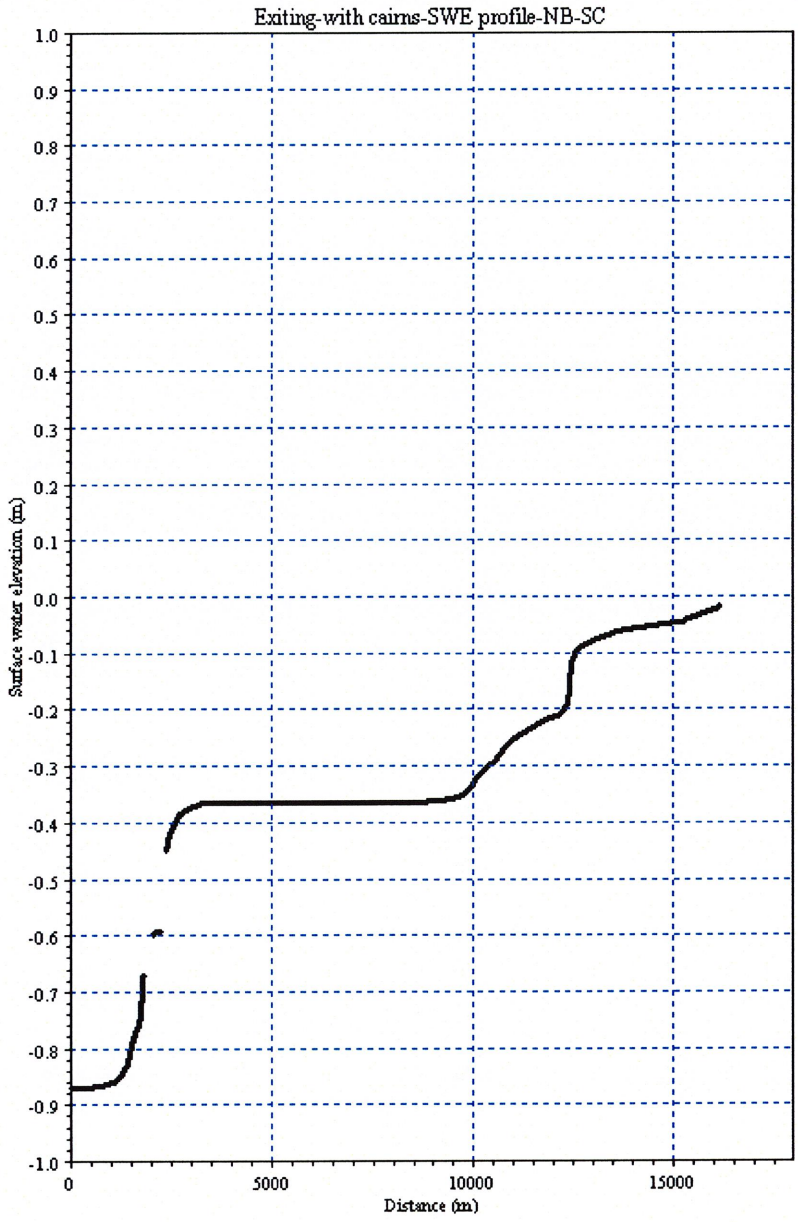
Figure 3.16 (a, b, c and d): shows water surface profile of flood and ebb along the points indicated in Figure 3.13

b) Minimum flood into Tubli Bay:

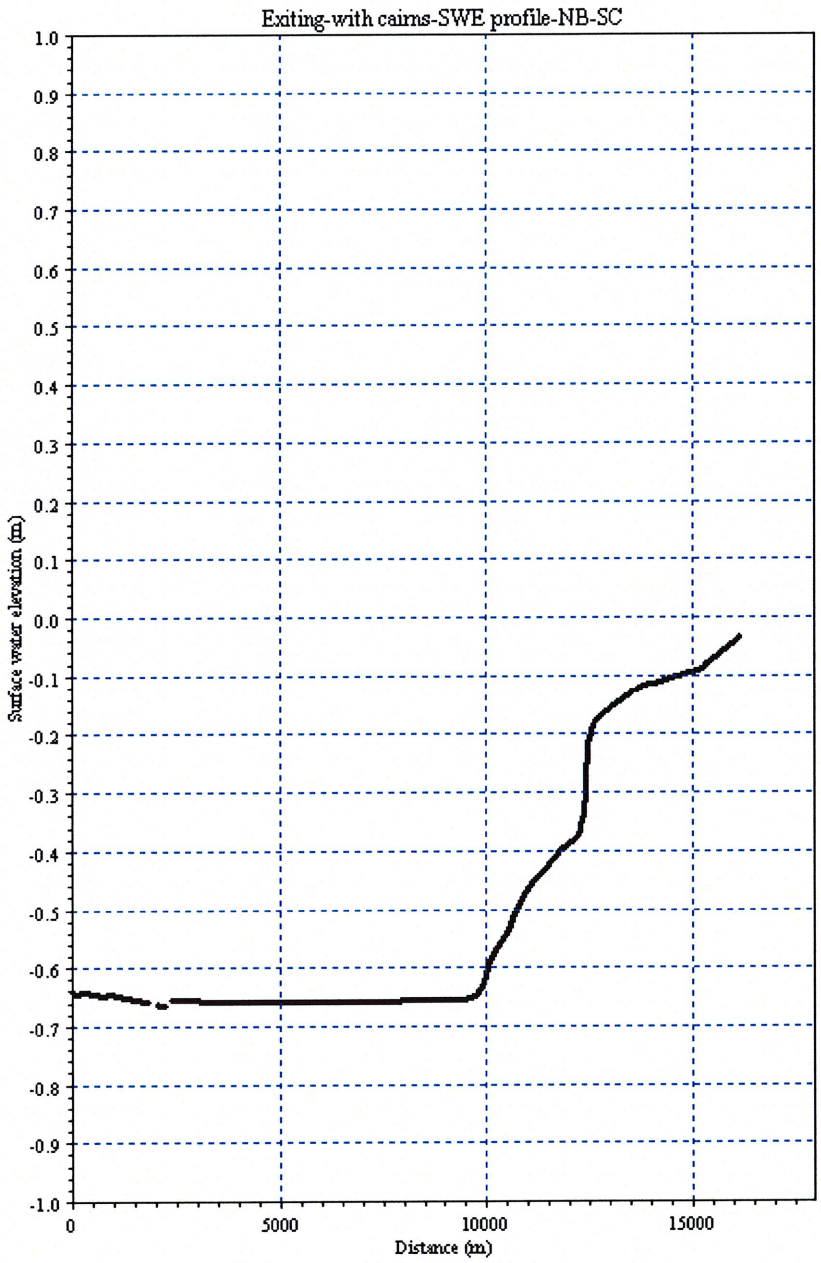


2- EBB:

c) Minimum ebb from Tubli Bay:



d) Maximum ebb from Tubli Bay:



Now to study the contribution of tidal and water circulation mean in, out and net discharges over the 14-day flood-neap cycle at sections: Sitra north bridge, Sitra south bridge, and the culvert or Ma'ameer Channel were calculated. As it is evident from the discharge calculations shown in Table 3.4 that the tidal prism contribution to flushing in Tubli Bay is about 34% (123.18/358.6) at Sitra north bridge, 58% at Sitra south bridge, and 4% at the culvert or Ma'ameer channel. On the other hand water circulation contribution is about 1% [(12.15-8.29)/358.6] around Nabih Saleh Island and about 0.7% through the culvert or the channel. These calculations indicate the weak role water circulation plays in flushing of the Bay and tidal prism is of profound effect and improvement scenarios should concentrate on it.

Table 3.4: In and outflow across sections outlined in Figure 3.13

	Mean outflow m^3/s	Mean inflow m^3/s	Average flow m^3/s	Mean net flow m^3/s	Outflow mean speed m/s	Inflow mean speed m/s
Sitra North Bridge	-127.57	118.79	123.18	-8.79	-0.19	0.17
Sitra South Bridge	-199.83	211.99	205.91	12.15	-0.11	0.12
Culvert	-13.63	16.05	14.84	2.42	-0.23	0.27
Ma'ameer Channel	-13.47	15.88	14.68	2.41	-0.14	0.17

3.12.3 Improvement Scenarios

The calibrated and validated model was put to investigate the flushing improvement scenarios. A number of scenarios that describe the most realistic cases in the Bay and at the same other scenarios could be easily deduced from them were tried (Table 3.5). Some scenarios belonging to shortening south which were previously tried by CAG EIA study, but the presentation here will be different, in GAC study their sole concern was to find the length of the southern bridge that keeps the in- and outflow through it unchanged, whilst here is to investigate options that can enhance flushing in the Bay.

Table 3.5: Proposed Scenarios

Scenario No.	Description	Length of Sitra North Bridge (meter)	Length of Sitra South Bridge (meter)
0	Existing situation- with cairns	217	452
1	Existing situation- No cairns	217	452
2	Elongating north bridge by 270 m - No cairns	487	452
3	Shortening south bridge by 90 m - No cairns	217	362
4	Shortening south bridge by 180 m - No cairns	217	272
5	Shortening south bridge by 270 m - No cairns	217	182
6	Dredged channel (3m deep, 45m wide) from southern Tubli bay to Ma'meer Channel	217	452
7	Dredged channel (3m deep, 135m wide) from southern Tubli bay to Ma'meer Channel	217	452

As presented in Figures 3.15 and 3.16 the scenarios in Table 3.5 have been drawn for high and low tide of 14-day flood-neap cycle at points in Figure 3.13 above. As the graphs indicate shortening Sitra southern bridge in the above scenarios has little effect on the tide high level in the Bay, and similarly the same could be concluded of the low time. However, the removal of cairns without shortening the bridge has increased the low tide level south of the culvert. Thus, it can be concluded that the removal of cairns and shortening the south bridge has little effect on the water level in the Bay.

As presented in Figure 3.17 and 3.18 the deepening the Bay south of the Tubli Bay and through the culvert and the channel has little effect on the high or low tide levels in the Bay before the culvert, after the culvert the effect is a gradual decrease or increase in water level and therefore the culvert or the channel will no longer become a control to flow and this improves flushing in the Bay.

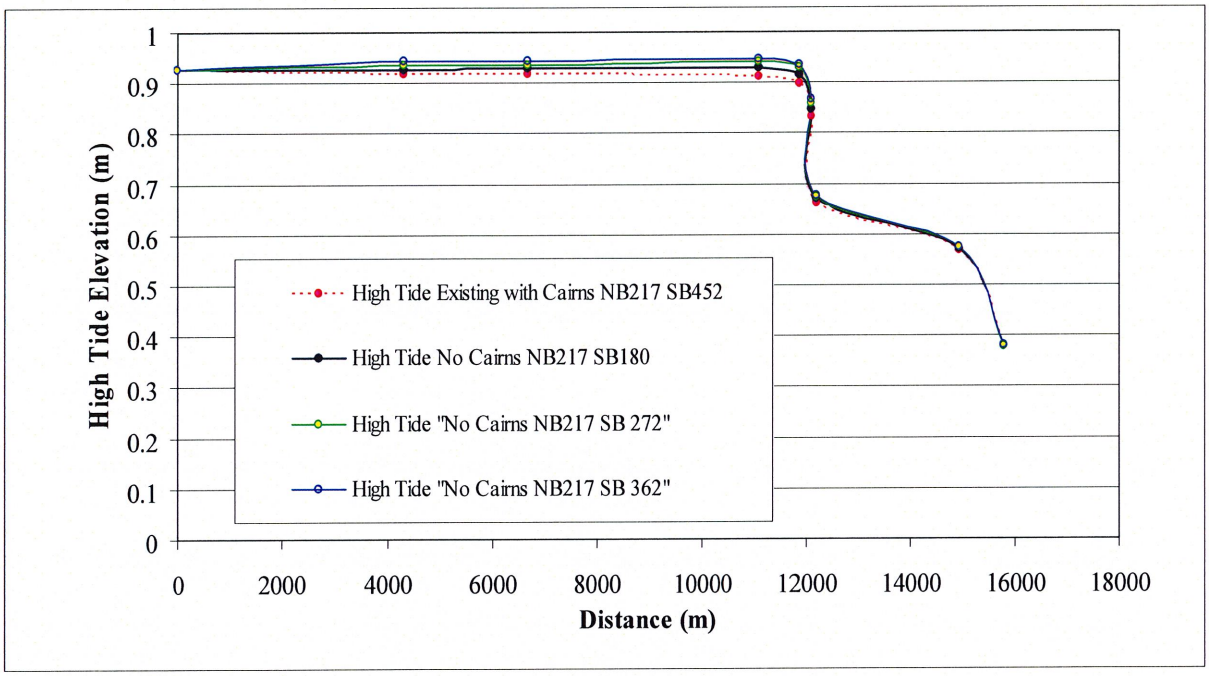


Figure 3.17: High tide level in Tubli Bay over the 14-day cycle for various south bridge openings

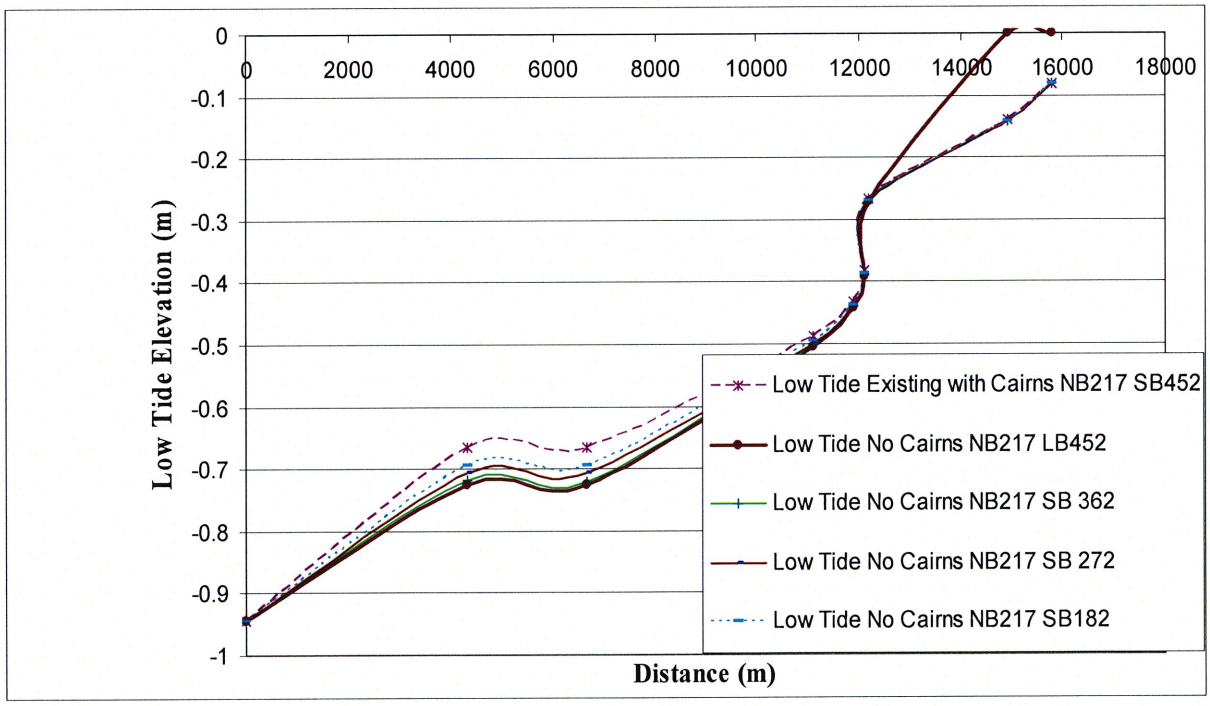


Figure 3.18: Low tide level in Tubli Bay over the 14-day cycle for various south bridge openings

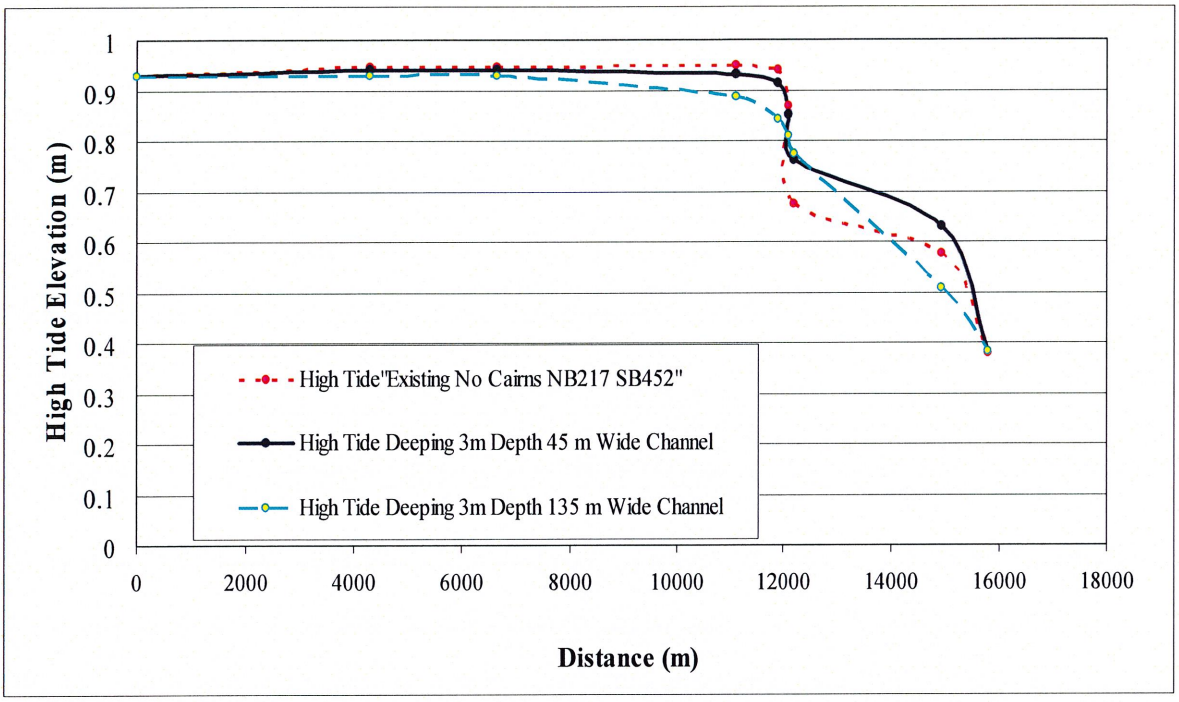


Figure 3.19: High tide level in Tubli Bay over the 14-day cycle for deepening south of the Bay to Ma'ameer Tide Channel

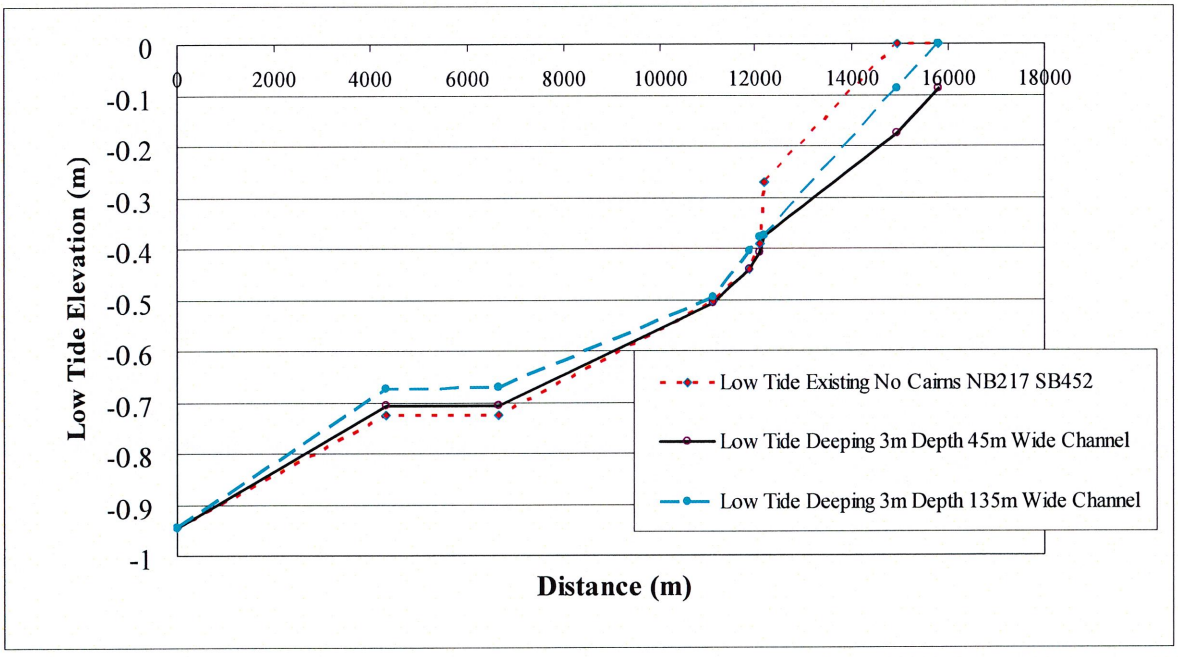


Figure 3.20 Low tide level in Tubli Bay over the 14-day cycle for deepening south of the Bay to Ma'ameer Channel

To study flushing in these scenarios calculation of discharge was made across sections of northern bridge, southern bridge, section at Ras Sanad and the culvert. The result of these calculations is presented in Table 3.6. A graph of values in Table was drawn in Figure 3.20.

Table 3.6: Discharge through various sections in Tubli Bay for various scenarios

	Q_{out} m^3/s	Q_{in} m^3/s	Q_{net} m^3/s
Scenario 1			
North Bridge	-139.21	134.72	-4.48
South Bridge	-201.99	211.82	9.84
Ras Sanad	-39.77	42.61	2.84
Culvert	-14.24	16.9	2.66
Channel	-13.22	15.87	2.65
Tubli Bay	**-408.43**	**421.92**	
Scenario 2			
North Bridge	-155.22	153.36	-1.85
South Bridge	-188.84	196.09	7.24
Ras Sanad	-39.91	42.83	2.91
Culvert	-14.36	17.07	2.71
Channel	-13.17	15.87	2.7
Tubli Bay	**-411.5**	**425.22**	
Scenario 3			
North Bridge	-144.66	140.98	-3.68
South Bridge	-194.68	204.56	9.89
Ras Sanad	-39.62	42.45	2.83
Culvert	-14.13	16.78	2.66
Channel	-13.25	15.89	2.64
Tubli Bay	**-406.34**	**420.66**	
Scenario 4			
North Bridge	-151.87	149.16	-2.7
South Bridge	-183.58	192.41	8.83
Ras Sanad	-39.37	42.17	2.7
Culvert	-13.98	16.6	2.62
Channel	-13.31	15.92	2.61
Tubli Bay	**-402.11**	**416.26**	

Table 3.6 (cont'd)

Scenario 5			
North Bridge	-158.55	157.42	-1.13
South Bridge	-173.4	179.35	5.96
Ras Sanad	-39.06	41.77	2.7
Culvert	-13.84	16.43	2.59
Channel	-13.37	15.94	2.58
Tubli Bay	**-398.22**	**410.91**	
Scenario 6			
North Bridge	-137.91	133.07	-4.84
South Bridge	-199.77	210.63	10.86
Ras Sanad	-45.04	48.61	3.57
Culvert	-25.59	28.89	3.3
Channel	-26.68	29.92	3.25
Tubli Bay	**-434.99**	**451.12**	
Scenario 7			
North Bridge	-133.33	128.7	-4.63
South Bridge	-190.34	205.66	15.28
Ras Sanad	-54.9	62.78	7.88
Culvert	-58.09	65.85	8.19
Channel	-59.31	67.57	
Tubli Bay	**-495.97**	**530.56**	

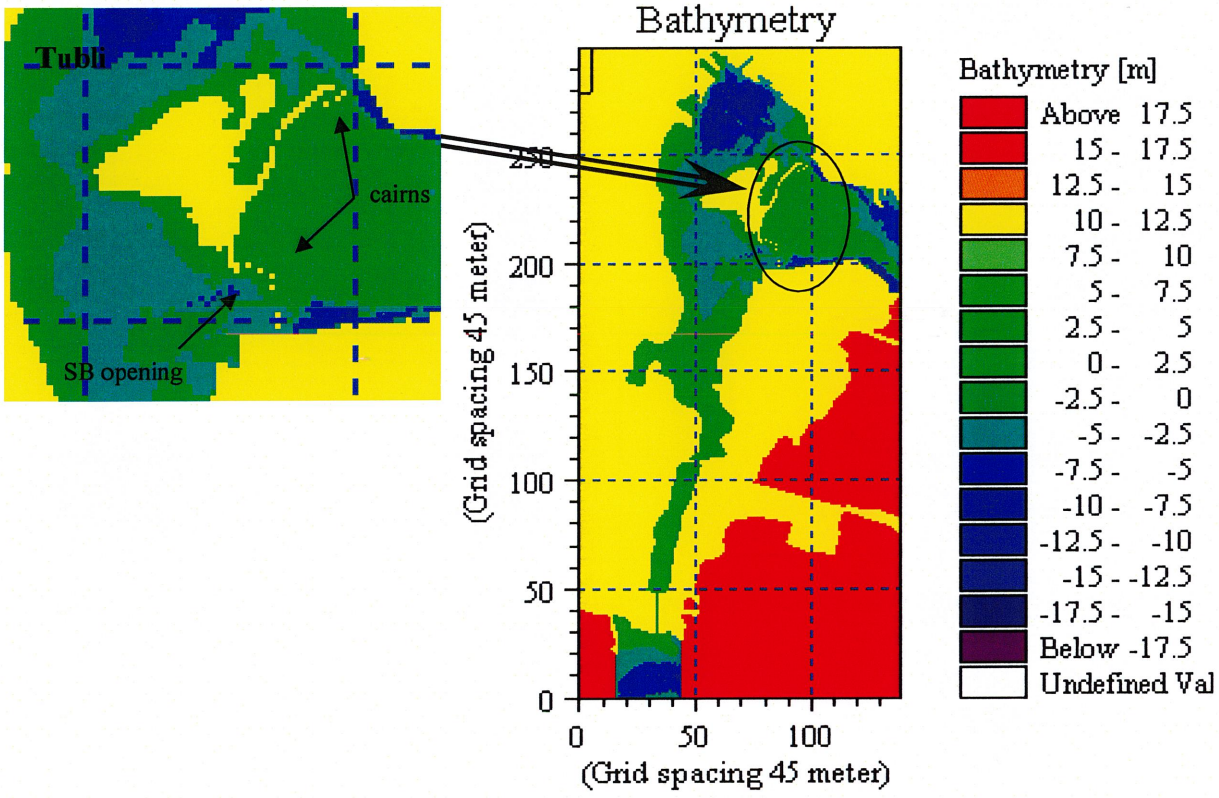


Figure 3.21: Location of cairns in the Tubli Bay

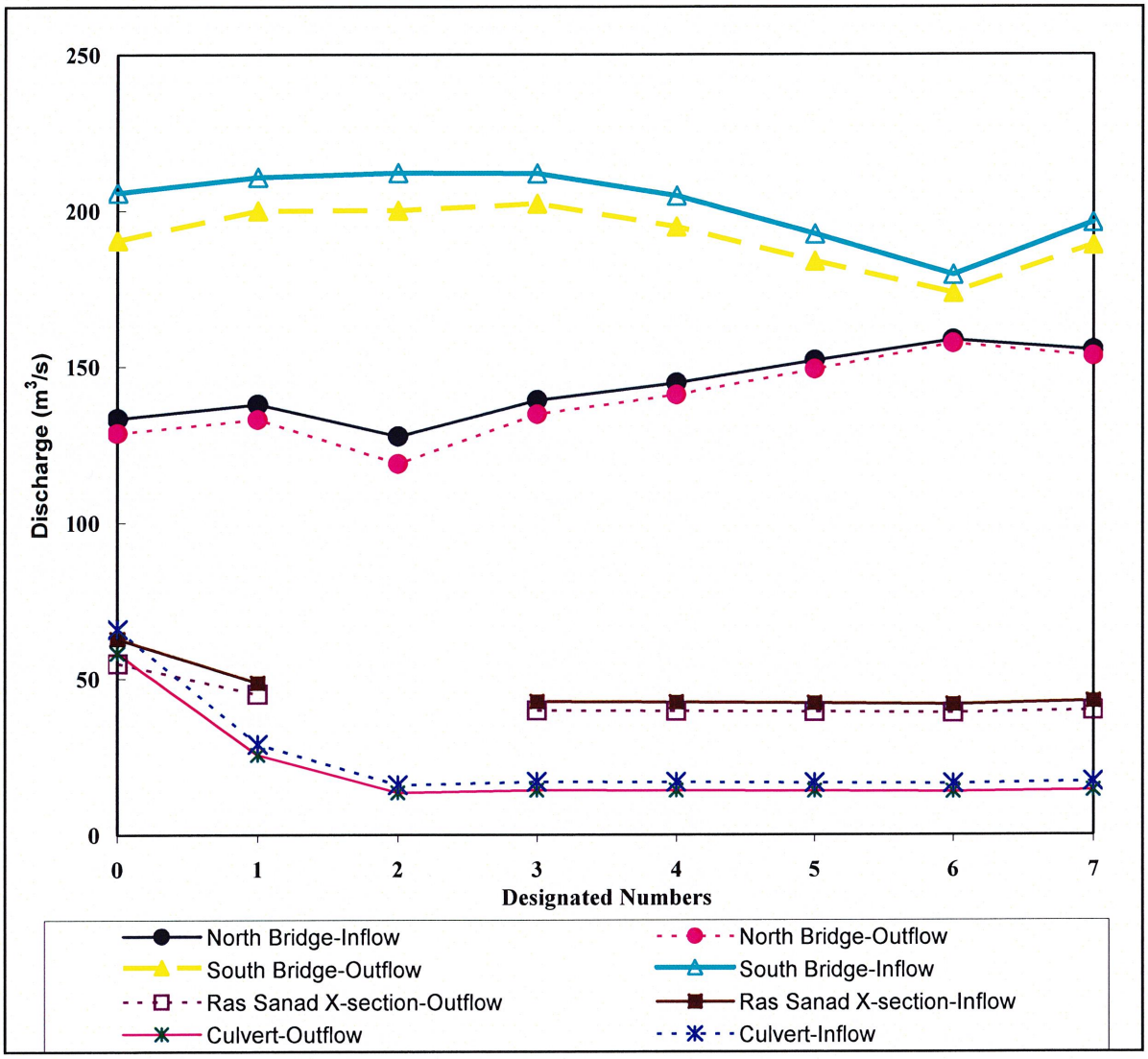
As observed in Figure 3.20 removing the cairns (scenario 1) increases the flow passing the northern bridge by 9.1%, but the southern bridge flow stays almost unchanged. Decreasing the southern bridge opening by 90 m (scenario 3) increases the flow crossing the northern bridge by 3.9%, 9.1% for 272 m southern bridge opening (scenario 4) and by 13.1% for 182 m southern bridge opening (scenario 5). On the contrary decreasing the southern bridge opening decreases flow crossing it by 3.4% for 362 m southern bridge opening, 9.1% for 272 m southern bridge opening and 15.2% for 182 m opening (Figure 3.19).

On the other hand, increasing the opening of the northern bridge by 270 m (Scenario 2) increases the flow crossing it from the existing situation without cairns (Scenario 1) by 11.5% and decreases the flow crossing the southern bridge by 7.4% from the existing without cairns. The amount of flow increase in the northern bridge is not big, which means that the most important opening for flushing Tubli Bay could be the southern bridge.

Dredging a channel of 3 m depth extending from south Tubli Bay and passing the culvert to the Ma'ameer Channel affect the flow crossing the northern and southern bridge slightly (Scenario 6 and 7). In case of the northern bridge the flow increase by 8.1% when the dredged channel has 45 m width and by 4.5% when the channel is 135 m width. The flow in the southern bridge decreases slightly when the channel is dredged or when its width is increased. This behavior is strange since dredging this channel or increasing the channel width should lead to an increase in the flow passing the northern and southern bridges. This behavior could be explained by the increase of water flooded into the Bay from southern channel and culvert which caused both waters coming from south and north to meet at some point south of Nabih Saleh Island, the collision of both waters reduces the flow passing the bridges.

However, dredging the channel has increased the interaction between the Bay and south of Ma'ameer Channel appreciably. For 45 m width channel the increase is about 63% and for 135 m channel it is 266%. One can use these values as guidance for dredging channel like the one here. In comparison with southern and northern bridge flow contributions combined it is about 7.5% for 45 m channel and 20% for 135 m channel. This contribution could not be practical on the basis of cost but definitely will improve the water quality in the bay.

From the last two paragraphs it can be concluded that the exchange between Tubli Bay and the south of Ma'meer Channel is very weak, either at the existing situation with cairns or without. This could be enhanced by dredging a channel down to south of Ma'ameer channel.



0	1	2	3	4	5	6	7
Scenario 7	Scenario 6	Scenario 0	Scenario 1	Scenario 3	Scenario 4	Scenario 5	Scenario 2

Figure 3.22: Discharge at various cross-sections in Tubli Bay for various scenarios

13.12.3.1 Residence Time

Residence time is the duration of persistence of a mass or substance in a medium or place. It can be calculated as follows:

Taken the Area of Tubli Bay as of 2002 = 12.56 Km^2 = 12.56X10^6 m^2, and
assuming Tubli Bay average depth is 6 m, then :

Residence Time = Volume / Q_{in}

The table below shows the residence time calculation for each scenario in Tubli Bay.

Table 3.7: Residence Time Calculation for each scenario in Tubli Bay

Scenario	Q_{in} in Tubli Bay m^3/s	Time Residence s	Time Residence d
1	421.92	178612.06	2.07
2	425.22	177225.91	2.05
3	420.66	179147.05	2.07
4	416.26	181040.70	2.10
5	410.91	183397.82	2.12
6	451.12	167050.90	1.93
7	530.56	142038.60	1.64

Based on the results presented in Table 3.7, it is clear that when the flow rate (Q_{in}) enter Tubli Bay is high, time residence will decrease which satisfies the formula as the residence time is proportional inversely with the flow rate.

Moreover, as it is known that flushing mechanism in the Ma'meer Channel in the south of Tubli Bay is contributed by bouncing flow. Due to shortest residence time (1.64 days) as indicated by table 3.7 for scenario 7 (dredging Ma'eer Channel 3m deep and 135m wide) the water quality in Ma'maar channel will be highly enhanced.

3.12.4 The behavior of contaminant in the Bay

To study the behavioral of contaminants transport in the Bay a number of simulations characterizing the various contaminant scenarios had been tried. Because dispersion coefficient in the Bay was not measured on site, it becomes necessary to search for a number of dispersion coefficients, but these coefficients vary largely and for our case we need a range that can be realistic to the bay situation. The literature was consulted and the one we found appropriate for bay was of DHI researchers, they found that in a case similar to the Bay and for similar cell dimensions of 45x45m as used in this work a 2.5 cm^2/s is appropriate.

Using this value two contaminant scenarios were tried, the first is by filling the inner of the Bay with a conservative contaminant of 10 (unitless) concentration (Figure 3.21). The reason the contaminant was placed in the inner of the bay is to reduce the effect of the boundaries conditions at Mina Salman and south of Ma'ameer Channel, which were assumed to stay at zero concentration during the simulations.

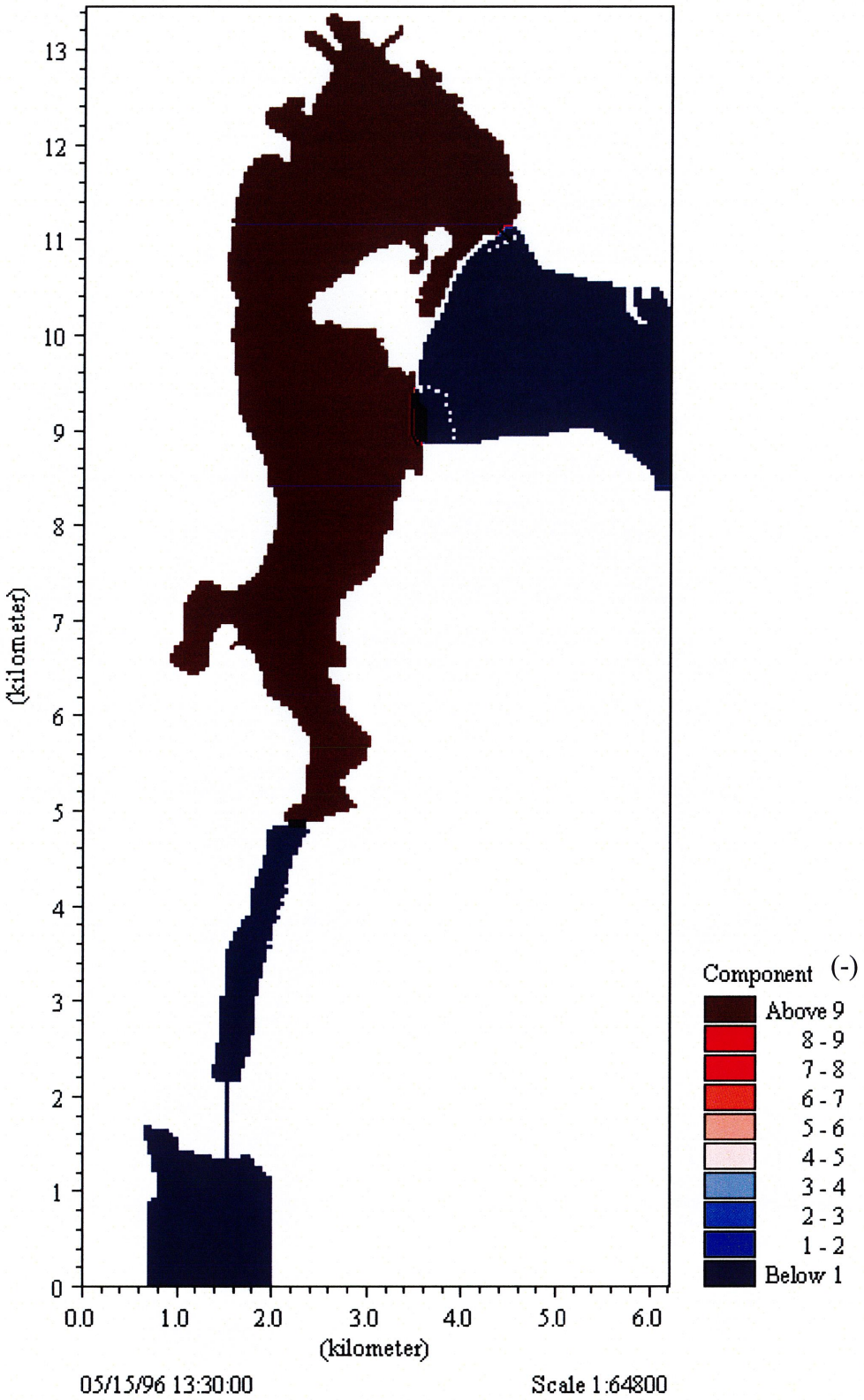


Figure 3.23: Contaminant initial concentration distribution in the Bay

The simulation results at maximum flow into the Bay is presented in Figure 3.22. According to this figure there are two unfortunate areas in the Bay and contaminant takes much longer to be removed from there, these are the north west corner of the Bay near Tubli wastewater treatment plant and the other is south of the southern bridge near Ras Sanad.

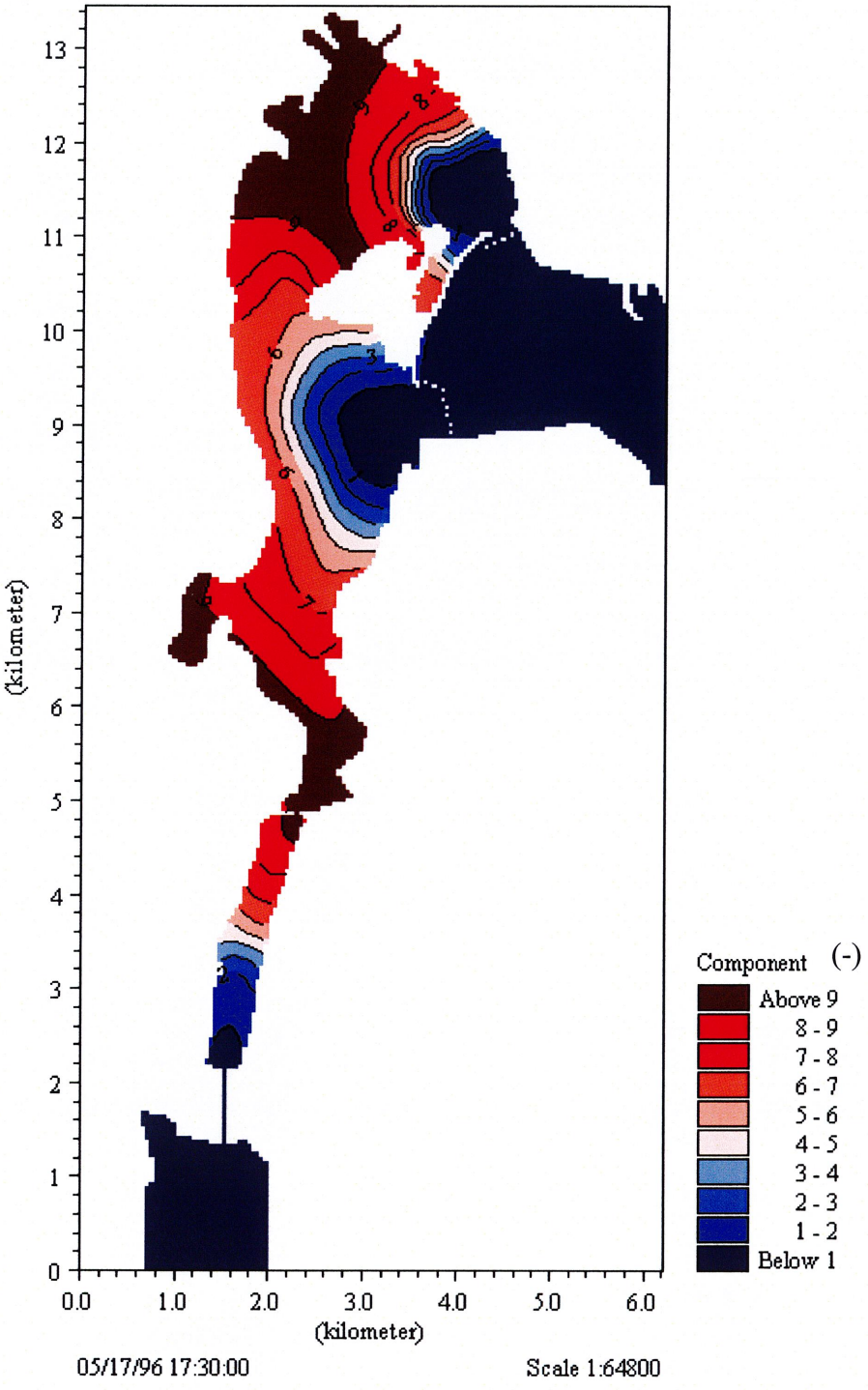


Figure 3.24: Contaminant concentration distribution in the Bay at the maximum flow

To understand how water at various areas of the Bay mix three spots of contaminant were placed north of the bay, at the middle near the southern bridge and south at Ras Sanad (Figure 3.23). The distribution of the contaminant also confirms the conclusion as shown in figure 3.24 that the same two unfortunate area exist, at the same the middle and north of the Bay water mixes, whilst water in the south seems difficult to mix with water north and it is flushed either through the southern bridge or the culvert, though the former is most probable.

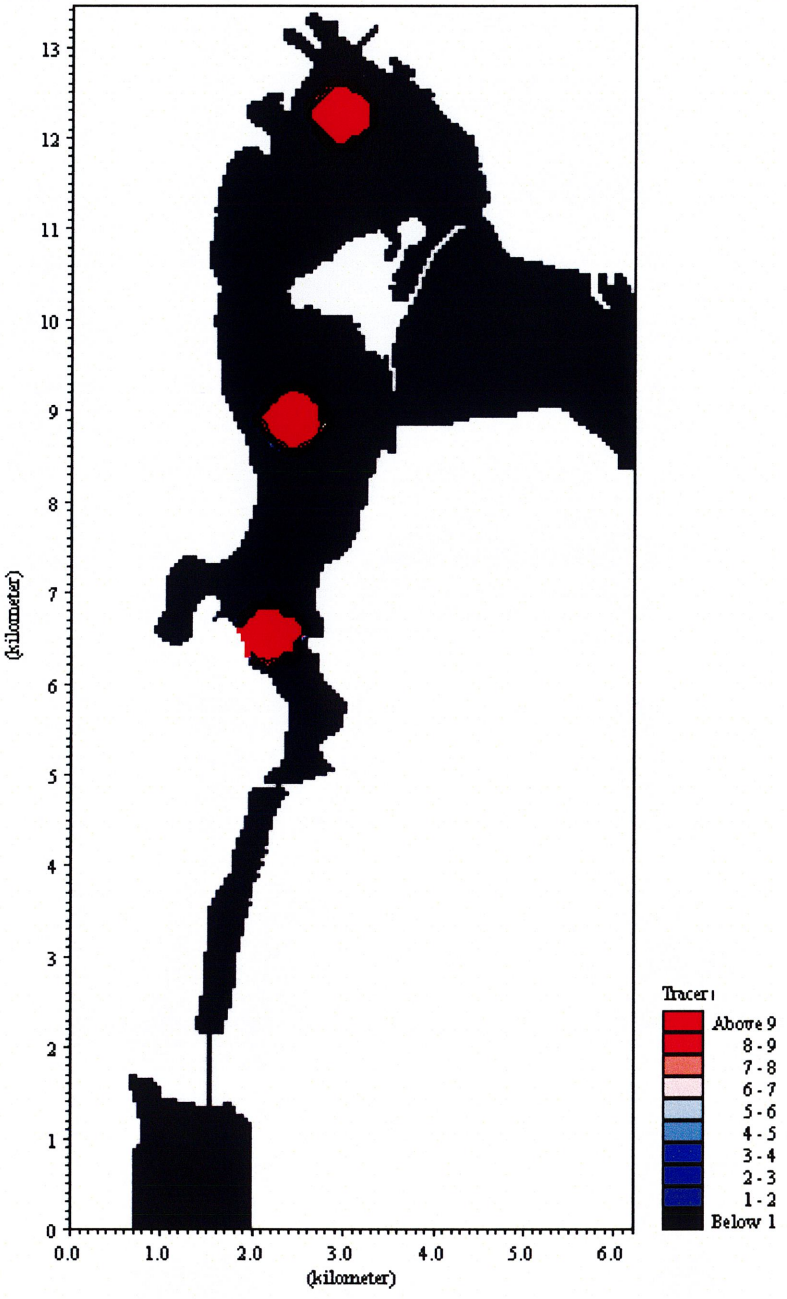


Figure 3.25: Initial concentration at three spots in the Bay

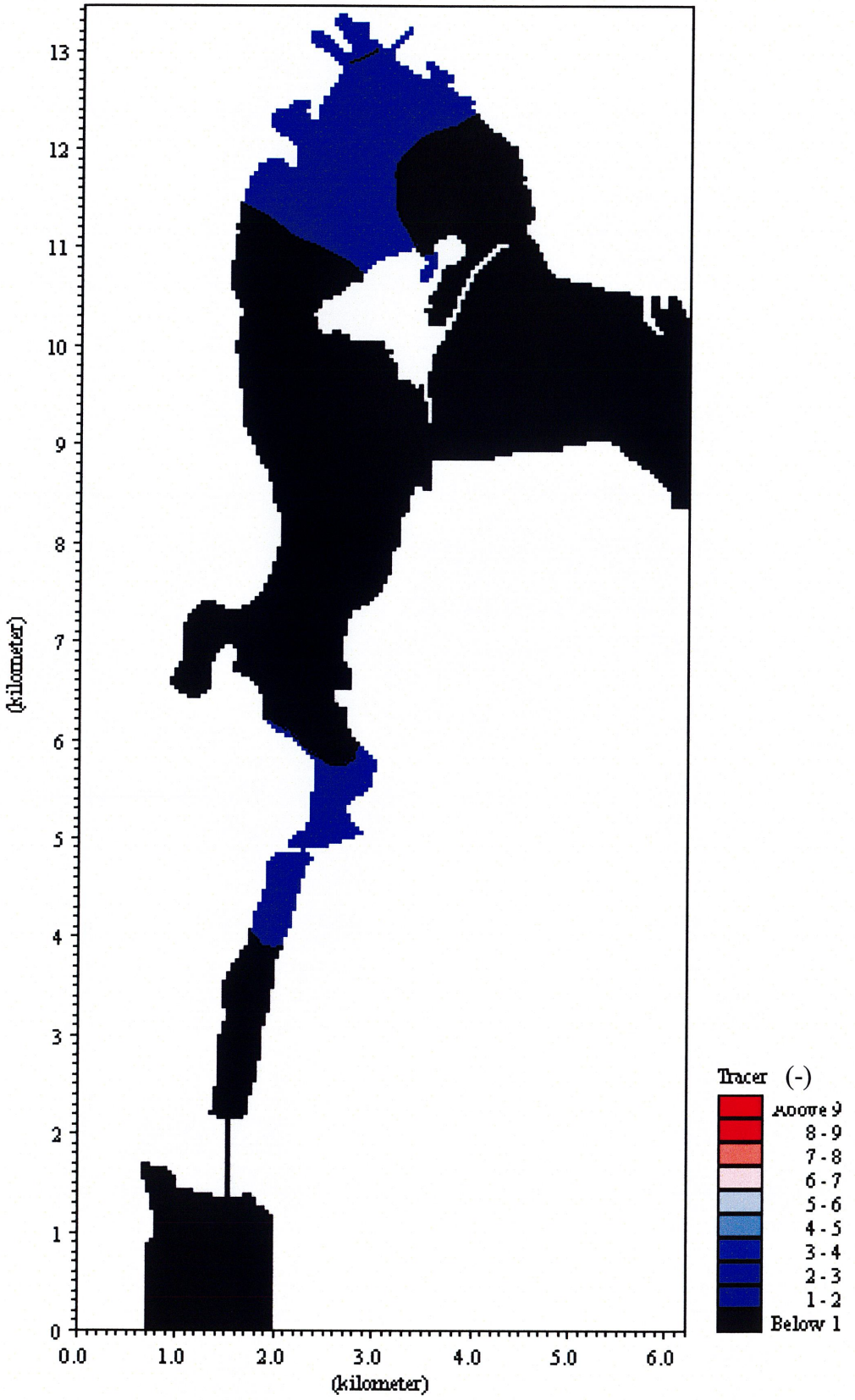


Figure 3.26: Concentration of three spots contaminant at the maximum flow

CHAPTER FOUR

CONCLUSIONS AND RECOMMENDATIONS

4.1 CONCLUSIONS

1. The model calibration with respect to water levels predicted by CAG was excellent at two points north and south of Nabih Saleh Island, at the culvert little deviations had been observed especially at low tide, and the reason could easily be attributed to the boundary conditions assigned south of Ma'meer Channel. With the exception of this the model could be considered representing tidal levels in Tubli Bay adequately.

2. The validation of the model with actual water level measurements at a point north of Nabih Saleh was excellent. On the contrary the validation of the model simulation with actual velocity at the same point north of Nabih Saleh Island can't be considered satisfactory, it is largely underestimated. CAG obtained similar results at this point and attributed the discrepancy to the place from which actual velocity was measured, which was just below the water surface. For the present study it is believed that this reason is not valid since velocity profile for shallow waters, dominated by bottom shear, is very coinciding with the mean velocity.

3. At present, the bay could be divided from flow and contaminant transport view into two regions, one representing the flow circulating around Nabih Saleh Island between Sitra north and south bridges, and the other represents the flow bouncing between Ras Sanad and south of the culvert or Ma'meer Channel. Whilst, the flow (in or out) of north Sitra bridge increases, the flow of the south bridge decreases by almost the same amount as the south bridge opening decreases (Figure 3.20 Designation Numbers 4, 5 and 6). At the same time flow through the culvert stays the unchanged in these scenarios.

4. Dredging a 3 m deep channel to connect south Tubli Bay with Ma'meer Channel increases the water exchange between them by almost two times for 45m wide channel and 4 times for 135m wide channel. In spite of this the flow through the existing Sitra bridge openings without cairns much overweighs the flow of the 135m wide dredged channel by two times for the north bridge and more than three times of south bridge. Accepting these figures one could conclude that a channel of 270m wide is required to let the flow south to Ma'meer Channel comparable with that of the north Sitra bridge. This clearly indicates

that one needs a very wide channel so as to make water flow south of Ras Sand affecting water circulation in the Bay.

5. From the simulations it seems that water flushing in Tubli Bay by tidal prism at various scenarios much overweighs water circulation around Nabih Saleh Island. (notice the total flow values and the net flow values in Table 3.4 for both north and south bridges). Therefore, flushing of contaminants in Tubli Bay is by tidal prism mechanism.

6. The simulation of a conservative contaminant in the inner Tubli Bay indicated that the reduction of its concentration by 50% takes about five to six days and to eliminate it by 95% takes about 21 days. This is a clear evidence of the good removal capacity of the Bay, if species and habitats can survive within these times. Furthermore, it was found that the area around the wastewater outflow is the most unfortunate area with respect to the removal of the contaminant; this confirms the findings of CAGs Study. Another unfortunate area exits also around Ras Sand and south to Ma'meer Channel.

7. Because the area around the wastewater outfall is unfortunate with respect to the distribution of contaminants and most importantly because wastewater settleable material settles easily in the deep area north of the Bay, it is expected that the bay will not recover from wastewater contamination in the short run, even if wastewater effluent is ceased. This settleable material will become a waste source because though upper water moves, deep water is almost stagnant.

8. Though the results have indicated that the proposed reduction of 300 m Sitra south bridge opening affects slightly the flow entering and leaving the Bay, but making a simulation with a domain of higher resolution around the bridge openings may indicate local fans or eddies that produces different erosion and siltation pattern in these areas. Siltation in these areas may produce a temptation for land infilling in them.

4.2 RECOMMENDATIONS

Based on the above features it is recommended that:

1. Further study is highly recommended to be conduct on the bay.

2. All waste effluents to the Bay should be ceased.

3. The settled waste at the deeper area north of the Bay, either be removed or the deep area filled (both not practical), capped by a thin layer of gypsum to stop feeding the upper water with dissolved waste, or left and later capped naturally by suspended matter siltation.

4. Not to dredge a channel south of the bay to Ma'meer Channel, because it will not enhance water flushing in the inner Bay, but it improves the water quality only in the area south of Ras Sanad. However, dredging such a channel may produce adverse environmental implications.

5. Demarkation line should be set to protect the Bay from further reclamation's or sea infilling.

6. The Bay should be developed in an environmental friendly way, this could make a good example of development environment internationally since the Bay is on the list of Ramsar Protected area.

CHAPTER FIVE

REFERENCES

REFERENCES

Abdulqader E. (1994). The role of Tubli Bay in the life cycle of the Penaeid shrimps of Bahrain. Proceedings of Symposium on Tubli Bay: Problems and Solutions, Bahrain.

Al Alawi Z. (1981). Oil spills in Bahrain waters during August-November 1980. Fisheries Journal, Arab Federation of Fish Producers Vol.3: 17-26.

Al Ansari M. (2002). Water Situation In Bahrain, GCC Greenery Jointly Symposium Japanese JCCP, Saudi Arabia.

Al Aradi A. (2006). Head Sewerage Treatment Plants Operation & Maintenance Department. Ministry of Works & Housing, Sewerage & Drainage Directorate. Personal Communication.

An Outlook to the State of the Tubli Bay Environment. Ministry of Housing, Municipalities, & Environment. Environmental Affairs, Directorate of Environmental Assessment & Planning, 11 May 1999.

Anon (1972). Statistical Abstracts. Statistical Bureau, Ministry of Finance and National Economy, State of Bahrain.

Anon (1992b). An Action Programme for the Conservation of Wetlands in South and West Asia. Asian Wetland Bureau, Kuala Lumpur, Malaysia, and IWRB, Slimbridge, U.K.

Al-Sayed H., Qureshi, A. & Al-Saad J. (1992). Some indicators of chemical and microbial pollution in the Al-Lawzy hypersaline pit, Bahrain. Biomedical Letters 47: 239-246.

Al-Sayed H. (1995). Ecological Characteristics of the Littorial Fauna at Tubli Bay, Bahrain. Qater University Science Journal, 15(1): 231 – 238.

Bird life Middle East, Bahrain – http://www.birdlifemed.org/Contries/barhin/barhin.html.

COWI M. (2004). Replacement of Sitra Bridges. Studies and surveys Environmental Impact Assessment.

CIA World Factbook - http://www.cia.gov/cia/publications/factbook/

First Report (2003). Millennium Development Goals, Bahrain - http://css.escwa.org.lb/scu-countryreports/Bahrain.pdf

General Commission for the Protection of the Marine Environment and Wildlife, Environmental Affairs, Bahrain. Personal Communication.

Google Earth - http://earth.google.com/download-earth.html

Halal A. (1996). Management plan for the viable sustainable development of Tubli Bay, State of Bahrain. Personal Communication

Janahi L. (2003). Water Resources in Kingdom of Bahrain. University of Bahrain, Report - Mater Program.

Kathy and Mike Hill, Bahrain - http://www.arabianwildlife.com/archive/vol2.2/bah.html.

Howard King, Bahrain Bird Report, http://www.geocities.com/Yosemite/5267/tubli.html.

Ibtisam K. (1993). Conservation of Tubli Bay, Symposium on "Tubli Bay- Problems and Solutions". Bahrain Centre of Studies & Research, Bahrain.

Kareema M. (2003). Sewage Treatment in Kingdom of Bahrain & Their Effects, University of Bahrain, Report - Mater Program.

Kareema M. (2003). The biological and ecological effects of domestic sewage outfall on Tubli Bay, University of Bahrain, Report - Mater Program.

Library of Congress Country Studies/Area Handbook – World Facts Index - http://worldfacts.us/Bahrain-geography.html

Mike 21 HD (2003). Reference Manual. Coastal Hydraulics and Oceanography Hydrodynamics Module, Scientific Documentation. DHI Water & Environment.

Mohamed S. (1991). On the movement and distribution of the greater flamingo, Phoenicopterus ruber in Bahrain. Arab Gulf J. Scient. Res. 9 (3): 133-142.

Mohamed S. (1993). Birds of Bahrain. Bahrain Centre for Studies and Research, Bahrain.

Mohamed S. (1994). Aquatic birds in Tubli Bay. In: Proceedings of Symposium on Tubli Bay: Problems and Solutions, Bahrain, 10 January 1994.

Raveendra E., Buali A., Al Sayed H. and Khalaf I. (1994). Physical and chemical. Characteristics of water and sediment in the vicinity of a major sewage treatment plant outfall. Contribute submitted to Symposium on Tubli Bay: Problems & Solutions, Bahrain.

Saleh, M. and Mohamed S. (1990). The western reef heron (Egretta gularis) in Bahrain. Fauna of Saudi Arabia 11: 306-317.

United Nations, Department of Economic and Social Affairs - httpl://www.un.org/dpcsd/earthsummit.html

United Nations, National Implementation of Agenda 21 – http:///www.un.org/esa/earthsummit/barin-cp.html

Vousden D. (1988). The Bahrain Marine Habitat Survey. A study of the marine habitats in the waters of Bahrain and their relationship to physical, chemical, biological and anthropogenic influences. Report and Volume Two: The Habitat Map.